Investigations of the Properties of Single Molecules of *Escherichia coli* β-galactosidase by Capillary Electrophoresis Laser-Induced Fluorescence

By

Jeremie Crawford

Thesis submitted to the Faculty of Graduate Studies of The University of Manitoba in partial fulfillment of the degree requirements of

Masters of Science

Department of Chemistry

University of Manitoba

Winnipeg, Manitoba

Abstract

Single molecules have been found to be functionally heterogeneous within a population with both static and dynamic heterogeneity identified throughout a variety of enzymes. It is widely accepted that heterogeneity is an applicable property for all enzyme molecules. Individual molecules have been shown to exhibit differences in both catalytic rate and electrophoretic mobility when under identical conditions as fluctuations over broad time scales creating a unique profile for each molecule. Both biological and structural sources behind the observed heterogeneity remain elusive. The studies presented within this body of work use *Escherichia coli* sourced β-galactosidase and capillary electrophoresis coupled with laser-induced fluorescence (CE-LIF) to investigate fundamental properties with regards to both static and dynamic heterogeneity. The fluorogenic substrate 9H-(1,3-dichloro-9,9-dimethyacridin-2-one-7-yl)-β-D-galactopyranoside (DDAO-gal) was used to provide both catalytic rate and electrophoretic mobility measurements as the enzymes are subjected to various conditions. It was found that dynamic heterogeneity gave rise to a conformational range for a given enzyme which increased with temperature. Enzyme formed in the presence or absence of specific heat shock chaperone systems were investigated with no measurable differences found. A novel assay for the application of dynamic capillary coatings for use in subjecting a single enzyme to multiple solutions was presented. Both K_m and K_I values were reported for individual molecules by subjecting each molecule to 3 separate solutions within the capillary. Heterogeneity was shown to exist for values of K_I within a population.

Acknowledgments

I would like to thank my advisor Dr. Doug Craig for all his support and guidance throughout my studies. His continued support has contributed greatly to my success both inside and outside of the laboratory.

I would also like to thank the members of my committee, Dr. Belay Ayele, Dr. Sean McKenna, and Dr. Hélène Perreault for their support throughout this endeavor.

Thank you to the Natural Sciences and Engineering Research Council for providing the funding that was required to complete the presented work.

I would also like to recognize others whose assistance is greatly appreciated. Thank you to Dr. Shakhawat Hossain for his assistance in the statistical analysis in Chapter 5 and to Dr. Joshua Hollett for his assistance in the mathematical modeling found in Chapter 7.

Table of Contents

List of Tables

List of Figures

List of Abbreviations and Symbols

A	Current (amperage)
ANOVA	Analysis of variance
APD	Avalanche Photodiode
atm	Atmosphere
ATP	Adenosine triphosphate
bp	Base pair
BSA	Bovine serum albumin
C_a	Concentration of analyte
CCD	Charge-coupled device
CE-LIF	Capillary electrophoresis laser-induced fluorescence
CS	Cover slip
D	Diffusion constant
Da	Daltons
DDAO	7-hydroxy-9H-(1,3-dichloro-9,9-dimethyacridin-2-one)
DDAO-gal	9H-(1,3-dichloro-9,9-dimethyacridin-2-one-7-yl)-β-D- galactopyranoside
DM	Dichroic mirror
DMSO	Dimethylsulfoxide
DNA	Deoxyribonucleic acid
E	Separation potential
e	Electronic charge
EE	Excitation emission
E_i	Injection potential
EOF	Electroosmotic flow
f	Frictional coefficient
FAD	Flavin adenine dinucleotide
FDG	Fluorescein Di-D-galactopyranoside
fL	Femtolitre
fM	Femtomolar
FRET	Förster resonance energy transfer
g	Times gravity
GFP	Green fluorescent protein
Glu	Glutamate
GS-6	Genescan polymer 6™
HEPES	*N*-2 Hydroxymethyl-piperazine-*N´*-2-ethanesulfonic acid
His	Histidine
HPLC	High performance liquid chromatography
Hz	Hertz
I	Ionic strength
I.D.	Internal Diameter
IPTG	Isopropyl-β-D-thiogalactoside
IR	Infrared
k_{cat}	Catalytic rate constant
K_I	Inhibition dissociation constant
K_m	Michaelis-Menten constant

L	Length of capillary
LB	Luria-Bertani
LDH	Lactate dehydrogenase
$MgCl_2$	Magnesium chloride
mM	Millimolar
mL	Milliliter
mW	Milliwatt
N	Theoretical plate number
N	Number of molecules
N_A	Avogadro's number
N.A.	Numerical aperture
NADH	Nicotinamide adenine dinucleotide
NaOH	Sodium hydroxide
nm	Nanometer
nL	Nanoliter
oNPG	*ortho*-nitrophenyl-β-D-galactopyranoside
PEG	Polyethylene glycol
PCR	Polymerase chain reaction
PMT	Photomultiplier tube
PVP	Polyvinylpyrrolidone
Q_a	Quantity of analyte
rpm	Revolutions per minute
r	Radius of particle
r_b	Average radius of buffer ions
r_c	Radius of capillary
r_p	Stokes radius of protein
R_s	Separation resolution between two analytes
RBG	Resorufin-β-D-galactopyranoside
RES	Resorufin
s	Second
S_0	Ground electronic state
S_1	First excited electronic state
SFC	Sheath flow cuvette
SiOH	silanol
SmFRET	Single molecule FRET
S/N	Signal to noise ratio
T	Triple state
T	Temperature
t	Analyte time to detector
t_{DDAO}	DDAO time to detector
t_i	Injection time
$t_{m,DDAO\text{-}gal}$	DDAO-gal time to detector
TIM	Triosephosphate isomerase
TIRF	Total internal reflective fluorescence
Trp	Tryptophan
Tyr	Tyrosine

V	volt
V	applied voltage
v	velocity of an ion in solution under an applied field
v_{act}	actual velocity of analyte
V_c	capillary volume
V_{app}	apparent velocity of enzyme
V_{eof}	velocity of EOF
V_{max}	Catalytic maximun
V_{rp}	velocity of enzyme relative to DDAO
w	peak width at half maximum
w/v	ratio of weight to volume
Z_p	net charge on protein
ε_r	relative permittivity
ζ	zeta potential
η	viscosity
μ	electrophoretic mobility
μ_{DDAO}	electrophoretic mobility of DDAO
μ_{eof}	electrophoretic mobility of EOF
μ_{Enzyme}	electrophoretic mobility of the enzyme
µg	microgram
µL	microliter
µM	micromolar
µm	micrometer
μ_p	electrophoretic mobility of protein
Z_a	Net charge
Å	angstrom

List of Copyright Materials Used

Page 47: Figure 1: Ribbon structure representation of β-galactosidase. Used with permission[101].

Page 49: Figure 9: Schematic of reaction mechanism for hydrolysis of galactopyranoside by β-galactosidase. Reprinted with permission from "Juers, D.H., Heightman, T.D., Vasella, A., McCarter, J.D., Mackenzie, L., Withers, S.G. and Matthews, B.D. (2001). A structural view of the action of *Escherichia coli* (*lacZ*) β-galactosidase. *Biochemistry* **40**(49): 14781-14794". Copyright 2001 American Chemical Society.

Page 63: Figure 2: Reported activity of individual β-galactosidase molecules between heat pulses of 47°C. A) Activity traces in a single experiment. Six images between taken between each heat pulse. B) Excerpt of 4 molecules to illustrate activity changes with each heat pulse. C, D, E, F) Histograms representing each molecules increase or decrease in activity based on turnover numbers (sec^{-1}). Used with permission[124].

Page 71: Figure 3: Conformational energy illustration. Each k represents local energy minima achieved by conformational shifts when the enzyme is provided with adequate energy to overcome the barrier. Used with permission[124].

1. Introduction

1.1. Background

Prior to 1959 the research industry was focused on everything that was "bigger and better" than it was in the previous years. The concept of more was the goal of most areas of research but sometimes less is more. In 1959 the quote "There's plenty of room at the bottom" came from renowned American physicist Richard Feynman's title of a talk he gave at the American Physical Society[1]. His goal was to promote the study of physical systems at the smallest possible scale, right down to the atoms and molecules. He stated that there should be no reason why the entire Encyclopedia Britannica could not be printed on the head of a pin[1]. Feynman offered one thousand dollars to be awarded to the first person who would reduce a book page 25,000 fold and to create the first 1/64 cubic inch rotating electric motor. Both feats were awarded, the motor in 1960 and the book page in 1986. This was the beginning for the generations to come to be focused on the world at the smallest possible level. From microscale medicine, nanotechnology, and single molecule research Feynman is considered to be the intellectual grandfather of the single molecule field.

1.2. Why Study Single Molecules?

The area of chemistry prior to the introduction of single molecule studies would measure properties based on solutions containing a large amount of sample. The experimental data resulting from the studies would represent an ensemble average of all the present components. For example an activity study for a given enzyme at a concentration of 1 mM in a 1 mL sample cuvette would contain 6.02×10^{17} molecules being analysed and a single average activity reported. However, this average is

eliminated when a single molecule is observed at a time, allowing heterogeneity within the population to be observed. The complexity of heterogeneity within a population is broken into two categories known as static or dynamic heterogeneity. With respect to an enzyme static heterogeneity refers to the assembly of the structure itself. The differences are permanent in the structure arising from, but not limited to, errors in transcription/translation of the primary sequence or differences in the post translational modification process. It is assumed that for small simple molecules structure is conserved completely as any variations would drastically alter the molecule. For large molecules these variations are often acceptable in the production of an enzyme and still yield a functional molecule. The homogeneity of a protein cannot be assumed and each molecule can be thought of like a unique snowflake with some varying combination not reproduced in the population. Single molecule experiments have shown that enzymes within a population have large differences in activity with nominally identical molecules that are stable and long-lived[2,3]. Dynamic heterogeneity encompasses the fluidity of a specific molecule once its structure has been established. Once assembled each molecule possesses different attributes leading to variations in measurable outputs. In order for this to be observed with a bulk assay approach it would require that the entire or at least the majority of the population be synchronized to one another producing a net effect as either an increase or decrease in signal. Single molecule studies on the other hand allow the alterations of each molecule to be observed individually. Most of these changes are short-lived intermediates that are rare to observe and are in constant flux with one another. Long-lived, stable alterations are possible but neither intermediate type is observable under bulk studies. It is thought that the static heterogeneity gives rise to a dynamic

profile for a given molecule. Dynamic fluctuations in structure may arise from reaction pathways[4,5] including; discrete steps of a motor protein[6], protein unfolding forces[7] and dynamic fluctuations of a protein[8]. In a bulk assay both static and dynamic heterogeneity goes unnoticed because it can be assumed that differences and fluctuations, either positive, negative or neutral will exist in a balanced state. This concept will be explored later in chapter 5.

It is important to note that the purpose of single molecule studies is not to disprove or create disconnect with the traditional biochemistry and molecular biology approaches. Instead it is designed to supplement the vast wealth of knowledge that these have provided us with. This means that the results from a single molecule study must coincide with its bulk assay counterpart. Therefore the combined single molecule measurements will approach that of the bulk assay with sufficient averaging. Rather than contradiction, single molecule studies aim to provide insight into how a population of molecules produce the effects that they do. A researcher in 2007 boldly projected that within the next 30 years research would solely be focused on single molecules[9]. Nine years later it is still too early to confirm whether the statement will hold true or not but from all areas of engineering, and science the trend continues to focus more and more on the fundamental workings of systems.

1.3. Overview of Single Molecule Studies

Biomolecules are primarily studied using two main branches of techniques chosen based on their ability to isolate and measure a single molecule without background interference. These are fluorescence spectroscopy and a variety of physical chemistry approaches measuring stretching and twisting forces. The use of fluorescence remains the

most dominant branch via natural fluorescence exploits or through the use of covalent fluorescent probes specific to the area of interest. Common exploits include fluorescent biomolecules but more often include the use of mildly or non-fluorescent substrates. These substrates are synthesized to take advantage of the specific selectivity of a particular enzyme allowing for the natural catalysis of the enzyme to create a highly fluorescent product[10]. The use of fluorescence spectrometry is the focus of the work being presented here.

The force based techniques include atomic force microscopy, optical tweezers and magnetic tweezers to analyse single molecules. Some examples include the study of molecular motors[11], DNA mechanisms[12], polysaccharide elasticity[13] and ATP generation by applied mechanical force to F1-ATPase[14]. This is meant to provide insight into the other branches of single molecule studies although force based techniques will not be discussed further in the presented research.

2. Theory and Literature Review

2.1. Fluorescence Spectroscopy

Biomolecules that exhibit highly fluorescent characteristics do so because of extensively conjugated π-electronic systems[15]. Typically this is found in molecules containing regions of polycyclic aromatic hydrocarbons which provides a basis for choosing a molecular probe for a particular study[16]. In solution fluorescence begins with the absorption of a photon with enough energy to promote an electron from the ground state (S_0) to excited singlet state (S_1) with the resulting transition being proportional to the absorbed energy[17]. A schematic is shown in Figure 1. In a particular molecule there exist many S_0 and S_1 states available for transition. As long as an energy gap is achieved between the two states the photon can be absorbed and fluorescence is possible.

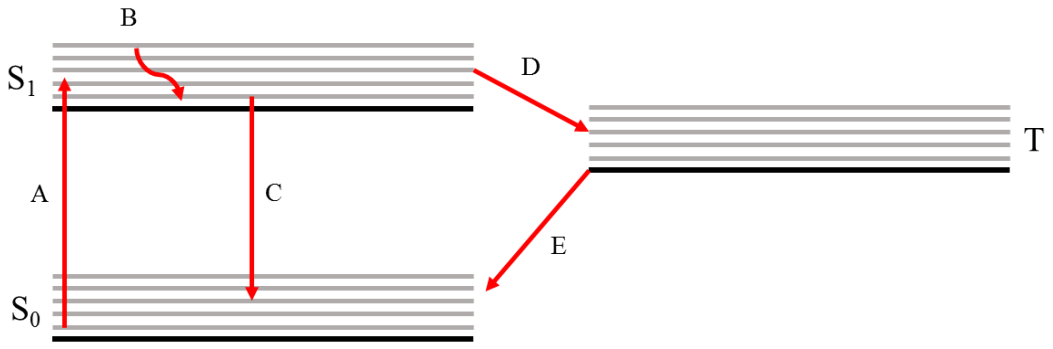

Figure 4: Electronic transition schematic for a fluorescent dye. S_0, S1 and T are the ground, first excited and triplet states respectively. The various horizontal lines (grey) represent vibrational and rotational levels within each state. A) Excitation B) Internal relaxation C) Emission D) Inter-system crossing E) Relaxation.

The S_0 to S_1 transition occurs for each photon absorbed of adequate energy followed by a very rapid ($<10^{-14}$ s) non-radiative relaxation (B) to the lowest S_1 state. At the lowest S_1 state the molecule will release the energy, returning to the ground state as either radiation (fluorescence) or non-radiative (heat, vibration) over a nanosecond time scale. Emission generally takes place from the lowest vibrational state of S_1 resulting in the return to any

of the S_0 states available. This creates a broadband emission spectrum for a given molecule reflective of its absorption spectra, shifted to higher wavelengths. Much of the emission spectra can be filtered out if it is not desired. Once emission is complete the molecule is ready to absorb another photon and repeat the cycle. Not every absorbed photon results in fluorescence emission. The ratio of emitted to absorbed photons is known as the quantum yield, which has a maximum value of 1. Another characteristic is known as the Stokes shift where there is energy lost by non-radiative processes between absorption and emission resulting in the emitted wavelength to be different from the absorbed[15]. A strong excitation source may produce saturation conditions for a molecule and when paired with a high quantum yield the resulting emission can be 10^6 photons or greater[16]. Fluorophore emission may be hindered by one or both of these two common issues; quenching occurs when another molecule present in solution is able to absorb the wavelength being emitted or a neighbouring molecule is able to absorb the energy through a non-radiative process. This factor is inversely proportional with the distance in solution that the emitted photon must travel before reaching the detector and materials present in the analyte solution. In theory the excitation/emission cycle is non-destructive but in actuality it is limited by a probability factor of photobleaching. This other hindering factor states that for each adsorption/emission cycle that the molecule achieves there is a small chance that the photochemical properties are destroyed in the process. Much like a catalyst will eventually break down from repeated reactions. Another possibility from the S_1 state is inter-system crossing (D) where the energy is passed from S_1 to the triplet state (T). Emission will then occur from this state (E) to the ground state at a millisecond or greater time scale. This effect is known as phosphorescence. Although

not utilized in the work presented here phosphorescent molecules exhibit very unique properties within the topic of fluorescence.

2.2. Detecting Single Molecules

There are two major difficulties when it comes to detecting single molecules: ensuring that a single molecule is observed and the signal to noise ratio (S/N). Efforts to maintain that single molecules are observed one at a time are made in the initial concentration of the solution in that it is sufficiently dilute. The remaining characteristics are taken into consideration after the experiment is complete. Maximizing the signal to noise ratio employs far more detailed processes focused on either maximizing signal or reducing the background noise. Typically lasers are used as the excitation source as they can be physically and optically controlled for a highly focused beam with minimal scatter. Any scatter present can be dealt with using optics, filters and detection placement. The emitted light passes through high numerical aperture (N.A.) objectives at 90° to the excitation source in order to collect signal while reducing scatter and focus it on a highly sensitive detector. The fluorophore itself will be limited on its maximum signal output and quantum yield and this maximum is often easily achieved with the high energy output of the laser excitation source.

2.2.1. Identifying Single Molecules

The book "Comprehensive Sampling and Sample Preparation" Chapter 3.16 by Craig & Nichols outlines 3 criteria that must be met in order to confirm that single molecules are being observed[18]. Firstly, the number of observed detections must correspond to the predicted number of molecules based on sample concentration and a given sample volume assuming a correct dilution. The detection events must also rise and

fall proportionally with the concentration of enzyme. Lastly the detections follow random sampling statistics for a given experiment[19]. When sampling, the data must represent a Poisson distribution, meaning that when sampling for single molecules, the observed peaks must follow a minimum of sampling noise. The minimum value begins at the square root of the mean.

A Poisson distribution also allows for the observation between concentration, volume and number of expected molecules in a particular volume. A low concentration of enzyme combined with a low sample volume can indicate the presence of between 0-2 molecules per volume to be observed on average. This represents a mean of 1 molecule per volume with the most frequent observations being 1 or a single standard deviation away (± square root of 1). Values beyond 2 molecules are rare but still exist as a probability. This concept will be discussed later as it pertains to the particular assay and the injection of single molecules.

2.2.2. Excitation Intensity

Fluorescence of a molecule obeys a general principle to a degree. That is the more photons in, the more photons out. The rate of photon emission (signal intensity) will depend on the on the rate at which the excitation photons are absorbed. This does not hold true when the molecule is already saturated with an excitation wavelength but as we approach excitation saturation, it will be observed. It is also important that the excitation intensity is not so great as to cause photobleaching in the sample being observed. Lasers are utilized for these studies because the high photon flux within a narrow wavelength range along with a stable and consistent output make them an excellent excitation source. The properties of a given laser can be tailored such that the intensity and duration

minimize the effects of photobleaching if signal collection is required over an extended time frame. Single biomolecules have been detected using alternative light sources however the setups are limited to where a large amount of fluorescent product must accumulate from an enzyme molecule in sub-nL volume containers before analysis is possible[20,21].

2.2.3. Background Signal Minimization

With respect to fluorescence the background signal primarily arises from light scattering but also from impurities in the solvents, other fluorophores and the solvent itself. The solvent produces Raman and Rayleigh scattering from elastic and inelastic laser scatter. In each case there are procedures taken to minimize background noise. All solutions are made using ultra-pure water and filtered through sub-micron filters to reduce the amount of impurities. Solvent responsible light scattering (Raman) can be reduced through a reduction in the volume of solvent that the excitation and emission photons must travel through[22]. Primarily it is avoided through optics which provide filtering for those specific wavelengths. In order to use a very small detection volume the laser must be precisely focused on a discrete spot. This is achieved through the manipulation of the optical geometry using prisms, mirrors and microscope objective lenses. CE relies heavily on the above two procedures when it comes to minimizing background noise. Another approach is to isolate single molecules in stationary suspensions in ultra-small volume containers. This can be achieved with oil-dispersion droplets[23,24], liposomes[25], fL microarrays[26] or by a modified fibre optic cable etched with wells[27]. Between photon emission and detection background noise can also be minimized using pinholes and slits. These spatial filters are physical barriers used to selectively

block photons from reaching the detector that are not in focus[28]. An optical filter is also placed between the detector and emission source to block out photons not in the wavelength range set by the filter while allowing the emission light to pass through unimpeded.

When working with very small volumes and even smaller detection probe ranges, the diffusion of analyte outside the probe range is often a problem faced. This can be solved by physically restricting the movement of the molecule or by using a volume small enough such that the probe covers the entire range. One common method of molecule immobilization is to fix the molecule to a microscope coverslip and by either moving the molecule to the laser or the laser to the molecule for analysis. A typical molecular tethering strategy relies on the high affinity of streptavidin for biotin[5] or by hexahistidine tags selective for Ni^{+}-NTA[29]. These tags will bind to both the glass and enzyme molecule fixing it in place. Non-specific interactions between the glass and enzyme are prevented through the initial treatment with BSA or PEG which will cover the glass leaving only the linker accessible to the enzyme. The flexible linker PEG is often used to increase the glass to molecule distance to promote translational rotation freedom allowing for more fluid-like range of motions[5]. Another method of molecular confinement is a dilute agarose gel (1%) with pores that will hold the molecule in place but allow substrate and product to diffuse freely[4]. The concern with tethering or confinement methods is whether or not the enzyme retains identical properties as if it was free in solution. In the case of confinement this case is rarely of concern although still tested for unless previously shown. Tethering molecules has the potential to introduce unpredictable physical barriers altering the activity of the enzyme[19]. If an affinity tag

binds to enzyme in more than one location it is possible that the active site will be oriented in different positions with respect to the binding surface. For example if the active site is oriented away from the binding surface activity should remain unaltered. If the active site is oriented facing the binding surface the substrate may lose accessibility altering the activity in an unpredictable manner. Methods that use molecules free in solution are sought after as they pertain more directly to cellular conditions. This will be discussed in more detail at a later point.

2.2.4. Optical Detectors

When performing a single molecule assay the use of highly sensitive detectors is absolutely necessary. The signal resulting from a single enzyme product formation will always be small even with a high activity enzyme. In order to maximize the collected signal high N.A. objective lens are oriented such that the emitted photons are collected and focused towards the detector. Two major classes of detectors are utilized: point detectors and wide-field detectors. Point detectors such as photomultiplier tubes (PMT's) and avalanche photodiodes (APD's) are extremely sensitive with μs temporal resolution but are limited in that they are only to collect data from a single source at a time. They are unable to differentiate spatially distinct photons so one molecule must be focused for data to be collected. Wide-field detectors such as charge coupled devices (CCD's) have lower resolution on an ms time scale but are able to register photon collection spatially. Either many spatially distinct signals can be measured simultaneously or the migration of a fluorescent signal may be monitored[30].

2.2.5. Post-Column LIF Detection

Post column LIF detection involves the excitation of fluorescent molecules as they exit a capillary. Figure 2 illustrates the post-column detection method. As fluorescent molecules exit the capillary they are excited by a focused laser beam with the resulting fluorescence collected before the molecules are washed away by a continuous sheath flow of appropriate buffer. The high sensitivity of this method has allowed for the detection of subattomolar concentrations of fluorescein isothiocyanate amino acid derivatives[28] and even yoctomoles of rhodamine 6G[31] to name two examples.

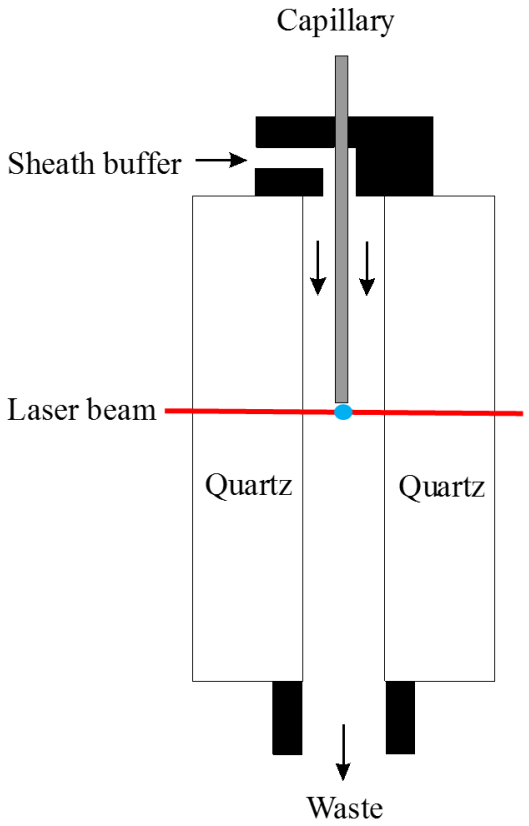

Figure 5: Illustration of a sheath flow cuvette for laser-induced detection. The blue circle represents resulting fluorescence emission as molecules exit the capillary.

The sheath flow provides a continuously flowing environment around the detection end of the capillary which prevents material from collecting within the path of the laser beam. A molecule will exit the capillary, become excited, provide fluorescent emissions and

then be washed away, providing detectable signal for only a short period of time. This also greatly reduces the possibility of photobleaching as mentioned above. It is this highly sensitive technique which is utilized in the studies presented here and will be discussed further with the entire instrument.

2.2.6. Additional Fluorescence Spectroscopy Methods

Two single molecule experimental methodologies will be discussed in this section. CE-LIF will be the focus of a later section. Both confocal and total internal reflective fluorescence (TIRF) spectroscopy are common optical geometry focused methods used when observing molecule fluorescence. Figure 3 is a schematic representation for each of the outlined techniques. In each case the molecule being analyzed is tethered to a microscope coverslip in solution between the coverslip and slide.

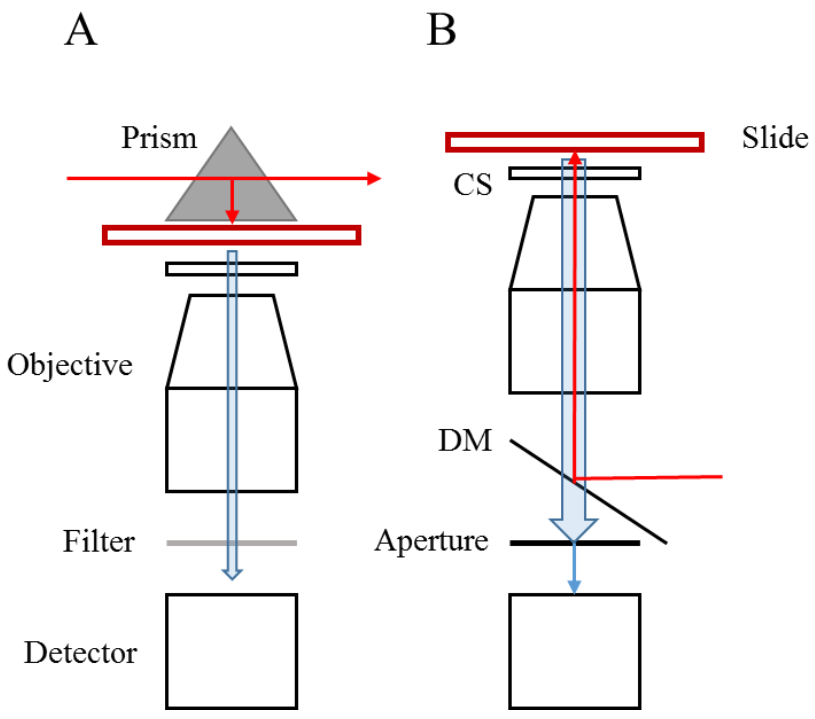

Figure 6: Schematic for TIRF (A) and confocal microscopy (B) setups with the laser beam depicted by the red arrow and fluorescence by the blue arrow. Cover slip (CS), dichroic mirror (DM).

The TIRF setup uses laser excitation by passing the beam through a prism which directs the beam towards the slide. The beam passes into the slide at an angle that exceeds the critical angle therefore is reflected back in full. However a portion of the excitation energy is able to pass about 100 nm into the solution past the slide and into the region between the slide and coverslip. Any waves not absorbed lack the energy to make it to the detector and quickly dissipate. The energy that does make it into solution excites the fluorescent molecules and the resulting emission is collected through a high N.A. objective and passed through a filter to the detector. Confocal microscopy uses a similar technique expect this time the excitation beam is reflected off a dichroic mirror, focused and directed to the sample by a high N.A. objective where excitation and emission occur. The resulting emission then travels back through the objective and dichroic mirror where it is collected by the detector. The mirror used must be such that it is opaque to the laser wavelength and transparent to the emission wavelength taking advantage of the Stokes shift for filtration of laser scatter. Although the filter is not 100% efficient it greatly reduces unwanted light from reaching the detector. A pinhole filter before the detector provides a final light filtration source selective for the emitted fluorescent wavelength from the point of excitation and discriminates against peripheral light.

2.3. Single Molecule Studies

2.3.1. Historical Background

The first fluorescence microscopy based single molecule experiment was performed using β-galactosidase from *E. coli*. Dilute enzyme and substrate were dispersed in fine droplets suspended in oil where product formation was measured over a period of hours[20]. Only if there was one or more enzyme molecule(s) present in a given

droplet would a detectable fluorescent signal be achieved. It was not then until 15 years later when Hirschfeld used fluorescein labeling to detect γ-globulin[32]. Each molecule was labeled with 80-100 fluorescein molecules. At the time it was not possible to detect a single fluorescent molecule so strategies used relied on the detection of many fluorescent molecules associated to a single enzyme. In 1984 single fluorophore detection was predicted[33] but it was not until the early 90's that the feat was met. Near-field scanning microscopy (NOSM) imaged carbocyanine dye molecules embedded in a polymethylmethacrylate-coated cover slip[34]. This technique was also able to provide insight into the lifetimes and dynamic properties of single sulforhodamine 101[35] and rhodamine 6G[36] molecules. Single molecule Förster resonance energy transfer (smFRET) was introduced[37] but was met with hesitation about the validity of the technique[38]. It involves the use of two fluorescent probes bound to different (known) locations on a molecule. The distance and position of the probes relative to each other can be monitored by exciting one probe which emits to the other before fluorescent emission is achieved and detected. Although originally smFRET experiments were scrutinized, today they are widely accepted for their ability to provide structural information of biomolecules in real time based on probe positioning.[39] Originally one of the major downfalls of the technique was the use of an aluminum-coated optical fibre excitation source. When the excitation source came within 10 nm of the dye molecule non-specific interactions were induced between the probe and dye molecule[40]. In 2004 Kapkiai reported a hybrid probing technique used for living cells using NOSM and atomic force microscopy (AFM).[41] Near-field techniques have since moved to scanning larger systems instead of single molecules as they have a tendency to damage the smaller molecules. Far-field techniques

now dominate the single molecule experiments. The first far-field single fluorophore detection used the confocal methodology described previously at room temperature. The study observed the effects of the local environment on fluorescent lifetime and emission maxima of single rhodamine 6G molecules[17]. Shortly after single fluorophore detection became well known it was modified to use a single fluorophore label to monitor biological molecules[42]. Although these techniques are of great value to single molecule research they are not applicable to the studies presented within this thesis and will not be discussed further.

2.3.2. Studies of Single Biological Macromolecules

Single molecule FRET uses fluorescent labels which can be applied to detect motions of a single protein molecule. These motions have included the conformational changes associated with catalysis[43] and protein folding[44]. An experiment conducted on the motions of rhodamine labeled myosin V on immobilized actin via TIRF demonstrated how the protein moved with a "hand over hand" motion instead of an inchworm mechanism as the protein traveled along a filament[6]. It was also found that myosin VI operating in the reverse direction acted in a similar motion[45]. TIRF has also been used to track motions of labeled components in live cells. Both the step size and rate of movement was measured for kinesin and dynein using the observed motion of GFP labelled peroxisomes in a living cell[46]. Through fluorescently labeling an actin filament with tetramethyrhodamine, the rotational motion of the F_1-ATPase motor component of F_0F_1-ATPase may be observed for the coupled transmembrane proton flow for ATP synthesis/hydrolysis[29]. The linkage was between the actin filament and the central stalk γ-subunit of the streptavidin-biotin linkage where the filament rotated counter-clockwise

(referenced from the membrane perspective) in the presence of 2 mM ATP. For every ATP hydrolysis performed the group was found to rotate 120° comprised of two smaller steps when the ATP became bound and then when the hydrolysis occurred[47].

When single molecule FRET is utilized two fluorophores are bound by site specific interactions to a given molecule. It is crucial that the binding take place in two known regions and not through non-specific interactions at other locations. The two fluorophores allow for non-radiative transfer of energy when one is excited which can be related to a nm scale ruler reporting continuous, real time distance data[38]. This technique has also been used to identify conformational changes along the reaction pathway for a hairpin ribozyme[48] and provided information on the conformational dynamics for the T4 lysozyme[43]. A study on *E coli* sourced adenylate kinase identified an open/closed conformational change where a lid-like structure was able to move over and off of the active site even without the presence of substrate[49]. When substrate was introduced the conformational equilibrium shifted to the closed state leading to the determination that the shift from closed to open to release the product was the rate limiting step.

2.3.3. Single Molecule Enzymology

2.3.3.1. The First Experiment

Single molecule enzymology represents and early branch of the single molecule research field. It is an ongoing topic of discussion throughout the work presented here as it has direct relevance in the justification of this thesis. As previously mentioned, Rotman was the first to publish single molecule enzymology work when he observed the activity of *E. coli* β-galactosidase[20]. This was achieved by using a dilute enzyme and fluorogenic substrate and dispersing them in a mist of fine droplets (~15 μm) trapped in silicon oil on

a microscope slide. After an incubation period of several hours, the accumulated fluorescent product was observed by fluorescence microscopy. The individual droplets were identified as having one or more enzymes based on presence of fluorescence within the droplet. Using Poisson statistics based on a ratio of fluorescent droplets to non-fluorescent ones Rotman was able to calculate the original concentration of the enzyme. It was also shown that the molecular weight of the enzyme could be calculated and proved closer to the actual weight than that of contemporary estimates. Rotman also went on using this approach to investigate if the residual activity and high K_ms measured in mutant enzymology studies were caused by the presence of some wild-type molecules retaining activity. He proved that even the mutants had very low activity. After Rotman, the single molecule enzymology field went dormant for about 30 years before regaining popularity in research.

2.3.3.2. Static Heterogeneity

It was not until 1995 that Xue and Yeung published their findings directly relating to the field of single molecule enzymology. Lactate dehydrogenase (LDH) was injected then incubated in a capillary for one hour in the presence of lactate and NAD^+ producing NADH. Taking advantage of the NADH fluorescence, the contents of the capillary were then passed through a laser-induced fluorescence detection system where the amount of NADH and the incubation time gave rise to the activity of individual molecules[2]. Capillary components moved electrokinetically to the detection end where they were excited by a focused 340 nm laser as they exited the capillary. A total of 79 molecules were reported all having different activities in a four-fold range of each other. To prove that the observed differences were valid, double incubations on single molecules were

conducted and were found to be reproducible for the individual molecule. An analogous experiment was conducted by the same group to investigate if the observed results were reproducible through a different technique. A single molecule assay for LDH was constructed using fL microarray wells produced by photolithography of fused silica. A similar activity range was observed[50]. A single metal ion catalyst was used in the place of a protein to demonstrate that the protein was in fact responsible for the different activities observed. The rate of product formed remained consistent for each of the observed metal ions indicating that the observed heterogeneity observed was due to the enzyme and not the experimental design. The variation in catalytic rates between single molecules of a population has come to be termed *static heterogeneity*.

The Dovichi group replicated the previous study and observed a catalytic distinction between single enzymes molecules shortly after, using CE-LIF[3]. The same group introduced a post-column sheath flow detection system (Figure 2) in order to measure the activity of bovine alkaline phosphatase. The product being measured was the synthetic fluorescent AttoFluor™. Due the greatly increased detection sensitivity, the assays no longer required a long incubation period for product to form. The assay time could be reduced down to a minute if desired. This time, a 10 fold range of activities were observed and shown to be independent of the assay duration. Multiple incubations were performed on the same molecule to illustrate this finding. A study of the catalytic activation energy was performed by measuring single enzymes activities at different temperatures. A heterogeneous relationship was found between molecules with no observed correlation between the activation energy and activity. This led to the interpretation that the ligand binding the enzyme was the dominant factor in terms of

catalytic rate. Ten years later Hsin and Yeung used liposomes to fuse single bovine alkaline phosphatase inside with a fluorescein-diphosphate substrate[25]. A 20-fold difference in static heterogeneity was reported providing support that the different techniques were in fact measuring the static heterogeneity of single molecules and that the observed phenomenon was not an artefact of the techniques themselves.

E. coli sourced β-galactosidase has been the focus of a great deal of single molecule research partially due to its inducible enzyme production. This is achieved through the extensively studied *lacZ* operon. When the bacterium is grown in a lactose free medium, β-galactosidase expression is less than 10 molecules in the cell. The addition of the non-hydrolysable inducer isopropyl-thio-β-D-galactopyranoside increases its expression more than 1000 fold, following a 3-5 min incubation period[51,52]. This allows *E. coli* to be grown first then induced to produce β-galactosidase for a period of time which then can be terminated with the introduction of glucose. The result is a population of β-galactosidase which is all roughly identical in age. There will be some residual molecules already present but there are very few when compared to the newly produced. The enzymes high catalytic rate and the availability of highly fluorescent commercially produced substrates allow for a diverse collection of assays. It may be purchased or produced/extracted from *E. coli* in the laboratory. Both methods were utilized in this body of work to obtain β-galactosidase. The enzyme-substrate interactions and special characteristics will be discussed in a later section as they are directly related to the research being presented. It was the Dovichi group who began applying contemporary single molecule techniques through monitoring the hydrolysis of the RES-gal fluorogenic substrate with CE-LIF. This was possible due to the relatively low RES-

gal fluorescence but very high RES fluorescence when hydrolyzed. A study demonstrated that prokaryotic enzymes also exhibit static heterogeneity when activities were measured by a single molecule approach[53]. Individual β-galactosidase molecules obtained from enzyme crystals were also assayed for activity using the same substrate with observed activities being reproducible within 15% of each other[54]. The catalytic heterogeneity was shown to be consistent throughout crystallized and non-crystallized enzymes. It has been shown that the enzyme relies on magnesium for it catalytic activity but this requirement was found to be heterogeneous at the single molecule level[55]. The catalytic rate between individual molecules has been shown to vary, however, the source of the enzyme also plays a role on the average activity observed[56]. This means the source organism, molecule age and production temperature can all be factors in the average activity outcome of their enzyme population. Another study, this time performed by Rissin *et al.*, monitored individual *E. coli* sourced β-galactosidase molecules using a fL array of well etched in modified optic cables[21]. Static heterogeneity was found in a 15 fold range at a variety of substrate concentrations with data collected every 15 seconds in the form of total product fluorescence. Activities were found to remain at a constant rate for the 3 minute trial. The observed differences in activities at the various substrate concentrations provided a distribution that led them to conclude that the activity differences where due to different K_{cat} values for each molecule. The substrate fluorescein di-D-galactopyranoside (FDG) has been shown to be effective in β-galactosidase assays however the study to illustrate this was that a microarray of fL containers constructed from a silicone elastomer was effective at single molecule detection[26]. Also individual β-galactosidase molecules have been detected using tryptophan fluorescence with

ultraviolet confocal microscopy[57]. Through the use of time-resolved single photon counting was able to identify single molecules without the use of substrate product detection.

Static heterogeneity has been found to be common amongst many single molecule studies. There are far too many to list all of the enzymes that have been studied, however specific examples will be shown. For example both alkaline phosphatase from *E. coli*[58] and *Thermus thermophilus*[59] have been shown to have a 12 fold activity range with single molecules detected by CE-LIF. A haloperoxidase from *Curvularia verruculosa* was monitored by confocal microscopy while in a dilute agarose gel with a 6 fold range of activities. *Brevibacterium* sp. sourced cholesterol oxidase has been studied taking advantage of the FAD cofactor and its natural fluorescence in the oxidized form. Single enzyme molecules were confined in agarose gel, which allowed solution components to diffuse freely to and from the enzyme while the enzyme remained stationary. Turnover rates were measured and were found to be different for each individual molecule with their ensemble average approaching that of the bulk study measurement[4]. Non-fluorescence based studies have also shown static heterogeneity in molecules being analysed. A study on λ-exonuclease showed a 4 fold catalytic range for the digestion of phage DNA[60]. It would be advantageous to assume that all enzyme molecules exhibit some level of static heterogeneity, although confirmation of such a statement would require an almost endless undertaking. Due to the wealth of static heterogeneity data, this statement is regarded as true throughout the scientific community. It is also thought that enzymatic heterogeneity may be an inherent evolutionary process allowing for biological molecules to adapt over time[61]. Through these “errors” enzymes are able to probe for

improvements based on sequence and conformation. Through the work to be presented on β-galactosidase, it will be assumed that the observed properties would be applicable to other enzymes.

2.3.3.3. Dynamic Heterogeneity

Static heterogeneity encompasses the variations in enzyme molecules at the time of formation giving rise to the observable differences such as catalytic rate. However, an enzyme is not a rigid molecule and may be subjected to alterations throughout its life time that include conformational changes. These fluctuations in conformation have been shown to alter an enzyme's turnover rate by increasing or decreasing the rate on a time scale of milliseconds to hundreds of seconds in length.[62] Dynamic heterogeneity describes the range of thermally induced fluctuations in conformation available to a particular enzyme once it has been folded. It has been shown that a single enzyme does not have the capabilities to achieve the entire range of observed activities indicating that once an enzyme has been folded the dynamic heterogeneity is subjected to limitations set by the static heterogeneity.[63] The dynamic fluctuations happen very rapidly due to low activation energy barriers between them, however, stable, long lived conformations are able to be adopted if the molecule shifts to a low energy state where the activation is increased. An early single molecule dynamics assay strategy was introduced by the Xie group (1998) using cholesterol oxidase from *Brevibacterium sp*. Instead of using a traditional assay where product was collected over a period of time and then analyzed, they monitored catalytic turnover numbers for a single enzyme[4]. This was made possible by exploiting fluorescent properties of oxidized flavin adenine dinucleotide (FAD) as a co-factor to the catalytic reaction. This provided an "on/off" fluorescent switch indirectly

for each turnover for a single enzyme trapped in an agarose gel. The time between turnovers was found to be highly variable and random in nature although a certain enzyme memory was observed. It was more likely for an enzyme with a short wait time in between turnovers to continue with short times and the same for an enzyme with long times to continue with them being long. The concept of conformational "memory" will be discussed in a later section.

Using the same style of analysis, the same group observed dynamic heterogeneity in *E. coli* β-galactosidase in 2006[5]. The enzyme in this case was tethered to a microscope slide through a biotinylated flexible cysteine-reactive PEG linker on a streptavidin coated bead biotinylated to the microscope slide with RES-gal substrate conversion to the fluorescent RES molecule being measured with confocal microscopy. In order to describe the range of turnover timing observed, the group stated that there must be more than ten unique conformations for the particular enzyme. The tethered molecule was found to follow Michaelis-Menten kinetics, however it was not always the case. The concept of enzymes bound or free in solution will be discussed later in this chapter.

Dynamic heterogeneity has also been observed by other researchers in cases where the individual turnovers may be measured, for example; horseradish peroxidase using the substrate dihydrorhodamine 6G which gets converted to the fluorescent product rhodamine 6G[64]. The activity was reported to have a wide range and when re-examined with TIRF the activities were reported an order of magnitude larger than the previous results with attributions to substrate properties; size, charge density and hydrophobicity[65]. Measurements on dynamic heterogeneity have also been made on hairpin ribozymes[48], *E. coli* Flavin reductase[66], and *Candida antartica* lipase B[67,68] to name a few. It would

appear that a similar claim may be made for dynamic heterogeneity as static in that it is an applicable feature across all enzymes.

As research techniques develop, measurements become more rapid with higher resolution and we are able to measure single enzyme molecular changes in real time. This allows for measurements to be taken on enzymes without the use of fluorogenic substrates. With the conformational energy barriers being low enough to allow room temperature conversions the subtle conformation changes take place very rapidly, identified as fast as femtoseconds for smaller alterations. Through kinetic isotope effects for H-transfers and 2D IR spectroscopy for transition/ground state complexes protein dynamics have be characterized.[69]

2.3.3.4. Relationship between Static and Dynamic Heterogeneity

The relationship between static and dynamic heterogeneity is a difficult link to make since it requires measurements both on the enzyme itself in a fixed state and a fluid state. Lu *et al.* measured a five-fold static heterogeneity in cholesterol oxidase between the enzyme substrate complex and the enzyme plus product[4]. However, it was not possible to distinguish if observed conformational differences were due to enzyme heterogeneity or substrate binding since the reactions proceeded faster than the measurements could take place. It was suggested by Edman *et al.* that both static and dynamic heterogeneity were in fact the same principle from two different viewpoints and that one does not exist without the other[64]. This statement was made based on the principle of ergodicity, in that many single measurements will converge at the same conclusion point as a single bulk measurement[22]. Through this statement, the validity of a single enzyme measurements can be confirmed as contributing to the average and not

contradicting it. It was later stated that the time frame for the convergence of activities from the point of static heterogeneity was between 10^3 and 10^4 times greater than the average single catalytic cycle rate[70]. Even on that basis the time scale when compared to a cell still signifies the importance of static heterogeneity[25].

Even with the difficulties presented in the past, static and dynamic heterogeneity continue to be a focus of research around the world. Static heterogeneity in particular requires closer observations. The *E. coli* sourced β-galactosidase has continued to be a front runner in heterogeneity research with the most extensive profiles on both static and dynamic properties. Min *et al.*[62] reproduced a set of experiments originally performed by English *et al.*[5] observing β-galactosidase turnover rates using RES-gal at approximately 200 s^{-1}. Based on the above statement that the activity should converge at 10^4 times the turnover rate, it can be calculated that the convergence should take place for an assay lasting 50 seconds. The 50 seconds represent the top of the heterogeneity diminishing scale. A 15 minute CE-LIF assay using the same enzyme and substrate found that static heterogeneity remained at values greater than 10-fold[53–55]. This signifies that the magnitude of static heterogeneity affecting enzymes is more than just a short lived single molecule observation.

2.3.3.5. Sources of Static Heterogeneity

Static heterogeneity can be envisioned to be the result of a variety of factors. These can include errors in transcription/translation of the primary sequence or differences in the post translational modifications. The concept of static heterogeneity has continued to grow in acceptance throughout the years as it was originally met with a great deal of speculation. For example Xue and Yeung attributed catalytically distinct LDH

molecules to distinct conformations achieved after protein translation[2]. Craig *et al.* focused on the post-translational glycosylation of bovine alkaline phosphatase as the source of its static heterogeneity[3]. It was reported that enzymes stored with the absence of protease inhibitors exhibited greater static heterogeneity[58]. This finding can be interpreted such that even functioning enzymes will be hydrolyzed by proteases if their sequence varies too much. Without the proteases all enzymes will remain for detection provided that they remain active. It is also important to note that the observed static heterogeneity only accounts for the enzyme population that retains a measurable activity. If a particular enzyme is created with too great of an error it will not be observed in terms of measurable activity. Therefore, the structural differences associated with static heterogeneity are likely to be subtle. For example heterogeneity between re-dissolved crystallized β-galactosidase and the original source were identical[54]. However, the heterogeneity is also attributed to the active site directly or indirectly due to many of the measurements being based on activity. Small changes in the orientation of the active site have been shown to have a great impact on activity when they are associated with catalytically important residues or cofactors[71]. This would also suggest that much of the static heterogeneity will go unnoticed when the focus of the assay is activity. As we move to higher resolution, fluid structural observation techniques it will become possible to observe the rest of the enzyme in greater detail.

2.3.3.6. Free in Solution vs. Bound Assays

It has been long debated whether tethering an enzyme to solid support surface allows for an accurate representation of enzymatic properties. It has been shown that tethering alkaline phosphatase by covalent interactions to the inner wall of a fused silica

capillary produced a K_m which was greater than the bulk ensemble free in solution[19]. The concept of tethering enzyme molecules to solid support surfaces will be discussed in more detail at a later point. The purpose of single molecule studies are to observe subtle changes and differences in a representative sample of molecules. Tethering enzymes is itself a source of subtle alterations to the structure which may cascade the change through the enzyme resulting in a significant alteration taking place. For example lysine residues are used to create interactions between an enzyme and a surface and each bound lysine alters the structure slightly in an unpredictable way. An enzyme bound to glass also results in a great deal of negative charges being in close proximity to the outermost residues. It is uncertain what effects this may have as it is residue dependant. There is also the issue of the binding orientation of the enzyme. When dealing with lysine tethering for example a given enzyme will have many accessible residues for binding. This means that the enzyme could end up being bound face up or face down with respect to the active site. An enzyme with the active site open down towards the negatively charged glass would not be able to have the same substrate interaction as one open directly to the substrate solution. It is considerably more difficult to perform single molecule assays free in solution however when it comes to observing the subtle properties in a cell like environment it is a necessity to do so. This concept will be discussed in greater deal in Chapter 8.

2.4. Objectives and Rationale

A large amount of this chapter has been focused on static heterogeneity and catalytically distinct enzymes within a single population. It has been shown that heterogeneity types, both static and dynamic are also characteristic of non-enzyme

proteins suggesting that these principles span across all proteins[72]. Since the first published study of heterogeneity amongst proteins, the concept has continued to grow in both reputation and wealth of knowledge. However, there continues to be much yet to study. As higher resolution techniques become available, the field of single molecule research continues to expand. For many years 3 main concepts have been the overarching goals of single molecule research. The first is how enzyme structure relates to static heterogeneity. Techniques relative to protein structure continue to develop but are yet to achieve the resolution required for detecting these subtle differences. Secondly of interest is the link between static and dynamic heterogeneity. This area has seen the most development and will be a large focus of later chapters. Lastly is the significance of static and dynamic heterogeneity in a cell system. There is a debate on the relevance of this particular area due to the knowledge that bulk averages do not show heterogeneity. The roles of heterogeneity in a cell system may only be applicable if the number of enzymes is small.

The main objective of this thesis is to further the research in single molecule enzymology based on the fundamental principles faced with β-galactosidase from *E. coli*. This includes more in depth investigations into both static and dynamic heterogeneity through activity and mobility studies. Measurements of single molecule Michaelis-Menten kinetics will also be performed along with the calculations traditionally applied to bulk assays. In order to achieve this, a new CE-LIF assay was prepared and tested in the hope of providing further insight into the already abundant knowledge of β-galactosidase. Due to CE-LIF and β-galactosidase being the focus of this thesis they have been given their own chapter in the coming section in order to provide a detailed

background. Chapters 5-8 will focus on the results of the experiments in the order that they were performed followed by overall discussion, and future directions chapters.

Here is a brief outline of the four results chapters and final chapters. Chapter 5 examines activity and mobility of single β-galactosidase molecules and how temperature can induce conformational changes altering the above mentioned properties. Chapter 6 outlines the observed effects of heat shock proteins on conformation through activity and mobility of the enzyme. Chapter 7 introduces a novel assay designed to subject a single enzyme molecule to multiple different solutions while the enzyme itself remains free in solution. The goal is to use catalytic rates in the presence of different solutions to allow for the calculation of both K_m and K_I from a single enzyme molecule. Chapter 8 will focus on the further development of material presented in Chapter 7. It will outline new approaches to the concept of subjecting a single enzyme molecule to multiple different solutions in order to investigate single molecule properties. Chapter 9 consists of an overall discussion and summary, bridging the past and current research by CE-LIF on β-galactosidase and the potential implications of the findings. The final chapter (10) will outline the future directions and any outstanding experimental approaches that may be carried forward.

3. CE-LIF and β-galactosidase

3.1. CE-LIF

3.1.1. Background

Traditional electrophoresis relies on the use of solid supports of gel based systems in order to achieve separations. Band broadening, setup time and the amount of materials required are limitations of this technique[73]. In the 1970's a technique known as capillary zone electrophoresis was pioneered making use of thin glass tubes, open on both ends with narrow diameter bore through the length of capillary. At the most basic level the CE system involves the use a high voltage power supply providing an applied voltage across the length of capillary which needs only to be submerged at both ends in an electrolyte solution. The bore of the capillary acts as a single channel separation chamber for anything flowing from one end to the other. Capillaries are often far more efficient than the tradition solid gel based separations however they cannot simply replace the latter. A clear benefit to CE is the ability to perform a separation at a much higher applied potential. Typical gel based systems are run between 10 and 20 V/cm while a capillary has been shown to withstand up to 1200 V/cm totalling 30 kV[74]. The ability to apply increased voltage to the separation medium has two distinct benefits: the first being that material will travel through the capillary much faster making for run times as low as a minute. The second is an increased resolution based on resolution being proportional to the square root of the applied voltage[74]. The separation efficiency of CE is much greater than a gel based system. It is also a very low load technique in that an assay may consist of picoliters of sample where a gel would require micro to millilitres of sample. There are however a few disadvantages to CE which is why gel based systems remain popular for

specific methodologies. One issue is that a capillary only provides a single separation lane allowing for only one sample to be analyzed at a time. This may be an issue if a particular study involves a large number of samples[75]. The other disadvantage is that CE offers no preparative abilities for the sample. Unlike a gel which is able to separate the multiple samples out into distinct bands which then may be extracted. CE however, does not allow for the practical collection of separated components due to such low analyte concentrations and very small fraction volumes. Separations performed throughout this body of work were often kept a 400 V/cm with capillaries ranging between 40 and 60 cm in length. In order to provide support for the fused silica capillaries they are externally coated with a thin polymer which adds to the flexibility and durability of the capillary. The coating is often polyimide. Capillaries typically have an inner diameter ranging from 10 to 75 μm and may range in length from 30 to 100 cm. In more recent years capillaries with inner diameters of 5 or 2 μm have become increasingly popular. Limitations in the resulting current from the applied voltage reduce the ability to run them at exceedingly high voltages. The smaller the internal diameter of the capillary the more susceptible it is to being damaged by a high applied voltage, however, a capillary withstands many fold higher applied voltages than a gel support[75].

Experiments conducted by CE rely on the use of chemical and electrically inert material for the separation chamber. Glass is most common today, however polytetrafluoroethylene was used in early CE experiments where it was demonstrated that even small anions were separated.[76] A few years later dansyl derivatized amino acids were separated with high efficiency in a short time frame by Jorgenson *et al*. in the early 1980's via drawn glass tubes[77]. Highly efficient protein separation was achieved shortly

following the amino acid success. A mixture of fluorescently labeled tryptic digested peptides was separated with close to one million theoretical plates achieved indicating that complex labeled mixtures could be easily identified[78].

Various detection methods can be utilized either as on-column or post-column detection. On-column detection involves the removal of a small amount of the capillary coating in order to gain optical access to analytes as they pass by and is typically UV absorption[78,79] or fluorescence[77,80]. Post-column detection collects the appropriate data as the analytes exit the capillary. This form has been used for electrochemical[81,82] and mass spectrometric analysis[83], as well as fluorescence. Post-column LIF is the detection method of choice in the research presented here.

The utilization of post-column detection coupled with sheath flow and LIF excitation provides a highly enhanced capability for the detection of analytes provided that they are fluorescent[31]. With these components combined with the separation efficiency of CE[28] the limit of detection of an analyte as little as yoctomoles[31,84]. This is achieved by minimizing the background noise while taking advantage of analyte properties. The high emission intensity and short fluorescence lifetimes allow a low concentration of analyte to produce sufficient signal. CE-LIF in this thesis has been focused primarily on the quantification of product formed from an enzyme catalyzed reaction, however, various other protein based studies have been and are currently being performed including: DNA sequencing[85], organelle heterogeneity[86], individual cell enzyme activity assays[87], and also the heterogeneity of cancer cell protein expression[88].

When a single enzyme molecule enters the capillary in the presence of substrate it begins to form product. If the enzyme and substrate were already in the presence of one

another prior to injection (in sample vial) the product formed will result in a rising background signal however a molecule in the capillary will produce product sufficient for a detectable signal. While an enzyme is traversing the capillary or if it is left stationary to incubate, product is continuously formed around the enzyme. As long as the enzyme and product have different mobilities they will migrate at different rates in the capillary and constantly separate from one another while voltage is applied. The enzyme may lead or trail behind the product being formed depending on the molecules and the buffer conditions. This creates a characteristic box shaped peak that will be described in greater detail at a later point. The benefit to such a narrow bore of the capillary is that there is minimal product zone distortion. In any given solution diffusion will take place over time in all directions. Two conditions will factor into the product zone distortion being available volume for diffusion and time. As the internal diameter of the capillary is so small product may only diffuse horizontally leaving only a small volume to diffuse into on either side of the product zone. Typically run times are in the range of minutes but even when exceeding an hour with incubations, diffusion does not present significant concern. This means that resolved product zones will remain well resolved as they traverse the capillary and can be attributed to single enzyme molecules with greater ease.

3.1.2. Mobility of a Charged Particle in an Applied Field

The fundamentals behind CE separations rely on an applied potential between two electrodes producing a potential distribution (E) which is the applied voltage (V) divided by the distance between the two ends of the capillary. When calculated, the resulting value is a V/cm of capillary length. When a charged particle is introduced into the capillary it will accelerate with a force equal to the product of E and its net charge (Z_a).

The acceleration will increase until the opposing frictional force (*f*) equals the driving force and a steady state velocity (*v*) is now maintained following:

$$v = \frac{EZ_a}{f} \tag{3.1}$$

With the frictional coefficient based on the size and shape of the charged particle as described by the Stokes expression:

$$f = 6r\pi\eta \tag{3.2}$$

Where *r* is the radius of the charged particle and η is the viscosity of the separation medium[89]. The given radius of a protein will be an assumption that the molecule is a sphere. Even though this is rarely the case it avoids complex individual expressions for each different molecule. Therefore we are able to express the migration of a charged particle as a ratio of velocity to electric field. The expression for electrophoretic mobility (μ) commonly follows:

$$\mu = \frac{Z_a}{6r\pi\eta} \tag{3.3}$$

Along with the assumption indicated above this expression is limited in the fact that it does not account for solvent ion interaction with the charged particle as well as shape irregularities[89].

3.1.3. Separation Efficiency

With respect to chromatography the separation efficiency for any given analytes is described as a theoretical plate number. This number represents the amount of relative theoretical equilibrium zones in a given length of separation medium. The higher the number of plates the greater the separation efficiency. However, if diffusion is the source

of peak broadening for an analyte, an expression can be written proportional to the applied potential and independent of capillary length or separation time. The expression for the number of theoretical plates (*N*) is as follows:

$$N = \frac{\mu V}{2D} \tag{3.4}$$

Where *D* is the diffusion constant for a particular analyte and the other terms are as they were described before[77]. For given separation conditions the number of theoretical plates can be calculated using time to the detector (*t*) and full peak at half-maximum (*w*):

$$N = 5.54\left[\frac{t}{w}\right]^2 \tag{3.5}$$

By increasing voltage it can be shown that the number of theoretical plates will increase regardless of using equation 3.4 or 3.5. Either by increasing the voltage directly or the increased voltage resulting in a faster time to the detector. This, however, results in a current-induced effect known as Joule heating. Joule heating is brought on by the heat generated as a current is passed through an electrolyte solution and is common to electrophoretic separations. This effect can result in the destruction of the separation medium but can be minimized through gel supports or by heat dispersion. CE takes advantage of its volume to surface area ratio for heat dispersion. Capillaries used in CE typically have inner diameters between 10 and 50 μm with outer diameters between 150 to 360 μm. The capillaries used can be as small as 2 μm inner diameter which means that there is a very high surface area to volume ratio. This property allows for very effective heat dispersion allowing for higher applied voltages[78]. As stated previously this will allow for a higher number of theoretical plates to be achieved. The capillary in CE does

experience a small radial heat gradient meaning that the center of the capillary will be a different temperature that the outer section. The difference in heat has the potential to affect electrophoretic mobility through viscosity but due to the extremely narrow bore of the capillary and uniform analyte dispersal the effects are not a concern[78].

3.1.4. Electroosmotic Flow

Electroosmotic flow (EOF) is the main driving force within the capillary as a result of the applied potential. This effect is caused by the silanol groups (SiOH) present on the surface of the capillary glass in contact with the internal solution. When the pH of the solution is greater than 2 the silanol groups deprotonate resulting in a dense layer of negative charges between the capillary wall and the buffer shown on Figure 4[90]. In order to balance the negative charges a positively charged layer accumulates as counter ions resulting in a double layer. The double layer is made up of a negative static layer as the capillary wall and a secondary layer whose thickness is dependent on the ionic strength of the solution. The secondary layer is composed of stationary counter ions as well as a diffuse layer. For example at an ionic strength of 10 mM the double layer will be approximately 3 nm thick[91]. When a voltage potential is applied across the capillary the positive counter ions in the diffuse layer will migrate with their associated solvation shells towards the negative pole. The result is the bulk solvent being carried from the positive pole to the negative pole which is EOF.

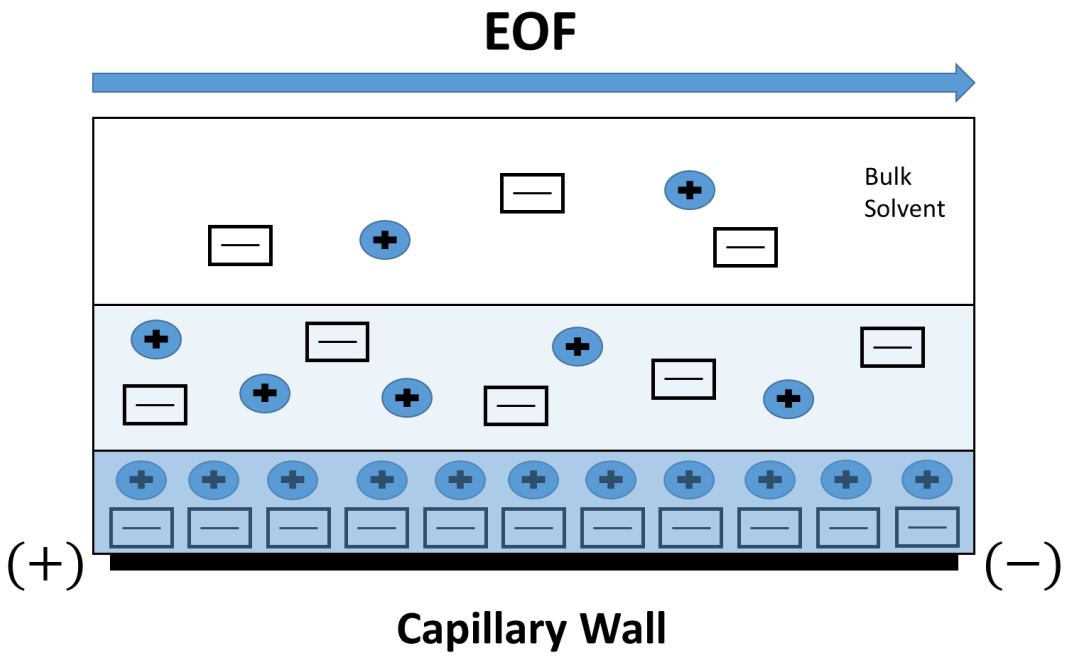

Figure 7: Charge profile of a capillary illustrating the formation of EOF. The darker semi-transparent blue region is the static layer and the lighter region above it is the diffuse layer.

Two types of flow profiles can be observed in these systems being either laminar flow of plug-like flow represented in Figure 5. Plug-like flow results in a flat leading edge on the solvent as it passes through the capillary and is achieved if the capillary radius is at least seven times the thickness of the double layer[91]. The flat edge of the plug-like flow contributes to the high separation efficiency of CE and minimized band broadening.

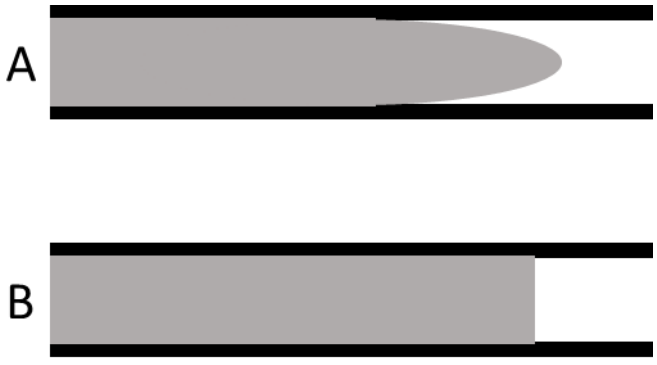

Figure 8: Schematic of laminar and plug-like flow inside a capillary. A) Laminar flow B) Plug-Like flow.

Band broadening is common in HPLC and other liquid chromatography techniques due to laminar flow with in the column. The linear velocity of EOF (V_{EOF}) can be calculated by the following expression:

$$V_{EOF} = \frac{\varepsilon_r}{4\pi\eta}(E\zeta) \tag{3.6}$$

Where ε_r is the relative permittivity of the buffer, ζ is the zeta potential and the other terms are as they were previously described. Relative permittivity refers to the permittivity of the buffer relative to the permittivity in a vacuum, accounting for the resistance produced when forming an electric field within the buffer. The zeta potential represents a potential difference between the bulk solvent and the region separating the static and diffuse layers. For any given molecule the net migration (apparent velocity, V_{app}) will be the sum of V_{EOF} and velocity resulting from the electrophoretic properties of the molecule (V_{act}):

$$V_{app} = V_{act} + V_{EOF} \tag{3.7}$$

Typically the capillary has a positive injection potential and a negative detection end resulting in EOF in the direction of the detector. Molecules may then have one of three different V_{act} properties with the magnitudes varying based on charge, shape, etc. A neutral molecule will migrate at V_{EOF} with no V_{act} so V_{app} will equal V_{EOF}. A positive molecule will migrate with an increased velocity towards the detector and a negatively charged molecule will migrate slower as V_{act} will be a negative value. As long as EOF is larger than the actual velocity of a negatively charged molecule it will enter the capillary. If that is not the case than those negative molecules will not enter the capillary and will

remain in the sample solution. The resolution between two different analytes (R_s) can be written as:

$$R_s = 0.177(\mu_1 - \mu_2)\left[\frac{\mathrm{V}}{D(\overline{\mu} + \mu_{\mathrm{eof}})}\right]^{1/2} \tag{3.8}$$

Where μ_1 and μ_2 represent the electrophoretic mobilities of each analyte[77]. From this expression it can be concluded that the maximum resolution is achieved as EOF approaches the negative value (opposite direction) of the mean mobility for the two analytes. This will result in the denominator to approach 0 and the expression to approach infinity in theory. Separation efficiency with respect to CE can decreased by some well characterized processes. This include width of the injection zone, conductivity differences between buffers entering the capillary, analyte-capillary wall interactions and hydrodynamic flow[92].

As we have seen, capillaries have a very high charge density on the interior surface. Most of the time this property is exploited to our advantage for separations however it is not always an ideal situation. When desired, the charged surface of the capillary may be shielded with various polymers thereby decreasing or removing EOF entirely. These coatings can allow separations to take place for components that would otherwise be subject to band broadening or permanent retention, for example small basic proteins. A coating may reduce band broadening by reducing the laminar flow characteristic of the flowing solution as mentioned earlier. Polyacrylamide and polyoxyethylene are possible permanent coatings but are expensive, time consuming and difficult to prepare[93]. Due to the viscosity of these polymers it is also very difficult to produce a working coated capillary with a narrow bore since the coating process often

results in the capillary becoming plugged. Another method of coating is a temporary dynamic coating achieved when the capillary is pressure injected with a buffer solution containing a coating polymer or analogue. For example phospholipid bilayers[94], polyvinylpyrrolidone (PVP)[95] and a variety of patented polymers[96] have been employed for dynamic coatings. These methods are far more cost effective and easier to use, however, the coatings are prone to degradation and inconsistency resulting in uneven interactions between the analytes and the capillary wall/coating. Dynamic coatings on narrow bore capillaries will be explored in a later section.

3.1.5. CE-LIF Setup

CE-LIF paired with a sheath flow cuvette allows for very high sensitivity to be achieved. The instrument has been described previously[97]. This is because the instrument takes advantage of five properties. They include; i) high fluorescent emission obtained from high quantum yield fluorophores excited via a focused laser, ii) reduced excitation volume, iii) efficient photon collection by focused emission collection through high numerical aperture microscope objective lenses, both optical and spatial filtering to minimize background signal, v) and a highly sensitive photon detector. The experiments outlined in the sections to follow rely on the setup scheme shown in Figure 6 although other setups and configurations are possible. The injection carousel is used to house a buffer containing vessel with the capillary and a platinum wire submerged in solution. The power supply generates a potential for the wire, through the capillary which is grounded at the detection end by the sheath flow buffer. The carousel is equipped with a safety lock which breaks the circuit at any point that the electrode is exposed.

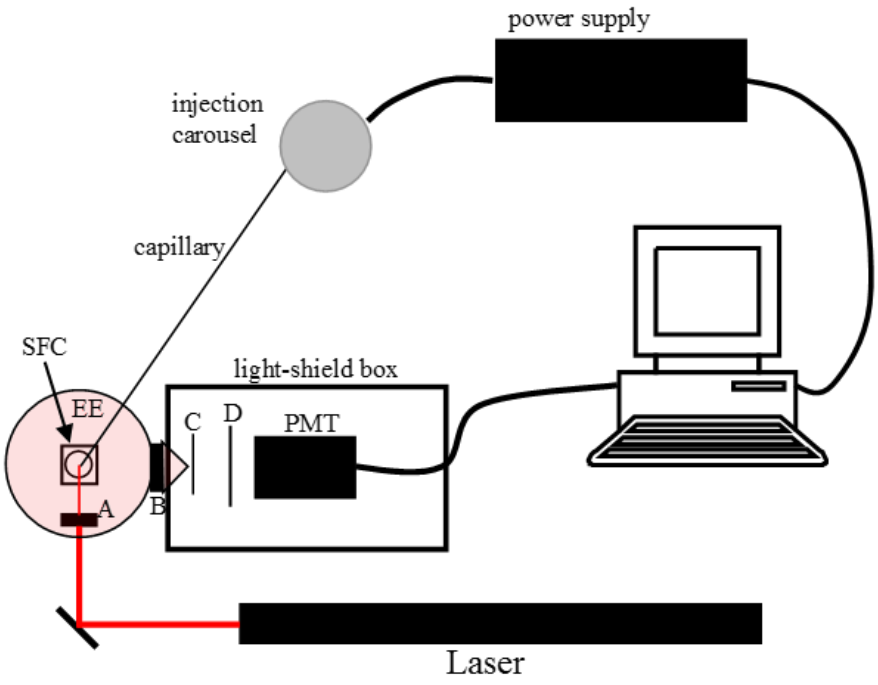

Figure 9: Schematic drawing for a basic CE-LIF instrument. Relative component positions may vary between setups. Lightly shaded red circle represents fluorescent emission. Sheath flow cuvette (SFC), excitation emission (EE); A) 6.3X 0.2 N.A. objective B) 60X 0.7 N.A. objective C) Optical filter D) Pinhole filter.

There are two ways that sample can be introduced into the capillary. Electrokinetic injection uses the applied potential for a specific period of time to introduce a small plug of sample into the capillary. The capillary can then be placed into a buffer vessel for the separation to take place. The quantity of analyte injected (Q_a) can be calculated by:

$$Q_a = \mu_a \cdot E_i \cdot t_i \cdot \pi \cdot r_c^2 \cdot C_a \tag{3.9}$$

Where μ_a is the net electrophoretic mobility of the analyte, t_i and E_i are the electrokinetic injection time and potential respectively, r_c is the internal radius of the capillary and C_a is the concentration of the analyte[98]. The other form of sample introduction is by pressure injection which is performed using a syringe filled with sample placed on the end of the capillary. The syringe contains a small amount of sample with the remaining volume

being compressed air between the sample and the syringe plunger. This allows the air on top of the sample to be compressed forcing the sample into the capillary. Using this method does not allow for an injected volume calculation so it is typically used to fill the entire length of capillary with sample as it is faster than electrokinetic injections. That statement holds true only for capillaries larger than 5 μm. Once the capillary inner bore becomes very small pressure injection times greatly exceed electrokinetic times. Pressure injections may also be used for compounds that would otherwise not enter the capillary electrokinetically or if the experimenter wishes to alter the direction that a molecule will flow in the capillary. For example the capillary may be filled with buffer containing substrate at one set potential. Upon reversing the potential applied to the capillary, the substrate will migrate back to the injection end, however, the enzyme will migrate into the capillary forming product along the way. Both the enzyme and the product (detectable) will migrate to the detection end while any unreacted substrate will exit the capillary at the detection end. This particular method relies on very specific charge profiles on the substrate, enzyme and product but provides and effective reduction of the background noise. This particular type of assay will be discussed further in Chapter 8.

The detection end of the capillary utilizes a sheath flow cuvette made of high grade quartz mounted in a stainless steel holder. The fine details about the instrument can be found in section 4.2.2. The sheath flow provides constant laminar flow of buffer at the detection end of the capillary from the top of the cuvette down. This effect hydrodynamically focuses the emerging analytes, reducing post-capillary sample broadening[28]. The capillary eluent is excited by the laser, the emitted photons are collected and the material is washed away. This all happens quickly, taking advantage of

the rapid fluorescent emission of the analytes while reducing signal stacking from lingering analytes. The small volume surrounding the analyte also reduces quenching possibilities, and the rapid passing of material ensures that photobleaching is limited. It is highly important that the sheath flow and running buffers be made of the same components. This is required to maintain an even potential across the capillary as well as to provide a consistent optical profile for the analyte excitation to take place.

3.2. *E. coli* β-galactosidase

3.2.1. Background

The β-galactosidase (E.C. 3.2.1.23) used was sourced from *E. coli* which was encoded with the *lacZ* gene. This enzyme is a 465 kDa homotetramer retaining glycosidase, whose function is to hydrolyze lactose (Figure 7) into glucose and galactose[99]. The binding of β-lactose to β-galactosidase relies primarily on the recognition of the galactose moiety while the glucose or aglycon portion is non-specific. This property allows the glucose moiety to be substituted with a variety of synthetic aglycons in order to exploit chromo or fluorogenic properties when bound or separated[100].

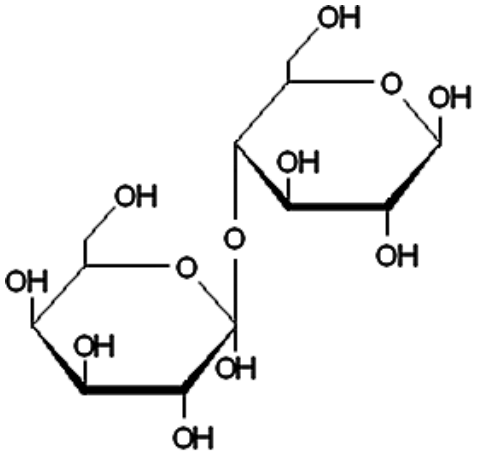

Figure 10: Molecular structure of β-lactose.

The enzyme is also responsible for the catalysis of the β1→4 transglycosylation linkage between glucose and galactose to a β1-6 linkage forming an allolactose. The enzyme is naturally induced by this allolactose[101]. The allolactose may be substituted with analogues such as isopropyl-β-D-thiogalactoside (IPTG) for enzyme induction purposes resulting in a non-hydrolysable compound. A study by Jacob and Monod observed a lactose induced response causing an increase in β-galactosidase activity leading them to an operon based gene regulation model[102]. Three genes make up the *lac* operon: *lacZ*, and *lacY* code for a transmembrane lactose transporter and *lacA* codes for a transacetylase but has been shown to have no connection to metabolism[103]. The *lacA* function continues to remain unexplained in its specific nature but is a requirement for the *lac* operon.[104] Growth medium with lactose was used to demonstrate the bacterial permease taking up the lactose into the cells. Upon entering the cell, a portion of the lactose is transglycosylated to allolactose by the small amount of β-galactosidase present. The allolactose, or IPTG in the experimental case, binds to a repressor protein located in the operator region of the operon[105]. The resulting induced conformational change from allolactose or IPTG binding lowers the repressors affinity for DNA thereby liberating the operator. Provided that glucose levels are low in the cell, the *lac* operon will open to transcription, producing a rapid increase in β-galactosidase molecules. Data showed that the level of β-galactosidase can increase as much as 1000 times within the hour[103].

3.2.2. Structure and Catalysis

E. coli β-Galactosidase is a well characterized enzyme; its amino acid sequence[106], nucleotide sequence[107] and crystal structure[108,109] have all been determined. Four identical 1023 amino acid protein monomers make up the enzyme with each

monomer being made up of five distinct folding domains[108]. The enzymes activity is based on its tetrameric structure with each monomer being active[99]. However, dissociated monomers are not active[100], neither are higher order oligomers[110]. Dimers may form but lose their activity as well as trimers will readily dissociate as they are not stable. Analysis by circular dichroism shows that the enzyme has secondary structures amounting to 14% α-helix and 48% β-sheets[111]. No disulfide bonds are present in the structure[112] and it has been shown that Mg^{2+} is required for both the stability of the tetramer[111] and the catalytic activity[113,114]. Levels greater than 10 mM magnesium will impair tetramer formation[115]. A typical concentration of Mg^{2+} used in the CE-LIF assays presented here is 1 mM, allowing for stability and high activity of the enzyme while keeping the ionic strength of the buffer low. The four monomers making up a β-galactosidase enzyme are oriented as shown in Figure 8. They are oriented along three mutually perpendicular axis of symmetry with two interfaces per monomer, one on each side. The "long interface" sections of the enzyme are areas of approximately 4000 $Å^2$, which is the linking surface between monomer A with B, and on the other side C with D. The molecule as a whole is planar and not overly structured. The region labeled "activating interface" has a slightly larger area of 4600 $Å^2$ for two regions corresponding to the linkage of A with D and B with C. The contact of this interface between the two monomers is greater than the previous long interface region. It is also an essential monomer interaction for the catalytic activity of the enzyme. This is due to residues 272-288 extending from one monomer to its counterpart across the activating interface completing the others active site[108].

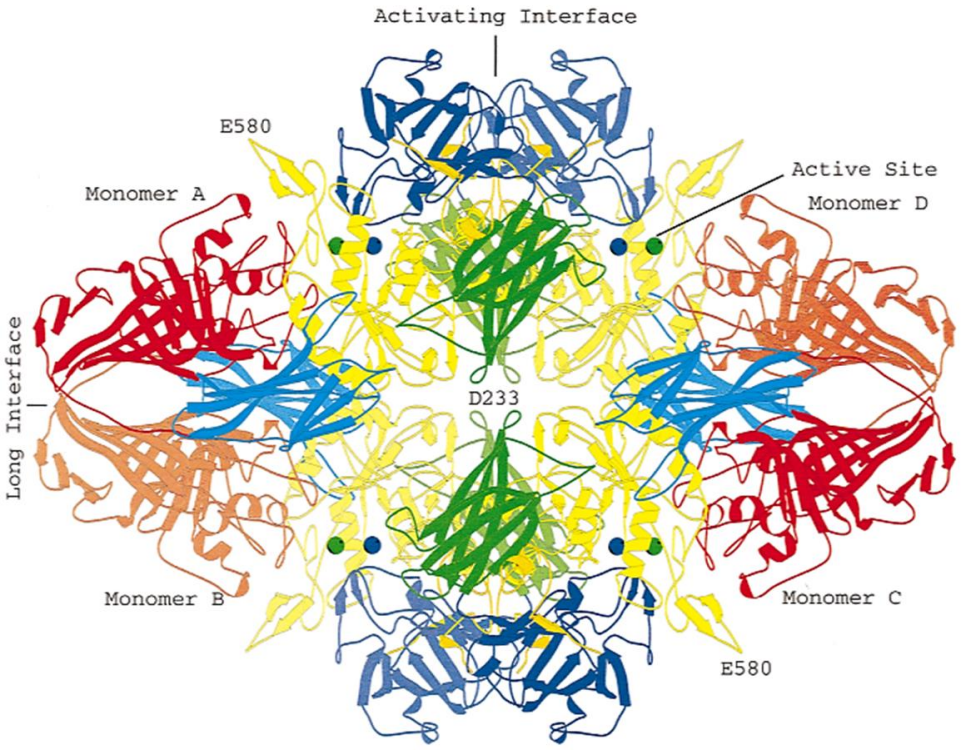

Figure 11: Ribbon structure representation of β-galactosidase. Used with permission[100].

The last interface between the monomers connects A with C and B with D. It is only 230 $Å^2$ but is an important bordering interface for the active site and the activity of the enzyme. As mentioned above, dimer formation is a possibility with this enzyme and occurs along the long interface portion although the interactions here are weaker than that of the activating surface. The inactivity of the formed dimers is best described as unfavorable to the activity of the enzyme through a rearrangement. It will be shown in a section to follow that the conformations taken by the four monomers are fluid in nature and the enzyme is not rigid in nature.

When bound, the tetramer forms each active site which in turn operates independently from residues of the first, third and fifth domain in a given monomer with a loop forming in the second domain across the activating interface. Each active site is

made of a TIM barrel structure creating a deep pit out of domain three. Both Mg^{2+} and Na^{+} are associated and required for activity. Residues in a monomer have been identified for their crucial role in activity: Glu461[116], Tyr503[117], Glu537[118], His540[119], and Trp999[120]. The loop formed between monomers has been indicated to be a stabilizing region of Mg^{2+} binding residues and not necessarily directly associated with catalytic activity[108].

Substrate hydrolysis is achieved through a double displacement reaction with a covalent intermediate supported by acid/base catalysis[121]. Shown in Figure 9 is a representation of the binding and hydrolysis of galactose with "OR" which may be glucose or a synthetic replacement. The glucose is initially bound at the opening of the active site shallowly stacking on Trp999[120]. The substrate then moves deeper into the active site for nucleophilic attack by Glu537 where the galactosyl group is lost to this residue through the cleavage of the glycosidic bond. This results in an α-D-galactosyl intermediate and the release of the OR group with the reaction assisted by acid catalysis by either Glu461 or Mg^{2+}. The end result is the release of the galactosyl by the removal of a proton from Glu461 which returns the enzyme to its original state allowing for another catalytic cycle.

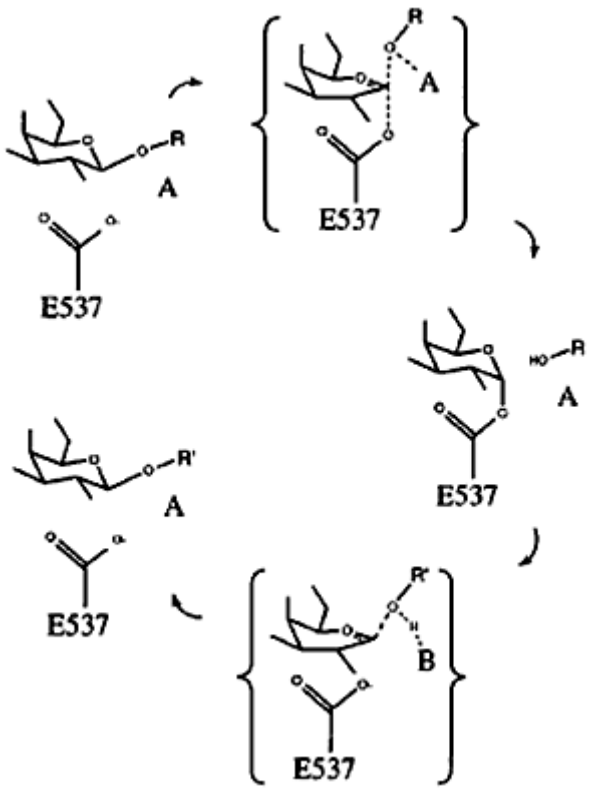

Figure 12: Hydrolysis schematic of galactopyranoside by β-galactosidase where OR represents aglycon and HOR` represents the acceptor. A and B represent either acid or base respectively. Used with permission[121].

β-Galactosidase is an excellent candidate for single molecule analysis due to a variety of characteristics that can be exploited. The enzyme can be expressed in high quantities over a short period of time with easily achieved growth conditions of E. *coli*. There are many available substrates that are highly fluorescent and the enzyme itself has a relatively high catalytic rate which is able to generate a measurable amount of product in a short period of time. Since β-galactosidase operates by primary recognition of the β-galactoside moiety, the glucose portion may be substituted with a variety of fluorescent molecules. In Figure 10 glucose is shown to be replaced with 9H-(1,3-dichloro-9,9-dimethyacridin-2-one-7-yl) (DDAO).

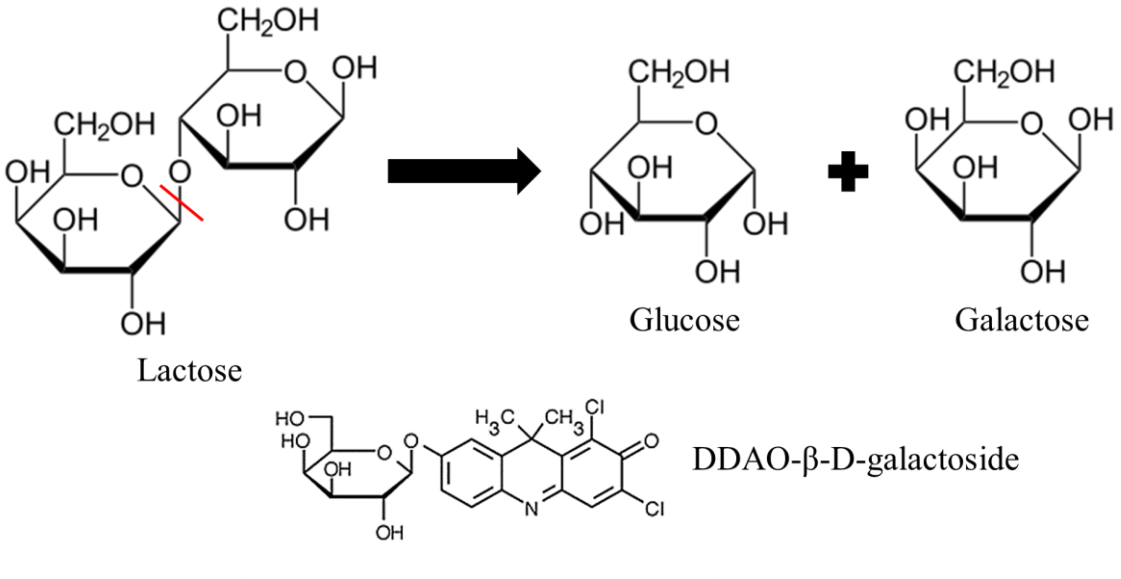

Figure 13: Hydrolysis of lactose. Cleavage of the β1→4 transglycosylation linkage shown by the red line. Substrate structure shown in the bottom portion of the figure.

The 9H-(1,3-dichloro-9,9-dimethyacridin-2-one-7-yl)-β-D-galactopyranoside (DDAO-gal) molecule remains virtually non-fluorescent until the DDAO is cleaved where it becomes highly fluorescent. This remains a highly exploited feature of β-galactosidase in single molecule research allowing for a wide range of substrates to be utilized for various assays.

4. Materials and Methods

4.1. List of Chemicals

Table 1: Chemicals used with supplier.

Name	Supplier
Ampicillin	Sigma (St. Louis, MO)
DDAO	Invitrogen (Eugene, OR)
DDAO-gal	Invitrogen (Eugene, OR)
D-(+)-Galactose	Sigma (St. Louis, MO)
DMSO	Sigma (St. Louis, MO)
GS-6	Applied Biosystems (Foster City, CA)
Glycerol	Sigma (St. Louis, MO)
HEPES	Sigma (St. Louis, MO)
LB media	Difco (BD, Sparks, MD)
L-(+)-Ribose	Sigma (St. Louis, MO)
Magnesium chloride	Sigma (St. Louis, MO)
oNPG	Sigma (St. Louis, MO)
Potassium Chloride	Sigma (St. Louis, MO)
Protease inhibitor cocktail	Sigma (St. Louis, MO)
PVP	Aldrich (Milwaukee, WI)
Resorufin	Invitrogen (Eugene, OR)
Sodium citrate	Sigma (St. Louis, MO)
Sodium hydroxide	Sigma (St. Louis, MO)
Toluene	Sigma (St. Louis, MO)

4.2. Capillaries and Instrumentation

4.2.1. Capillaries

Fused silica capillaries externally coated with polyimide were used with 3 different diameters (Polymicro Technologies, Phoenix, AZ). In order of decreasing size; 10 µm internal diameter 151.8 µm outer diameter, 5/152.7 and 2/151.5 µm diameters respectively. Capillaries were cut on the longitudinal axis of the capillary with a sapphire capillary cutter (Supelco, Oakville, ON) at the detection end and approximately 1-2 mm of the polyimide was removed by flame to expose the silica. A straight cut along with the removal of the polyimide coating ensured that the laser could be focused as close to the

detection end as possible while minimizing light scattering. The quality of the cut was determined visually under microscope prior to insertion into the instrument to ensure that no jagged edges or polyimide was present. The injection end was given a rough cut to give the capillary a final length determined by the specifics of the experiment. The exact lengths will be given in the methods of each individual experiment.

4.2.2. Instrumentation

The single molecule assays throughout the research being presented were performed on one of three laboratory constructed CE instruments. Each instrument is equipped with a post-column LIF detection system. At the injection end of the system a 0.5 mm diameter platinum wire connected to a high voltage power supply (Spellman model CZE 2000, Hauppauge, NY) was placed into a sample container along with the capillary on a rotating carousel. Samples were primarily buffer based solutions with analyte components specific to the experiment. At the detection end of the instrument, the capillary was placed into a quartz sheath flow cuvette with a 250 x 250 inner bore diameter (Hellma, Concord, ON). The cuvette was mounted onto a custom stainless steel holder attached to 3 translational stages allowing for precise positioning in the *x*, *y* and *z* axes and covered by a retractable light shield to block ambient light. The light shield contains two slits, one for the laser to enter, make contact with the sample and the other on the opposite side to let the excess light pass through. In each case the laser beam was reflected off a single mirror then focused with a 6.3X, N.A. 0.7 microscope objective (Melles Griot, Nepean, ON) approximately 10 μm below the capillary's detection end. Fluorescence emission from this point was collected at a 90° to the excitation using a 60X, N.A. 0.7 microscope objective (Universe Kogaku, Oyster Bay, NY), passed through

a 670DF40 optical filter (Omega Optical) and a slit onto a PMT detector (Hamamatsu model 1477, Bridgewater, NJ). The analog PMT signal was collected and digitally converted onto a computer loaded with a PCI-MIO-16XE I/O board utilizing LabView™ software (National Instruments, Austin, TX) between 10-50 Hz. The same software was used to control the PMT bias of 1000V as well as the electrophoresis voltage and time delays for specific procedures. The assays utilized a 10 mW 633 nm red HeNe laser (MellesGriot) as the excitation source. All the sheath flow buffer and capillary eluent flows from the cuvette to a waste container.

4.2.3. Buffers/Solution Preparation

All buffers and solutions used in conjunction with CE-LIF and spectrophotometric analysis were prepared with milli Q (18 MΩ) deionized water and passed through 0.45 µm filters (Nalgene, Lima, OH) to remove particulate matter. Buffers used in both separations and sheath flow were 10 mM or 50 mM *N*-2, hydroxymethyl-piperazine-*N´*-2-ethanesulfonic acid (HEPES), adjusted to pH 7.3 with NaOH, containing 1 mM $MgCl_2$ and 1 mM sodium citrate. Two types of capillary coating assays were used, each being made with 50 mM HEPES and 1 mM $MgCl_2$ with a pH adjustment to 7.3. Separation and sheath buffers contained 0.02% (w/v) polyvinylpyrrolidone (PVP), with an average molecular weight 1.3 MDa, or 0.0007% Genescan polymer 6™ (GS-6). The coating buffers were made identical to the separation/sheath buffers except for an increase in the polymer concentrations. PVP was increased to 0.5% (w/v) and GS-6 was increased 0.007%. A capillary rinsing solution of 100 mM NaOH was prepared and filtered for daily use. All buffers, containers and pipette tips were autoclaved prior to use which the exception of the NaOH solution and

GS-6 which was added to the buffer after the buffer had been autoclaved. DDAO-gal substrate was prepared each day as needed in the corresponding buffer. An appropriate amount of DDAO-gal was diluted to 200 µL in buffer then washed 3 times, each with an equivalent volume of toluene in order to remove the DDAO impurity. The concentration at this stage was 0.2 mM. The washed substrate was then diluted to its experimental concentration as either 50 µM or 30 µM with the experimental components: buffer or buffer and dilute enzyme. Inhibitor solutions of L-ribose were prepared at 1.05 mM in 10 mM HEPES, 1 mM $MgCl_2$ and 1 mM citrate at pH 7.3. From there 100 µL was transferred into a solution of the same buffer plus substrate. This resulted in a substrate concentration of 50 µM and an inhibitor concentration of 210 µM.

4.2.4. Capillary Preparation

At the start of each day a solution of Resorufin and 7-hydroxy-9H-(1,3-dichloro-9,9-dimethyacridin-2-one) (Res + DDAO) combination alignment dye was used to check the alignment of the instrument followed by 100 mM NaOH rinse for 30 min and then a buffer rinse for 30 min before experiments took place. If a coating was used in the capillary the specific coating (PVP or GS6) was pressure injected with 100 mM NaOH and then dynamically coated by pressure injection (approx. 5 atm) for a minimum of 30 min with coating buffer. Excess coating buffer was removed by flushing with running buffer. A new capillary was pressure injected with 100 mM NaOH for a minimum of 30 min to remove the air before running with alignment dye and aligning the capillary.

4.3. Experimental Procedures

4.3.1. Activity and Mobility Assays

4.3.1.1. Activity Assay

The assay was performed on a 5 µm capillary 60 cm in length with two temperature controlled sections. The first 15 cm of capillary was suspended in the air followed by a 5 cm section fastened against an aluminum pipe, 20 cm in the air and another 5 cm on the pipe with the final 15 cm in the air. Water flowed through the pipe by using a recirculating heater/cooler maintaining a constant temperature for the two 5 cm sections at 50, 28 or 10°C. Room temperature was 21°C. The running, sheath, and sample buffer was 50 mM HEPES with 1 mM $MgCl_2$ and 1 mM citrate (pH 7.3), with a sampling rate of 10 Hz. The enzyme β-galactosidase was purchased in a purified form from Sigma, sourced from *E. coli* and diluted sufficiently to have enzyme molecules enter with sufficient space between them. The sufficient space is defined as a minimum of 30 seconds in between molecules when continuously injected at 200 V/cm with data being collected at 10 Hz. This range provides enough data points to calculate a baseline average prior to and post enzyme product zone.

4.3.1.2. Mobility Assay

This assay was performed on a single 5 µm capillary 60 cm in length with a single temperature controlled section. Due to mobility differences between capillaries, a single cut capillary was used to collect the data for this assay. The injection end of the capillary was secured to the carousel, submerged in the sample vial with the first 27.5 cm in the air followed be a 5 cm section fastened to an aluminum pipe as described previously. Water was pumped through the pipe and maintained at a constant temperature for the duration

of the assay. Room temperature remained 21°C. The running, sheath and sample buffers remained the same along with the sample preparation. The data was acquired at a rate of 50 Hz and the assay was performed by continuous flow at 200 V/cm.

4.3.2. *E. coli* Transformation and Cell Harvesting

E. coli strains BW25113, JW0013-4, JW0054-1, and JW4103-1 were obtained from the Coli Genetic Stock Center (Yale University) and were each transformed with the pTNA plasmid containing wild-type *E. coli* LacZ (wtLacZ). The transformation was performed in a previous study by Craig et al., 2012.[122] Wild type LacZ was amplified from genomic DNA using the following primers: 5'LacZ_SphI (5'-TTT GCA TGC ATG ACC ATG ATT ACG GAT-3') and 3'LacZ_HindIII (5'-TTT AAG CTT TTA TTT TTG ACA CCA GAC-3') (SphI and HindIII sites are italicized). The resulting PCR products were digested and inserted into the pTNA plasmid, containing an ampicillin resistance gene.[123] The transformed *E. coli* cells were grown in LuriaBertani (LB) media containing 100 µg/mL ampicillin overnight at 37°C or 42°C. Each strain of *E. coli* was grown under each temperature conditions making for a total of 8 different conditions. The resulting suspension was taken in the morning and centrifuged at 3300g for 20 min, maintained at a temperature of 4°C. The supernatant was discarded and the remaining pellet was re-suspended in 1 mL of 100 mM HEPES (pH 7.3) with 2 mM $MgCl_2$ and 2% (w/w) Sigma Protease Inhibitor Cocktail without the presence of metal chelators. In order to lyse the cells a freeze, crush, thaw and repeat approach was taken. Each sample was frozen with liquid nitrogen, ground by physical force and thawed. This process was repeated for a total of 5 complete cycles for each sample. Once the lysis procedure was complete an additional 3 mL of the solution described above was added to each sample. The samples

were then centrifuged at 12000g and the resulting pellet was discarded. The supernatant was taken and passed through a 0.45 µm filter, then diluted with an equivalent volume of glycerol and stored at -20°C until required.

4.3.3. Heat Shock Assay

This assay utilized the β-galactosidase extracted from 4 different strains of *E. coli* described above, each grown under two different temperature conditions. A 40 cm, 5 µm diameter capillary was used with data acquired at 10 Hz. The entire length of capillary was maintained at room temperature (21°C) and was run by continuous flow at 400 V/cm. A DDAO standard was run in triplicate prior to running the sample at $1.1x10^{-8}$ M for a 60 second injection at 400 V/cm then run to completion with running buffer in between each of the 3 standard runs. The running, sheath and sample buffers were all 50 mM HEPES with 1 mM $MgCl_2$ (pH 7.3). The enzyme was diluted to a point where there was an average of 5 molecules present per capillary volume.

4.3.4. Capillary Coatings

4.3.4.1. Genescan Coating

A 40 cm, 10 µm capillary was used and the running, sheath and sample buffer was 50 mM HEPES and 1 mM $MgCl_2$ (pH 7.3) with 0.02% (w/v) GS-6 added after the solution was autoclaved. The coating buffer was 0.2% (w/v) GS-6, a 10 fold increase compared to the sample buffer, added to a portion of the buffer described. Each day the capillary was flushed with NaOH, set with a negative injection potential. Only the hydroxide would enter the capillary initially due to the reduced EOF, and it migrated to the positive potential detection end. The capillary was then pressure injected for 30 min with coating buffer followed by an additional 30 min with running buffer to remove any

excess coating and loose material. The alignment procedure was then performed set at a positive injection potential and the capillary was flushed with running buffer after the alignment was confirmed. The capillary was then filled with DDAO-gal substrate at 50 µM. Once the capillary was filled with substrate a dilute β-galactosidase solution in sample buffer was run continuously at a negative injection potential of 400 V/cm.

4.3.4.2. PVP Coating

A capillary with the same specifications as described in the previous section was used. The running, sheath and sample buffer was composed of 50 mM HEPES and 1 mM $MgCl_2$ (pH 7.3) with 0.02% PVP (w/v) added prior to being autoclaved. An aliquot of the buffer was removed to make the coating buffer which was the same as above with the addition of 0.5% (w/v) PVP. An identical procedure as was described in section 4.3.4.1 was taken in preparing and running the sample with the PVP in place of the GS-6.

4.3.5. Salt Suppression of EOF

The assay used a 40 cm, 2 µm capillary with running, sheath and sample buffer at 50 mM HEPES, 50 mM $MgCl_2$, 200 mM KCl (pH 7.3). A negative injection potential was used for all instrument runs, except for an initial capillary fill with substrate which was done on positive potential. Post alignment check, the capillary was filled with DDAO-gal substrate 50 µM for 60 min, then with 25 µM for 20 min. The enzyme was diluted to a point where there were only a few molecules per capillary volume and the assay was run continuously until completion.

4.3.6. Kinetics Assay

In this assay a 50 cm, 5 µm capillary was used with the running, sheath and sample buffer 10 mM HEPES, 1 mM $MgCl_2$, and 1 mM citrate (pH 7.3). Three substrate

solutions were produced post DDAO-gal washing procedures. All were prepared using the described buffer, the first being a standard substrate (*S*) at 50 µM, then a second substrate concentration (*S2*) at 30 µM and a substrate/inhibitor solution (*I*) with 50 µM substrate and 210 µM L-ribose. The capillary was first filled with S, while the enzyme was diluted to a point that resulted in a single enzyme molecule entering the capillary during the injection phase. The enzyme dilution was injected for 5 seconds at 100 V/cm, followed by an injection of *S2* for 15 seconds at 400 V/cm and a 30 minute incubation period. The *S* was injected for 150 seconds at 400 V/cm followed by another 30 minute incubation. Lastly *I* was injected for 240 seconds at 400 V/cm with a final 30 minute incubation before being run to completion.

5. Temperature Induced Conformational Changes

The data presented in this chapter has been originally published as:

Jeremie J. Crawford, Frannie Itzkow, Joanna MacLean, and Douglas B. Craig (2015) Conformational change in individual enzyme molecules. *Biochemistry and Cell Biology*, Vol 93 (6), 611-618. Used with permission.

The manuscript was co-written and edited by Dr. D. Craig.

5.1. Introduction and Background

Analysis of single enzyme molecules provides insight into the heterogeneity within the population. These heterogeneities have been found with respect to catalytic rate, activation energy of catalysis, and electrophoretic mobility for a variety of enzymes[2,3,124]. Both static and dynamic heterogeneity can be measured, however a direct link between the two has been difficult to conclusively prove. As it was stated previously, static heterogeneity represents the fact that not all enzymes are created equally independent of their age in the population. Although it is not fully understood, static heterogeneity is thought to arise from errors in transcription/translation of the primary sequence, differences in post translational modifications or differences in conformation. Dynamic heterogeneity is the range of variation overtime within an already formed enzyme excluded alterations in post-translational modifications and changes in amino acids. The dynamic range does not encompass the loss or replacement of residues or denaturation of proteins. It is assumed that the enzyme amino acid sequence remains constant. As activity is the focus of the study, the molecule must remain active throughout the entire experiment for the data to be valid.

Dynamic heterogeneity most likely emerges from an enzyme's ability to switch between different active and stable conformations due to low energy transitions. A low

activation energy barrier between conformations would allow a protein to alter its conformation at ambient temperature to reach a new energy minimum. It has been shown that the full population range of observed catalytic rates is far larger than a given molecule's range. This suggests that once a molecule is formed and a given folding pattern has been established only a portion of the active conformations are now available[63].

In a study published by Rojek and Walt, the catalytic rates of β-galactosidase were measured before and after several brief periods of heating[125]. The assay consisted of an array of sealed microwells etched into an optical fibre bundle. Dilute enzyme was dispersed into each well such that probability dictated 0 or 1 enzyme molecule per well to be the most probable outcomes. Each well also contained the resorufin-β-D-galactopyranoside (RBG) substrate and a CCD detector was set in place to collect the resulting fluorescence from the catalytic turnovers. The wells could then be subjected to heat cycles for a period of 1 minute before being allowed to cool to room temperature. Figure 11 illustrates the main findings of the group. They reported that heating pulses resulted in an observable change in the enzyme molecules based on catalytic rates observed. This was attributed to conformational shifts from one stable conformation to another due to low activation energy barriers between the conformations. It was also reported that the enzymes have an equal probability of increasing or decreasing their catalytic rate as a result of the heating cycle. This equal probability concept explains why no net change was observed in bulk solution. Activity was measured before and after 47°C heat pulses and the change in activity was recorded. A data point was obtained for each change in measured activity. When plotted, a Gaussian distribution was observed,

indicating that small changes in activity, either as an increase or decrease in value were most probable.

This study provided the foundation for the principles being investigated in this chapter. Through the use of CE-LIF it was first sought to confirm or disprove the finding that temperature induces conformational changes that are stable and long lived through the measurement of catalytic activity and that the induced conformational changes had an equal probability of resulting in either increasing or decreasing observed activity. Single enzyme molecules were subjected to short periods of increased or decreased temperature as they traversed the capillary. If temperature does in fact induce conformational changes that result in catalytic rate alterations then it was assumed that as temperature increases so would the range of observed activities. It was also assumed that a difference in activity was caused by a conformational shift and not any other mode of action. Electrophoretic mobility was also a measured property as conformational changes may result in mobility alterations due to electrophoretic mobility being dependent on molecular shape of the enzyme. If conformational change increases proportional to temperature then the range of observed mobilities would also be assumed to increase with temperature. β-galactosidase has been found to be electrophoretically heterogeneous with a Stokes radius of 6.9 nm, an average buffer radius of 0.25 nm, an axial ratio of 1.31 and a net charge of -62.9 at pH 7.3 while a conformational change that results in a radius alteration of 0.3 nm is sufficient to account for the entire range of static electrophoretic mobilities[108,126,127]. Therefore a change in mobility would be indicative of a change in the enzymes radius due to conformational shifts. In both the activity and mobility studies, the temperature range was broadened to include both high and low temperatures using the same assay.

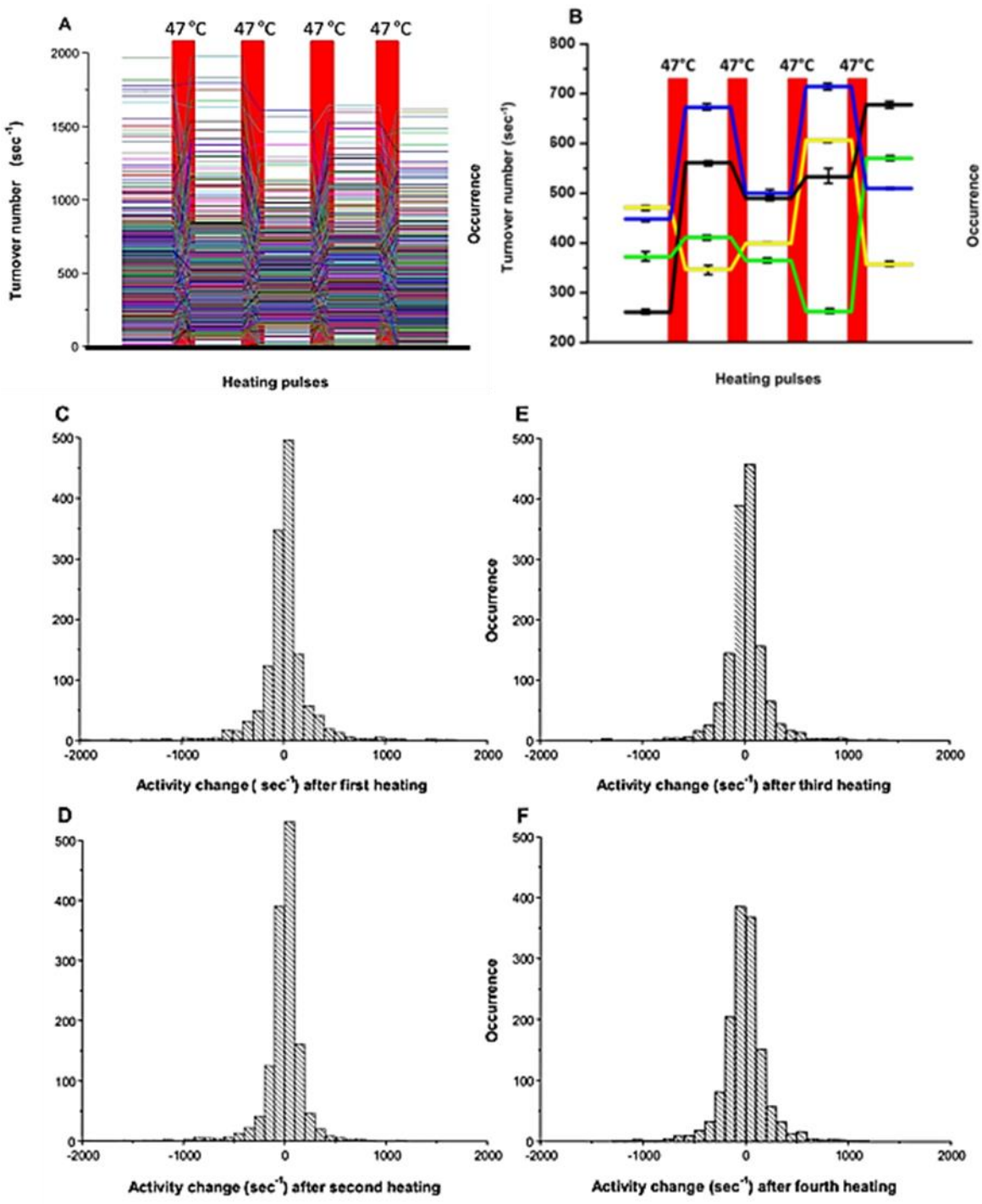

Figure 14: Reported activity of individual β-galactosidase molecules between heat pulses of 47°C. A) Activity traces in a single experiment. Six images between taken between each heat pulse. B) Excerpt of 4 molecules to illustrate activity changes with each heat pulse. C, D, E, F) Histograms representing each molecules increase or decrease in activity based on turnover numbers (sec^{-1}). Used with permission[125].

5.2.Materials and Methods

The CE instrument is as described previously along with the DDAO-gal sample preparation. Solutions for analysis were prepared with 125 µL of washed substrate, 5 µL diluted enzyme and 370 µL running buffer. The running, sheath flow and sample buffers were all 50 mM HEPES, 1 mM citrate and 1 mM $MgCl_2$, brought to pH 7.3 with concentrated NaOH. A 5 µm internal diameter fused silica capillary was cut to a length of 60 cm.

5.2.1. Standard Assay

A bulk solution activity assay of β-galactosidase was prepared using the buffer described above plus 0.5 mM o-nitrophenol-β-D-galactopyranoside as the substrate with β-galactosidase. Activity was monitored by measuring the rate of change in absorbance over time at 410 nm. An incubation period of 2 minutes at room temperature (21°C) was performed prior to analysis in order to establish a homogeneous environment.

5.2.2. Continuous Flow Assays

5.2.2.1. Activity Assay

For this assay portions of the capillary were fixed to a pipe connected to a recirculating water heater/cooler and the rest was left in the air subject to room temperature (21°C). The 60 cm capillary was portioned into the following 5 sections; the first 15 cm was suspended in the air followed by 5 cm fastened to the temperature controlled zone, 20 cm suspended in the air, 5 cm fastened down and then the final 15 cm suspended in the air. Figure 12 is an illustration of the capillary setup.

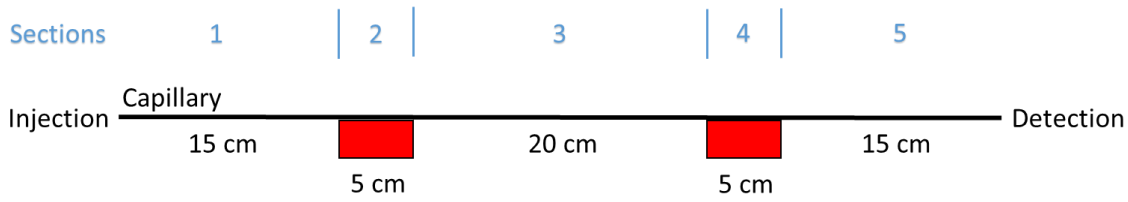

Figure 15: Activity assay setup schematic. Sections 2, 4 (red blocks) represent heater/cooler zones both set at 10, 28 or 50°C.

The sample was prepared as described above and set up for continuous injection at 200 V/cm with the data collected at 10 Hz. Activity was measured in the form of average signal for the duration of time that the enzyme was at room temperature in the capillary for each of the 3 sections (Section: 1, 3, 5).

5.2.2.2. Mobility Assay

A second assay was performed in a similar manner, this time with the focus on electrophoretic mobility before and after a single temperature controlled zone. Figure 13 is an illustration of the set up.

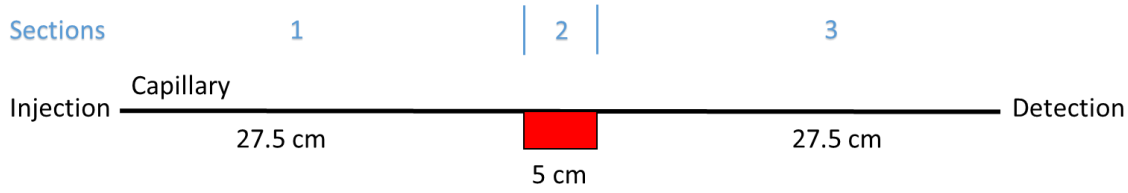

Figure 16: Mobility assay set up schematic. Section 2 (red block) represents heater/cooler zone set at 10, 28 or 50°C.

The sample was prepared the same and a continuous injection protocol was used at 200 V/cm. Data was collected at 50 Hz for this assay.

5.3. Results and Discussion

5.3.1. Temperature Controlled Incubation Effects on Catalytic Rate

In a continuous flow assay the applied potential remains constant throughout the entire assay and the enzyme is diluted sufficiently such that an individual enzyme entered

the capillary at a time with sufficient baseline separation between them. Baseline separation was defined as a minimum of 30 seconds between each enzyme. As a single enzyme traverses the capillary from injection to detection, end product will be continuously formed. When the enzyme reaches a zone of increased or decreased temperature the catalytic rate will differ, represented by a height difference in the electropherogram.

Under low ionic strength conditions, citrate present in the buffer binds to β-galactosidase, resulting in an increased negative charge on the enzyme. With a positive injection potential, EOF will be in the direction of the detector. Negatively charged species will migrate towards the detector at a slower rate than EOF based on the amount of negative charge present on the surface of the molecule. This created a situation where the DDAO product being formed moved faster than the enzyme through the capillary[128]. While the enzyme travels through the capillary, it remains at the trailing edge of the bulk product formed. The DDAO-gal molecule is neutral and will move at the rate of EOF, however, the negatively charged DDAO molecule formed through the enzyme catalyzed reaction then moves at slower rate than EOF. This difference in rate allows for fresh substrate to consistently surround the enzyme and for the DDAO product to move ahead of the enzyme. This means that the product that first reaches the detection end was made at the time that the enzyme entered the capillary. This creates a reversed effect in the box shaped peaks produced where the leading edge of the product peak represents the product formed when the enzyme first entered the capillary. Since there is diffusion of product taking place as time goes on it is expected that the leading edge will be less of a sharp increase compared to the just formed trailing edge. All the data points that the leading

and trailing edge of a single enzyme's peak correspond to the enzyme's production of DDAO product while traversing the capillary. Figure 14 illustrates the concept of a continuous flow assay under these conditions.

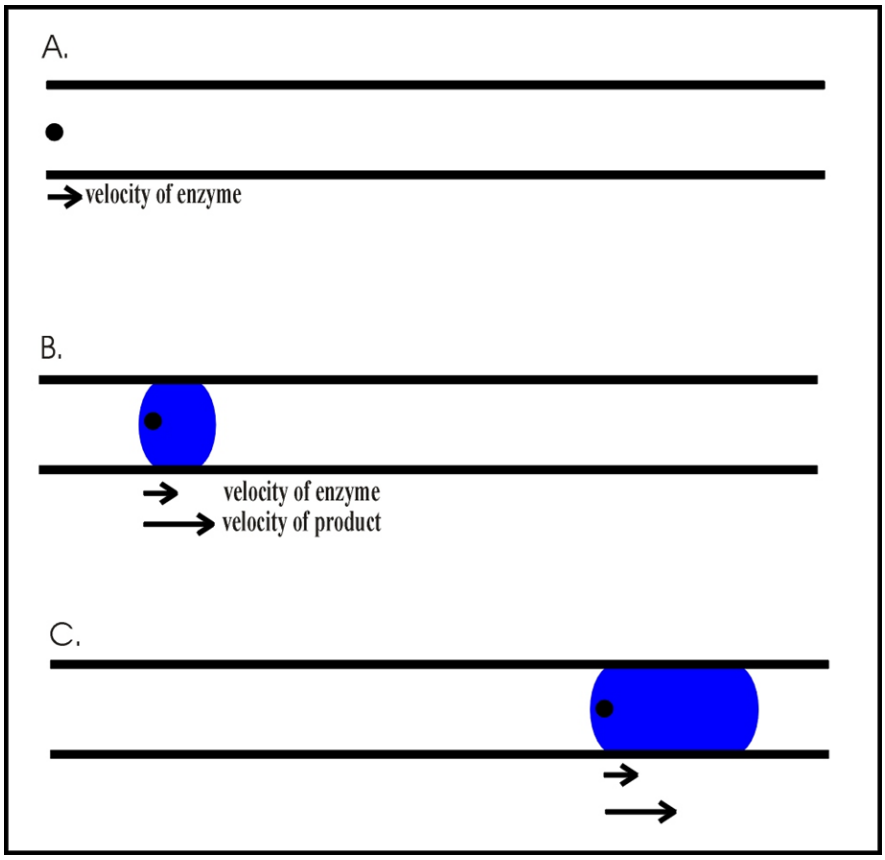

Figure 17: Continuous flow assay illustration. A) Injection of enzyme. B) Product begins to form moving ahead of the enzyme. C) Enzyme is run through the capillary continuously forming product.

In this set of experiments, β-galactosidase was subjected to a continuous flow assay where the capillary had two temperature controlled incubation sections described above in Figure 12. Data was collected at 10, 28 and 50°C with 22 sets for 10 and 28°C and 24 sets for 50°C. Figure 15 shows three electropherograms that are representative of each data set from each of the three temperature conditions.

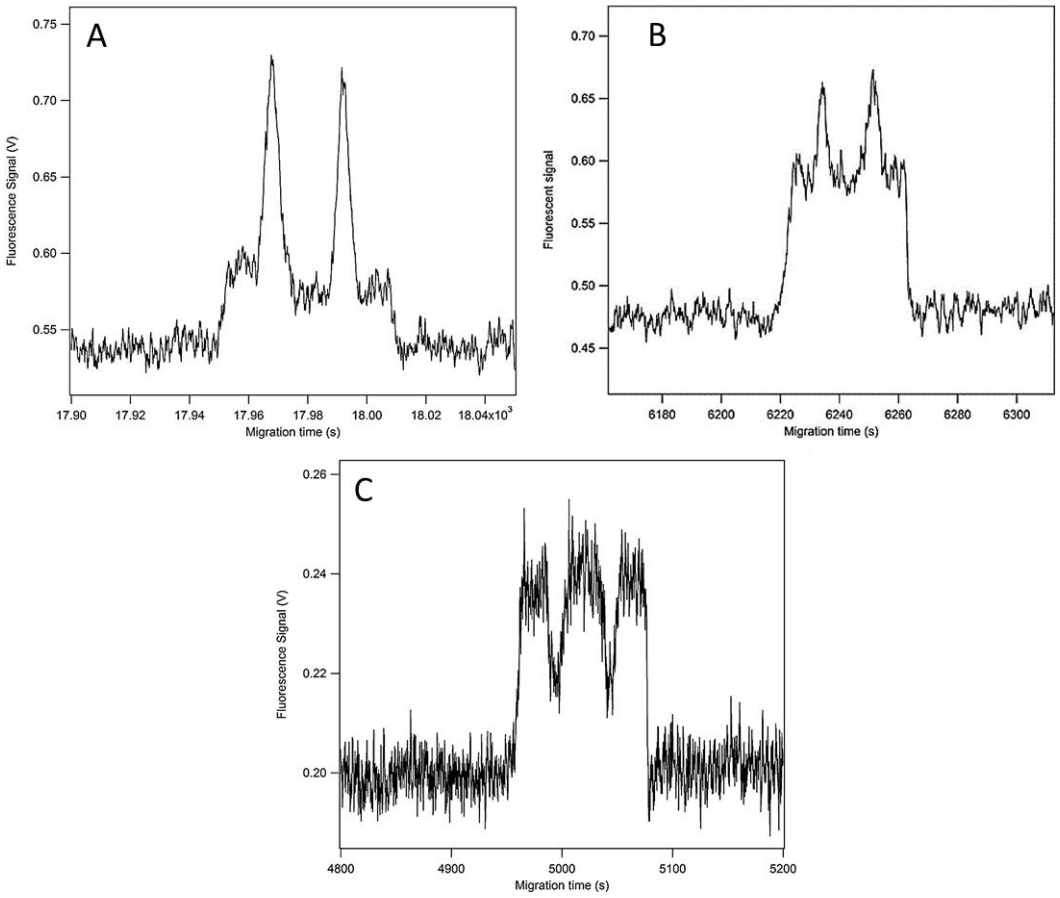

Figure 18: Continuous flow assay performed using dual temperature incubations. Each represent a single β-galactosidase molecule. Zone temperatures both held constant at: A) 50°C B) 28°C C) 10°C.

Each single molecule data set represents 5 distinct sections from left to right on the electropherogram. Sections 1, 3, and 5 are the plateaus representing activity of the enzyme of a period of time at room temperature. Sections 2 and 4 are the spikes representing an increase or decrease in temperature. Each of the plateaus was used to calculate an average activity for that section of the assay. The variation in signal over time is similar to that of the background noise, indicating that the catalytic rate was approximately constant over time as the enzyme traveled through a particular region[63]. A portion of the data points collected immediately before and after the product peak was averaged to determine a baseline equation. This equation was used to correct for a rising

background by subtracting the background component from each data point. Background hydrolysis causes a small portion of the DDAO-gal to hydrolyze as time goes on, as well the continuous assay involves both enzyme and substrate to be mixed together in a single injection vial, resulting in consistent DDAO production. The combination of the two sources of rising background are not sufficient to overtake the signal produced by the enzyme generated DDAO in the capillary.

Three temperatures were chosen to each represent a specific condition relative to ambient temperature. The capillary was cooled, heated and brought to a midrange close to that of room temperature. Rojek and Walt tested bulk solutions of the enzyme for its thermal stability and found that over 55°C the enzyme began to denature[125]. Therefore 50°C was set to test the maximum. At the low end of the temperatures, 10°C was tested under the hypothesis that if high temperature allows an enzyme to access multiple active conformations, then a low temperature should reduce the number of conformations available. Lastly, a midrange temperature of 28°C was chosen to represent a median value. Ideally this value would be set at room temperature but it had to be sufficiently high to produce a measurable activity spike as this was the basis for determining the different sections of the electropherogram. Twenty five degrees Celsius was initially tested but the relationship between the five sections on the electropherogram was not discernable. With sections 2 and 4 maintained at each of the selected temperatures the plateaus of section 1, 3 and 5 were each averaged. The calculated averages and standard deviations are shown in Table 2. As seen in Figure 15 the electropherograms behaved as expected with the peaks at sections 2 and 4 being the highest for 50°C, lower for 28°C and inverted when the temperature went below room temperature.

Table 2: Collected activity averages from sections 1, 3, and 5 with associated standard deviation. Sections 2, 4 were held constant at 10°C (N=22), 28°C (N=22) and 50°C (N=24).

Section 2/4 Temperature	Section 1 Height	Section 3 Height	Section 5 Height
10°C	0.056±0.027	0.058±0.028	0.057±0.028
28°C	0.049±0.020	0.048±0.020	0.048±0.020
50°C	0.060±0.029	0.050±0.026	0.052±0.025

The data was analyzed using analysis of variance (ANOVA) with the differences in catalytic rates tested at the 95% confidence level. The three average rates for a given (constant) temperature showed no significant difference in the average or variation between them. The rates were also compared between the other temperatures studied and also no significance between the average and variance was found. This finding suggests that catalytic dynamic heterogeneity was also indistinguishable. However, this does in fact coincide with knowledge that heterogeneity goes unobserved in bulk solution. Individual enzymes were observed to have their catalytic rates increase or decrease with equal probability of either event to occur as a result of the heated/cooled incubation sections. Due to enzymes showing both increasing and decreasing catalytic rates with an even distribution, there is no net effect to be observed in an ensemble average.

From this point it was concluded that individual molecule characteristics would have to be analyzed and not the averages. The relative differences in rate were compared between sections 1, 3 and 3, 5. When the temperature controlled sections were held at 50°C, the rates between sections 1 and 3 were found to differ by 22% and between 3 and 5 by 43%. However, one of the 24 molecules analyzed displayed a 6-fold rate change between sections 3 and 5. If that molecule is considered an outlier and removed from the data set, the percent difference drops to 19%. The number of molecules whose activity increased after each heating period was found to be equal to the number whose activity

decreased resulting in no net change in the average rate or variance. When the temperature was set to 28°C, the individual molecules showed rate changes equal to 7% and 6% for sections 1, 3 and 3, 5 respectively. Again approximately equal amounts of molecules showed an increased activity as a decreased one. Lastly the temperature was set to 10°C, the average rate change for the individual molecules was found to be 4% for both sections 1, 3 and 3, 5. The number of molecules that showed an increased activity roughly matched the number that decreased.

This data confirms previous findings that heterogeneity is lost in bulk solution. However, as temperature increases an enzyme gains access to a greater range of active conformations. The 50°C condition showed the highest individual molecule rate changes at 20% for the average between two sections. It was much less for the 28°C condition and negligible for 10°C. Figure 16 is an illustration representing the interconversion between active conformations for a single enzyme.

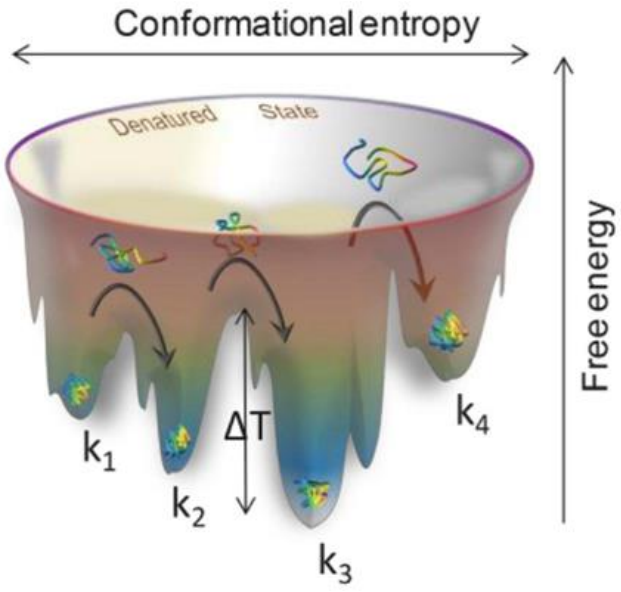

Figure 19: Conformational energy illustration. Each k represents local energy minima achieved by conformational shifts when the enzyme is provided with adequate energy to overcome the barrier. Used with permission[125].

A given molecule will have multiple stable active conformations available to it located at a variety of energy minima. An increase in temperature provides the energy required for the enzyme to loosen its structure and reposition itself into a new conformation. However, if the temperature increase is too great the enzyme will unfold into a denatured state that it is unable to recover from. This provides insight into the conformational changes taking place for a given enzyme being the result of small structural alterations. Larger conformational alterations would most likely result in the breakdown of the quaternary or tertiary structure.

Determining the relative change in activity for a given molecule does not lend itself to suggest what type of conformational change might be occurring. A very small conformational change in or near the active site could be envisaged as having dramatic effects on catalytic rate, whereas a change far away from the active site may not have much impact. It is also possible that large changes in conformation result in little or no changes in activity. Although it cannot be concluded to what degree the conformational shifts are taking place, it is evident that shifts are taking place resulting in stable, long lived and active new conformations. It is suggested that a given molecule does retain conformational "memory" in that the previous conformation has a certain effects on the new conformation possibilities for the enzyme at the next incubation.

A bulk solution assay on the enzyme was also conducted to measure the activity before and after the three temperature incubations. Two minute incubations were performed at 10, 28 or 50°C for a large ensemble enzyme solution and compared an identical mixture which was not incubated. After incubation at 10°C and 28°C the activity did not differ from that of the untreated sample. At 50°C the enzyme's activity

was found to decrease by 8%, suggesting that a portion of the sample denatured at this temperature. The single molecule assay showed no net change in average activity for the 50°C condition. This is due to the single molecule assay only taking account molecules which remained active for the entire assay. If an enzyme was to denature in the middle of the assay it would not have been included in the overall results. A previous study has shown that a fraction of the individual β-galactosidase molecules denature upon a short 50°C incubation[63]. Although speculative it is possible to include the principles of heterogeneity into the denaturation observed here. If individual molecules are created with slight differences resulting in different ranges of dynamic heterogeneity then the temperature at which denaturation occurs would also be a range. This would explain why a certain percentage of molecules denature at 50°C while it was previously stated that the molecules denature above 55°C.

The study reported by Rojek and Walt (2014) studied a much larger number of individual molecules of β-galactosidase for their alterations in catalytic rate upon 47°C sequential incubations. Different temperatures were not a focus of that study. The results at 50°C are in complete agreement with their findings at 47°C. Catalytic rates were found to randomly increase or decrease post heating in both studies for individual molecules with no change to the overall average activity. With the introduction of electrophoresis it is also possible to measure electrophoretic mobility changes which was not possible with the experimental approach taken by Rojek and Walt.

5.3.2. Temperature Controlled Incubation Effects on Electrophoretic Mobility

The second set of experiments performed under the temperature induced dynamic heterogeneity concept insisted of measuring electrophoretic mobility before and after a

temperature controlled incubation. The setup has been previously illustrated in Figure 13. This time the capillary was only split into 3 sections with 1 and 3 being suspended in the air at room temperature and section 2 fixed to the same pipe attached to the water heater/cooler. The same 3 temperatures were used in this study as in the activity assay. The use of longer sections at room temperature and data collection at 50 Hz allowed for a more accurate peak width measurement. Figure 17 shows a representative data set from the 50°C incubation trial. The shapes of the peaks resembled that of Figure 15 with the exception of only a single region where the peak height is above or below the plateau sections. The 28°C peak height was less than that of the 50°C and the 10°C peak height was inverted. Two widths were measured for each data set: the width from the half maximum height on the leading edge to the calculated mid-point of the central spike, then from the mid-point to the half maximum height of the trailing edge. It was these widths that were taken as representatives of the enzymes mobility before and after the incubation section.

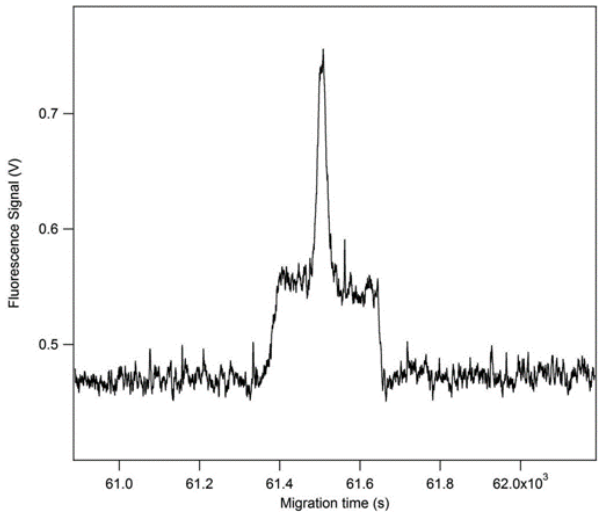

Figure 20: Single incubation at 50°C for a single β-galactosidase molecule following a continuous flow assay. Mobility before and after incubation obtained from electropherogram.

Measurements were made on individual molecules in the following quantities: 50°C (N=21), 28°C (N=18) and 10°C (N=20). The averaged data is shown in Table 3.

Table 3: Average width and standard deviations of sections 1 and 3 when section 2 was held constant at 10, 28 and 50°C. Section width interpreted as mobility of the enzyme within that section.

Section 2 Temperature	Section 1 Width	Section 3 Width
10°C	40.8±18.3	40.5±18.5
28°C	35.0±12.5	34.5±12.8
50°C	34.5±14.2	35.2±14.7

The data was analyzed using ANOVA with differences at the 95% confidence interval considered significant. The averages and variances corresponding to section 1 and 3 did not differ significantly within the same temperature condition or between the temperature groups. Again, the data was interpreted at the single molecule level. When the heated section was maintained at 50°C, the difference between section 1 and 3 was found to be an average of 8%. Roughly an equal portion of molecules showed an increase in peak width as a decrease in width. The same was found for 28°C and 10°C with differences being 5% and 3% respectively. This again confirms that heterogeneity is lost in the averaging effects of the data. On an individual molecule scale, temperature was shown to be a factor in conformational changes resulting in different observed activities. Mobility was observed to follow a similar pattern to that of the activity assay in that heterogeneity was observable at the individual molecule level and not in the averages.

This set of experiments was not concerned with the activity of the enzyme molecules prior to and after the heating or cooling periods. However, with respect to activity the same general trend of increasing and decreasing activities was observed. The plateau of section 3 was just as likely to be higher as it was to be lower compared with

the plateau in section 1. This is an important principle to observe because although this assay is focused on a different property, past conclusions must still hold true.

Electrophoretic theory allows one to predict how much of a change in enzyme shape or charge is required to illicit a given change in electrophoretic mobility[89,129]. The reported 8% change in widths of the box shaped peaks corresponds to a calculated electrophoretic mobility change of $1x10^{-6}$ $cm^2 \cdot V^{-1} \cdot cm^{-1}$. The enzyme β-galactosidase has been stated having a Stokes radius of 6.9 nm, an average buffer radius of 0.25 nm, an axial radius of 1.31 and a net charge of -62.9 at pH 7.3[127]. A conformational change that results in a change in the Stokes radius less than 0.1 nm is sufficient to change the mobility of an enzyme by the stated $1x10^{-6}$ $cm^2 \cdot V^{-1} \cdot cm^{-1}$. Each of the 4 monomers that make up a β-galactosidase molecule is made up of 5 independently folding domains. The first 50 amino acid residues of each monomer are in an extended form with the first 12 residues being highly disordered. Each monomer contains several solvent exposed loops, including those from residues 578-583, 654-690, and 727-733, all of which are highly mobile with multiple possible conformations[100,109]. Staphlococcyl nuclease was used in a study subjected to site-directed mutagenesis where a loss of a single hydrogen bond was shown to alter the CE determined electrophoretic mobility by $3x10^{-6}$ $cm^2 \cdot V^{-1} \cdot cm^{-1}$. The conversion of a single peptide from the *cis* to *trans* conformation through a glycine substitution for an alanine resulted in a $2x10^{-6}$ $cm^2 \cdot V^{-1} \cdot cm^{-1}$ mobility change[130]. The conformational changes associated with the incubations in this study are likely very subtle with no major changes taking place within the protein. Any significant structural change would result in a much larger mobility shift and may result in denaturation or inactivation of the enzyme. This change in mobility due to dynamic heterogeneity is far

smaller than the possible ranges set by the static heterogeneity. As it was observed in the previous study it implies that once a given protein is folded in a particular conformation the full range of conformational possibilities cannot be accessed by the enzyme through dynamic heterogeneity.

5.4. Summary and Conclusion

The studies presented in this chapter were based on and built upon the data collected by Rojek and Walt (2014) where individual molecules of β-galactosidase were subjected to temperature induced conformation changes. Short periods of incubation at elevated temperature resulted in an increase or decrease in activity with an equal probability for each event. Therefore, no net change in the average catalytic activity of the population will be observed. They proposed that this is due to the enzyme switching from one stable, active conformation to another stable conformation with a different catalytic rate upon heating. The findings within the experiment conducted agree in full with the findings of Rojek and Walt. CE-LIF assays performed on individual β-galactosidase molecules showed changes in conformation as a result of brief incubations at elevated temperature (50°C). However, no net change in the population will be observed because the molecules are just as likely to increase in activity as they are to decrease. This change in conformation cannot be explained by the binding of allosteric effectors, since the buffer composition remained constant. I propose that the conformational shifts are caused by a loosening or slight expansion of the molecule allowing for the flexibility for the shift to take place. An interpretation of this event could be that the thermal energy applied to the molecule is causing a disruption in the non-covalent interactions present with the current conformation. Hydrogen bonds and

hydrophobic interactions could break, allowing for the molecule to shift conformation and re-equilibrate at a new stable, low energy conformation. In order to confirm this, a highly sensitive structural measurement would be required at the time when heating occurred in real time. With a high enough resolution in theory the subtle movements would be able to be captured. Two additional temperatures were also tested (28°C and 10°C) in order to provide more information to the temperature induced conformational change hypothesis. It was found that the average catalytic change was dependent on temperature with the greatest range at 50°C. Furthermore, the CE-LIF system is capable of measuring electrophoretic mobility. Individual molecules subjected to a brief heating period demonstrated increasing and decreasing mobilities in equal proportions, resulting in no observable net difference in the mobility of the population. Again, this was found to be temperature dependent by testing 28°C and 10°C. Overall this study further supports the proposal that dynamic heterogeneity is due to conformational changes in individual molecules. It also supports that the heterogeneity becomes elusive to analysis methods with less than 20 molecules in an average. The results found with the activity and mobility studies suggest that these changes are subtle.

6. Effects of Heat shock Proteins on Static Heterogeneity

The data presented in this chapter has been originally published as a portion of:

Jeremie J. Crawford, Frannie Itzkow, Joanna MacLean, and Douglas B. Craig (2015) Conformational change in individual enzyme molecules. *Biochemistry and Cell Biology*, Vol 93 (6), 611-618. Used with permission.

The manuscript was co-written and edited by Dr. D. Craig. Frannie Itzkow was an undergraduate student who participated in the cell transformation process for each of the four cell lines utilized in this study. She was also responsible for the preliminary work for the development of the assay, however no data was obtained. Joanna MacLean provided assistance in the data collection of the 1211 enzyme peaks.

6.1. Background and Introduction

It has been stated previously that static heterogeneity can be envisioned as being caused by factors such as; errors in transcription/translation of the primary sequence or differences in post translational modifications. These differences then have the potential to alter how the molecules fold as they reach difference energy minima. Heat shock proteins play an important role in the proper folding of proteins when a system is under stress[131]. These proteins are present within a cell under standard conditions, however their increased production is the result of stress induced induction pathway resulting in many fold more becoming present in the cell. Therefore, heat shock proteins may be a potential factor in static heterogeneity.

The general theory behind this study was to compare β-galactosidase sourced from a standard *E. coli* strain to that of mutant strains containing various heat shock protein deletions. Both activity and mobility were simultaneously studied. *E. coli* β-galactosidase (EC 3.1.2.23) is encoded with the *lacZ* gene which contains 3075 base pairs. It functions as a homotetramer with 1023 amino acid subunits[108]. This study utilized 4 *E. coli* strains in total; one wild-type strain and then three mutant strains each

containing a single heat shock protein deletion. BW25113 is the parent *E. coli* strain and JW0013-4, JW0054-1, and JW4103-1 are part of the Keio collection as members in a single deletion mutant set *E. coli* K-12[132]. Each mutant strain contains a single deletion as the only variation from the parent strain and all contain strains the *lacZ* deletion. These conditions provided a situation where a comparison can be made between the parent and mutant strains with identical conditions except for the deletion in question. By comparing mutant strains to the wild-type strain through observed catalytic rates, differences due to static heterogeneity, if any, will be able to be observed. Cells were grown under two sets of conditions; 37°C and 42°C where 42°C is the temperature at which the heat shock proteins will be induced.[133] After the growth period the cells were lysed and β-galactosidase was extracted and purified. Assays were then run on the β-galactosidase obtained from each *E. coli* culture.

6.2. Materials and Methods

E. coli strains BW25113, JW0013-4, JW0054-1, and JW4103-1 were purchased from the Coli Genetic Stock Center, Yale University. BW25113 is the parent strain while the deletions are DnaK, DnaJ and GroEL respectively. The substrate was DDAO-gal as outlined previously and all other chemicals were purchased from Sigma-Aldrich.

6.2.1. Transformation, Culture and Harvesting

Each of the 4 *E. coli* strains was transformed with the plasmid pTNA containing wild-type *E. coli lacZ* prepared in a previous study[122]. This portion of the study's method was not performed by myself but as it is critical to the study it will be outlined. The *lacZ* gene protocol can be found in detail in Chapter 4, section 4.3.2. The section also outlines the β-galactosidase harvesting procedures. Enzyme concentrations were roughly equal at

this stage. The principles observed in this study are not dependent on concentration and samples prepared were adjusted for the necessary enzyme dilution.

6.2.2. Sample Preparation

The substrate DDAO-gal was used and prepared as previously stated with toluene washings. The sample, running and sheath buffers were all; 50 mM HEPES (pH 7.3) containing 1 mM $MgCl_2$. The samples were prepared with 125 µL washed substrate, 370 µL buffer and 5 µL diluted enzyme. The final dilution of the enzyme was prepared such that there were approximately 5 molecules on average per capillary volume (6.1 nL). The effective concentration of enzyme in the samples was ~1.4 fmol/L.

6.2.3. Capillary Electrophoresis Instrument

The set-up utilized in this study was identical to that described in the previous chapter (Chapter 5). Details outlining the specifications of the instrument and be found in section 4.2. A 40 cm long, 5 µm internal diameter, 145 µm external diameter uncoated fused silica capillary was used. The entire length of the capillary was suspended in the air maintained at a constant temperature of 21°C. Data was collected at 10 Hz.

6.2.4. Continuous Flow Assay

This experiment used a continuous flow (Figure 14) assay procedure for all of the analysis. Sample was continuously injected at 400 V/cm for the duration of the assay which ranged from hours to overnight.

6.3. Results and Discussion

The novel continuous flow assay was developed by Craig and Nichols (2008) where fluorogenic substrate and dilute enzyme are continuously mobilized through the capillary[63]. The enzyme was diluted to such a point where approximately 5 molecules, on

average, would enter per capillary volume. This provides enough peak separation on the electropherogram. As the molecule traverses the capillary it is continually forming product and since the enzyme and the product have different mobilities they are constantly separated from one another. This produces a smear of product in the capillary which when passed through the excitation beam. The resulting PMT signal produces a box shaped peak in the electropherogram. In this experiment citrate was not included in the buffer, resulting in a less negative enzyme molecule which will cause it to remain in front of the DDAO product smear.

As mentioned the effective concentration of the enzyme in the capillary was 1.4 fmol/L. In the past low concentration enzyme preparations were made in the presence of another protein such as BSA in an attempt to prevent the subunits from dissociating from each other[20]. These "stabilizing" proteins were not used in this study. Experimental evidence has shown that the concern of subunit dissociation is without merit in dilute solutions[134]. The β-galactosidase enzyme activity has been shown to remain linear down to 4.8 fmol/L as the lowest concentration assayed with no additional protein[135]. Alkaline phosphatase activity has also been shown to remain linear down to 460 amol/L without any additional protein[136]. The linear activity findings indicate that the subunits remain intact at low concentration. Figure 18 is a representative section of the electropherograms collected from the β-galactosidase *E. coli* lysates. There are two shifts in the background prior to any peak appearing in the electropherogram. These two shifts are present for all DDAO-gal assays and can be used calculate EOF and the mobility of the DDAO product. Since DDAO-gal is a neutral molecule it will move with EOF alone. The DDAO product is negative, therefore it will move at a lesser rate than EOF. In this case because we are

measuring mobility of each enzyme it will be shown how these two shifts can be used to do so.

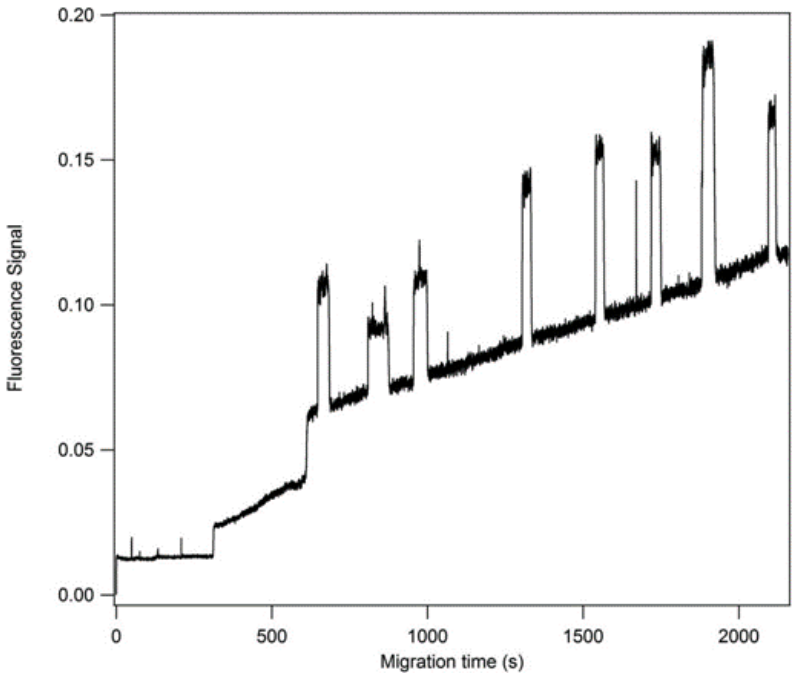

Figure 21: Resultant electropherogram for the continuous flow assay of *E. coli* β-galactosidase. Each box shaped product peak represents the activity and mobility of a single enzyme molecule.

The initial shift in the background is caused by the DDAO-gal beginning to elute from the capillary. Then a second shift occurs when DDAO, present as an impurity from non-enzymatic hydrolysis, begins to pass the detector. Following the two shifts, 8 box-shaped peaks are shown in Figure 18, each represents a single enzyme and its product formed as it traversed the capillary. The time of the first and second shifts are used to calculate the electroosmotic flow and the electrophoretic mobility of DDAO respectively with the following equations:

$$\mu_{EOF} = \frac{L}{t_{m,DDAO-gal}} E \qquad [6.1]$$

Where μ_{EOF} is the mobility of the electroosmotic flow, L is the capillary length, $t_{m,DDAO\text{-}gal}$ is the time of the first background shift and E is the electric field.

$$\mu_{DDAO} = \left(\frac{L}{t_{m,DDAO}} E \right) - \mu_{EOF} \quad [6.2]$$

Where μ_{DDAO} is the electrophoretic mobility of the DDAO and $t_{m,DDAO}$ is the time of the second background shift. The width of each peak was used to calculate the electrophoretic mobility of each enzyme according to the following equation:

$$\mu_{Enzyme} = \left[\frac{L}{\left(t_{m,DDAO} - w \right)} E \right] - \mu_{EOF} \quad [6.3]$$

Where μ_{Enzyme} is the electrophoretic mobility of a given enzyme molecule and *w* is the width of each box-shaped peak. Since the enzyme molecules had different electrophoretic mobilities the time taken to traverse the capillary and therefore incubation time varied. This transit time, *t*, was calculated as follows:

$$t = \frac{L}{\left(\mu_{EOF} - \mu_{Enzyme} \right)} E \quad [6.4]$$

The areas of each box shaped peak collected were compared to a daily standard injections of DDAO performed in triplicate, and divided by the transit time to determine the catalytic rate of each enzyme molecule[63,134]. Each standard injection consisted of a 60 second DDAO injection followed by buffer until completion.

As mentioned earlier there are four stains of *E. coli* sourced β-galactosidase being studied; a standard (BW25113) and three strains each containing a single deletion for a heat shock protein. The *E. coli* was grown at either 37°C (standard conditions) or 42°C (heat shock conditions) with β-galactosidase collected in each case. The specific deletions in the strains were chosen based on their relationship to two different heat shock chaperone systems. *E. coli* β-galactosidase utilizes the DnaK-DnaJ-GrpE but not the

GroEL-GroES system, both however, are chaperone systems for the prevention of misfolding and aggregation of newly formed peptides[131,137]. Protein misfolding increases with temperature and the added stress results in an activation of these systems past 37°C due to an increase in growth up to 42°C. Since only one heat shock system is used for β-galactosidase it was thought that the DnaK-DnaJ-GrpE system would be the one to produce differences in catalytic rates and mobilities due to conformational changes as were proposed in chapter 5.

Altering active heat shock proteins of the applicable system might manifest itself in the static heterogeneity of each enzyme. Table 4 shows the determined averages of catalytic rate and mobility for each lysate.

Table 4: The average and standard deviation corresponding to catalytic rate and electrophoretic mobility for β-galactosidase produced by 4 different *E. coli* strains grown at 37°C or 42°C. (N=Number of molecules).

Strain	Growth temp.	*N*	Catalytic rate (min^{-1})	μ_{enzyme} (×10–4 cm2·V–1·s–1)
BW25113	37 °C	145	27 000±8 000	–1.62±0.05
BW25113	42 °C	154	31 000±9 000	–1.67±0.06
JW0013	37 °C	165	29 000±10 000	–1.60±0.06
JW0013	42 °C	152	32 000±10 000	–1.64±0.04
JW0054	37 °C	144	36 000±17 000	–1.59±0.05
JW0054	42 °C	149	30 000±8 000	–1.61±0.06
JW4103	37 °C	151	30 000±10 000	–1.63±0.06
JW4103	42 °C	151	29 000±9 000	–1.64±0.03

In a previous study, single molecule assays were performed on lysates from BW25113, which contains the *lacZ* deletion and one that was transformed with the plasmid containing *wtlacZ*. The *lacZ* deletion case produced no detectable peaks under identical conditions[134]. Measurements of catalytic rate and electrophoretic mobility have been performed on highly purified β-galactosidase preparations as well as crude homogenates.

Neither case produced a detectable difference in the averages and ranges of mobilities[63]. This suggests that despite the presence of other proteins in crude homogenates from the lysates all peaks can be attributed to β-galactosidase. Furthermore, electrophoretic mobility measurements are not affected by the presence of any additional cellular material.

Assays of β-galactosidase from different wild-type strains of *E. coli* have shown catalytic rates that vary by up to a few fold[56]. As such caution must be used when comparing the data from different strains, despite the strains originating from a single parent. All samples showed relatively similar catalytic rates with no relationship between growth condition and average rate. However, samples grown under the heat shock conditions were slightly more negative ($P<0.05$) for all strains. Figure 19 shows the catalytic rate and electrophoretic mobility plotted against each other for the total collection of 1211 molecules assayed. Catalytic rate was found to be independent of mobility with an R^2 value of 0.03.

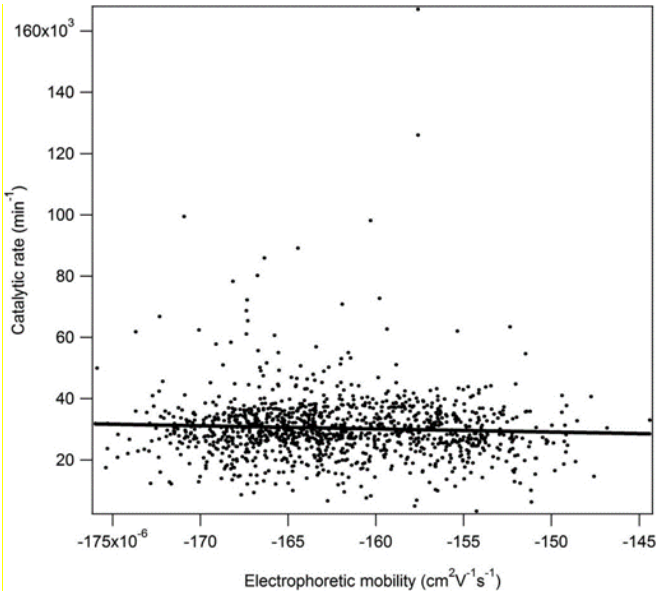

Figure 22: Plot of catalytic rate and electrophoretic mobility of 1211 individual β-galactosidase molecules.

It was previously stated that the enzyme in the capillary moves slower than the DDAO product in this case. This means that the trailing edge of the peak represents product that was formed as the enzyme first entered the capillary. This edge is less sharp because of the increased time spent in the capillary contributing to the diffusion of the product slightly. It is interesting to note that 9 out of the 1211 peaks analysed were opposite to what was just stated. This indicates that the net mobility in these enzyme molecules was less than that of the DDAO product. The population of enzyme molecules showed a distribution of mobilities with these 9 populating the leading edge of that distribution. The mobility of these 9 molecules was calculated from the modified equation 6.3 as follows:

$$\mu_{Enzyme} = \left[\frac{L}{\left(t_{m,DDAO} + w \right)} E \right] - \mu_{EOF} \qquad [6.5]$$

This set of experiments showed no clear effect of the alterations in heat shock protein expression on the heterogeneity of β-galactosidase. This includes comparing within the strains and across strains. The GroEL-GroES system has been found to not be involved in the proper folding and acquisition of activity of β-galactosidase fusion proteins. This is primarily due to the fact that the subunits are too large to be encapsulated by the GroEL-GroES complex although some interactions have been reported[137,138]. According to this statement no difference in heterogeneity for JW4103 was expected to be found when compared with the parent strain since it contained the GroEL deletion.

The folding of β-galactosidase and the associated fusion proteins utilizes the DnaK-DnaJ-GrpE system along with the α-complementation of the enzyme. This system

increases the folding yield of the active enzyme although its absence still allows a significant portion of the enzyme to attain activity. Of the fraction that folds, a subpopulation have been found to be "defective" in that they only retain about 10% of the specific activity compared to the fully functional β-galactosidase[137–141].

The assays performed in this study only analyze individual molecules of β-galactosidase that have sufficient activity for single molecule detection. No differences in heterogeneity were found between the wild-type strain and JW0013 or JW0054, which had the deletions for DnaK and DnaJ respectively. It is possible that no differences were observed due to them being lost in a fraction of β-galactosidase that does not have sufficient activity due to improper folding. Another possibility is that other heat shock proteins are able to compensate for the absence of either DnaK or DnaJ.

6.4. Summary and Conclusion

Analysis of heat shock proteins and their effects on the static heterogeneity of β-galactosidase showed no clear effects. Some speculations have been stated and it remains that no effects were observed by this study but that does not mean that there are no effects to observe. It is believed that single molecule structural analysis would provide further insight into the matter. It remains a possibility that alterations to the enzyme have gone unnoticed by this particular study and that a heat shock protein deletion does in fact produce a significant difference. Outlined in this study are the equations used to calculate mobility of individual molecules based on peak width. Two possibilities on the effects of heat shock proteins and heterogeneity have been presented as a result of this study. The first being that the affected enzyme has lost its activity thereby becoming unobservable by this assay. Therefore only active, unaffected enzymes would be observed. The second

possibility is that heat shock protein chaperone system was able to compensate for the loss of a single protein. Under these possibilities it could be seen that the role played by the deleted heat shock protein was compensated for by either another protein or the existing ones in the chaperone system. This would then allow the enzymes to remain unaltered in their characteristics as measured in this study. This concept remains an open area of research.

7. Kinetics: Determining K_m and K_I from Single Molecules

The material presented in chapter 7 has been accepted for publication in ELECTROPHORESIS (2016) currently in press.

Jeremie J. Crawford, Douglas B. Craig (2016). Determination of the Inhibitor Dissociation Constant of an Individual Unmodified Enzyme Molecule in Free Solution. *Electrophoresis.* DOI:10.1002/elps.201600201

Dr. D. Craig reviewed and edited the submitted manuscript.

7.1. Introduction and Background

Heterogeneity, static or dynamic, has become widely accepted as a property of biological molecules. However, in a large majority of heterogeneity studies the measurements were taken using the same buffer solution throughout the assay. Performing sequential assays on an individual enzyme molecule free in solution while changing the solution between assays is more challenging. Regardless, this is required to assess the effect of different concentrations of substrate or the presence or absence of an effector. A population of a given enzyme has been shown to be quite diverse in its range of catalytic rates. Therefore, if we are to compare the effects of changing substrate concentration we require a minimum of an initial rate at one concentration of substrate and a second rate at another concentration for the same molecule or no comparison may be made. One approach has been to immobilize the enzyme, allowing for the surrounding solution to be changed between assays[19]. This approach was used to determine K_m for individual molecules of alkaline phosphatase, although the values obtained were far greater than the ensemble average from bulk solution[19]. This was likely due to an artifact of the tethering itself which was performed by random covalent linkages between the enzyme's lysine residues and a solid support surface. Due to the enzyme containing a large number of external lysine residues, it is possible for the enzyme to adopt many

different bound positions. This means that the active site could be oriented away from or towards the solid support surface, or any position in between. Figure 20 shows an illustration of two possible orientations.

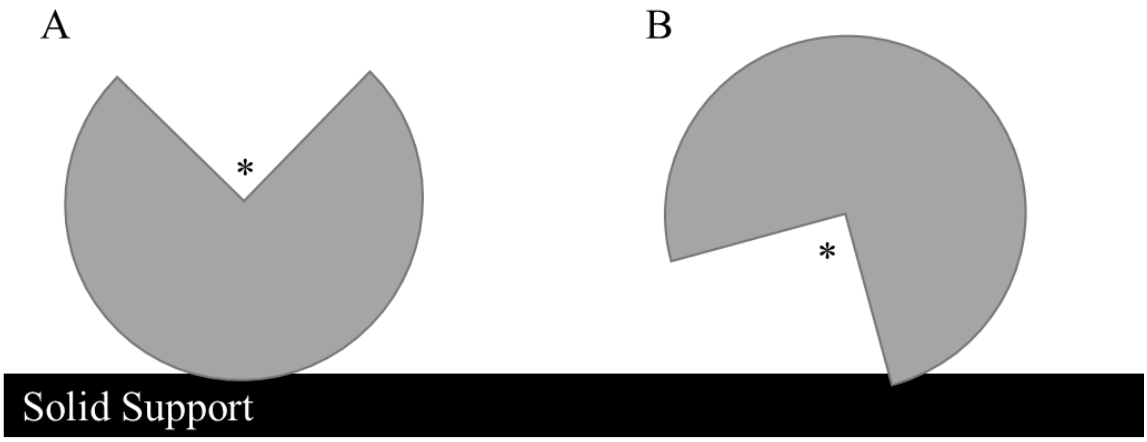

Figure 23: Illustration of two possible enzyme positions when bound to a solid support surface. *) Represents the enzymes active site. A) Active site face up with respect to solid support. B) Active site face down with respect to solid support.

The very nature of tethering may introduce its own heterogeneity. For example a tethered enzyme may be attached to a solid support surface such that its active site is oriented away from the support. The activity may remain as it would be observed free in solution. The tethering also has the potential to restrict substrate access to the active site if the enzyme's active site is oriented towards the support surface. Tethering the molecule may also introduce conformational changes throughout the enzyme itself. As shown in Chapter 5, a very small change in conformation can result in considerable activity differences. The portion of the illustration for the enzyme with its active site bound facing towards the support surface introduces other concerns along with the conformational ones. If the enzyme's active site is facing the surface it is possible that substrate does not have the same accessibility as the previous example. The active site is also now located in an area with a high negative charge density due to the tethering

surface. This may cause conformational changes or other active site related alterations. Tethering has been reported elsewhere in single molecule studies[5,142]. Although this theory is speculative, there is evidence to suggest that when studying enzyme heterogeneity, it would be prudent to avoid such methods that may artificially introduce or enhance heterogeneity.

As the method of choice in this study is CE-LIF, the enzyme and substrate will separate in the capillary due to their different mobilities as it has been described in section 3.1.2. It is therefore possible for enzyme molecules to be mobilized out of one substrate zone and into another of a different concentration. This concept has allowed the measuring of K_m of unmodified individual molecules free in solution. K_m has been found to be a heterogeneous property for *E. coli* β-galactosidase. As reported, most molecules had a K_m value in the range of 50 to 200 μM, with some falling in the 3 to 500 μM range[143].

The rate equation for an enzyme which follows Michaelis-Menten kinetics in the presence of a competitive inhibitor is[144]:

$$V = \frac{V_{\max} S}{(\alpha K_m + S)} \qquad [7.1]$$

Where α is given by:

$$\alpha = 1 + \frac{I}{K_I} \qquad [7.2]$$

Where I is the inhibitor concentration and K_I is the dissociation constant of the enzyme-inhibitor complex. An expression can then be formed to compare the rate in the absence and presence of inhibitor at identical substrate concentrations as follows:

$$\frac{V}{V_I} = \frac{V_{\max} S / (K_M + S)}{V_{\max} S / (\alpha K_M + S)} \quad [7.3]$$

Which simplifies to:

$$\frac{V}{V_I} = \frac{(\alpha K_M + S)}{(K_M + S)} \quad [7.4]$$

If $S << K_m$ this expression simplifies to:

$$\frac{V}{V_I} = \alpha = 1 + \frac{I}{K_I} \quad [7.5]$$

Under these conditions only 2 rates need to be obtained in order to provide a numerical value for K_I[145]. However, if S is not very low relative to K_m, and as K_m differs between individual molecules, then a numerical value for K_m for a given molecule is required to obtain K_I for that molecule as well. To determine both K_m and K_I for a particular enzyme it must be subjected to 3 separate single molecule assays. To first determine K_m, 2 rates must be determined at S_1 and S_2 according to the equation[143]:

$$K_M = \frac{[(V_2 - V_1)S_1 S_2]}{(V_1 S_2 - V_2 S_1)} \quad [7.6]$$

Once this value is known, the rate in the presence of either substrate concentration, S_1 or S_2 and the rate of the same substrate concentration plus the concentration of inhibitor can be used to calculate α and K_I according to equations 7.4 and 7.5 respectively.

β-galactosidase is an enzyme that follows Michaelis-Menten kinetics and is competitively inhibited by L-ribose[146,147]. The bulk solution ensemble value for K_I for β-galactosidase has been determined to be 210 μM, although a different buffer system was used with a much higher ionic strength then this study worked with[148]. The value of 210

μM provided a suitable starting point for this study. The objectives of this study were to create a novel assay in which a single enzyme molecule free in solution could be subjected to multiple solutions consisting of substrate and inhibitor, to determine K_m and K_I for individual molecules and to determine is K_I is a heterogeneous property for single *E. coli* β-galactosidase molecules. The principle idea of subjecting a single molecule to multiple solutions in order to measure more in depth properties is a continued interest and will be investigated further in Chapter 8.

7.2. Materials and Methods

L-Ribose was purchased from Sigma-Aldrich. All other material are as previously described and can be found in Chapter 4, Table 1.

7.2.1. CE Instrument

All assays were performed on the laboratory constructed CE instrument as described in previous sections. Both 10 and 5 μm internal diameter fused silica capillaries were used in this study and will be indicated based on the assay performed. Data was collected at 10 Hz.

7.2.2. Sample Preparation

The sample, running and sheath flow buffers were all prepared as 10 mM HEPES containing 1 mM $MgCl_2$ and 1 mM citrate following the same preparation protocol as was outlined in Chapter 4. The substrate DDAO-gal was washed and prepared as described previously. The enzyme was diluted about 10^8 fold in sample buffer. Three substrate based solutions were prepared as follows: 125 μL washed DDAO-gal in 375 μL buffer resulting in 50 μM substrate (S_1), 75 μL DDAO-gal in 425 μL buffer resulting in

30 µM substrate (S_2), and 125 µL DDAO-gal with 100 µL 1.05 mM L-Ribose in 275 µL buffer resulting in 50 µm substrate and 210 µM L-ribose (I).

7.2.3. Single Molecule Assays

Three different assays were performed in this study: The first was a double incubation assay where the catalytic rate of β-galactosidase molecules was determined by two separate incubations under the same substrate concentration (50 µM) in order to determine the reproducibility of the method. The second assay was also a double incubation where the catalytic rate was determined at 50 µM substrate and then again with a solution of 50 µM substrate plus 210 µM inhibitor. The third and final assay performed was a triple incubation assay of a single β-galactosidase molecule. Measurements were taken after a 30 µM substrate incubation, then 50 µM substrate and lastly 50 µM substrate plus 210 µM inhibitor. The first assay is outlined in Figure 21. Stock enzyme was diluted approximately 10^8 fold in running buffer and was injected into the capillary for 5 s at 125 V/cm. This was followed by a 120 s injection at 400 V/cm of S_1 and a 30 min incubation period where no electric field was applied. Subsequently a 240 s injection at 400 V/cm of the same S_1 solution was done, followed by a second 30 min incubation period. The sample was then subjected to a 400 V/cm potential until the capillary contents exited the capillary.

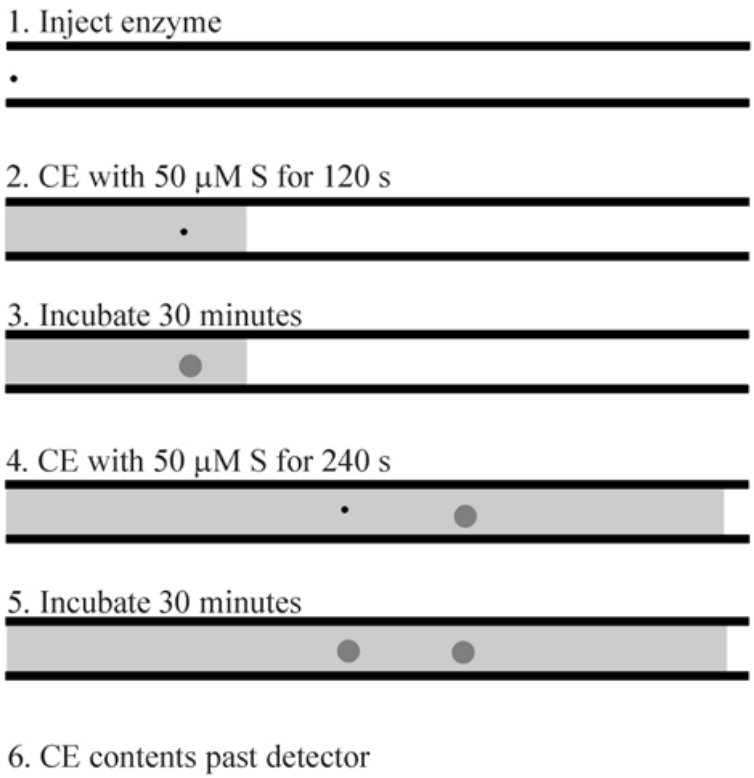

Figure 24: Schematic representing the protocol for a same solution double incubation of a single enzyme. Each incubation in 50 µM substrate with the product zone forming around the enzyme during incubation.

In the second assay, represented by Figure 22 the enzyme was diluted approximately 10^8 fold in sample buffer and injected into the capillary for 5 s at 125 V/cm. This was followed by a 120 s injection of S_1 at 400 V/cm and a 30 min incubation where no electric field was applied. Subsequently a 240 s injection at 400 V/cm was performed using the solution *I* followed by a second 30 min incubation period. The sample was then subjected to a 400 V/cm potential until the contents exited the capillary. In both the first and second assay a 40 cm long, 10 µm internal diameter capillary was used.

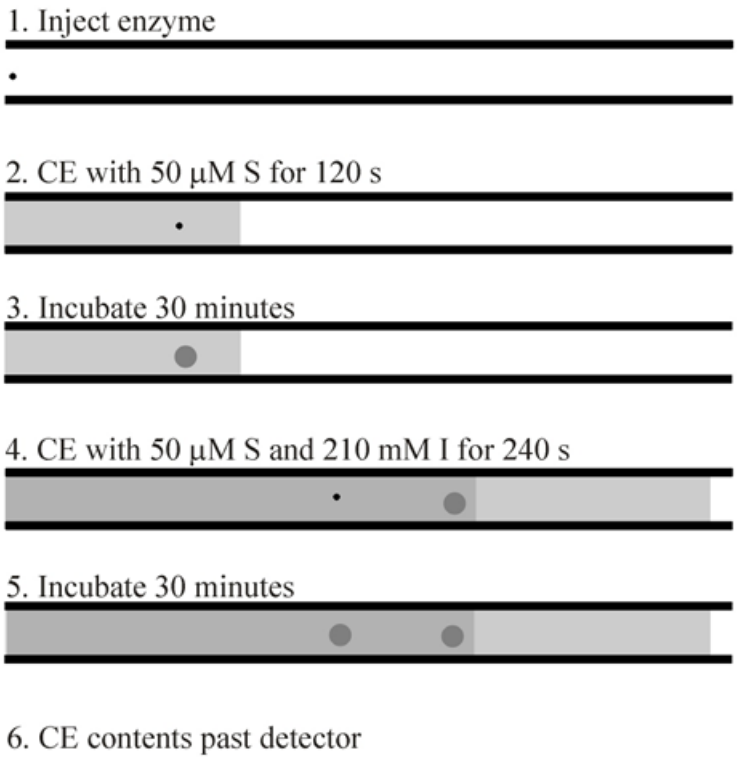

Figure 25: Schematic representing the protocol for a double incubation of a single enzyme with two different solutions. The first incubation in 50 µM substrate and the second in 50 µM substrate plus 210 µM inhibitor.

The third assay is represented in Figure 23 where the enzyme was subjected to 3 separate assay solutions. In this assay enzyme was again diluted 10^8 fold in sample buffer and injected into the capillary for 5 s at 125 V/cm. This was followed by a 15 s injection at 400 V/cm of S_2 and a 30 min incubation period where no electric field was applied. Subsequently a 105 s injection at 400 V/cm of S_1 was performed followed by a 30 min incubation period. Finally, a 240 s injection at 400 V/cm was performed with solution *I* followed by a third 30 min incubation period. The sample was then subjected to a 400 V/cm potential until the contents exited the capillary. In this assay a 40 cm long, 5 µm internal diameter capillary was used.

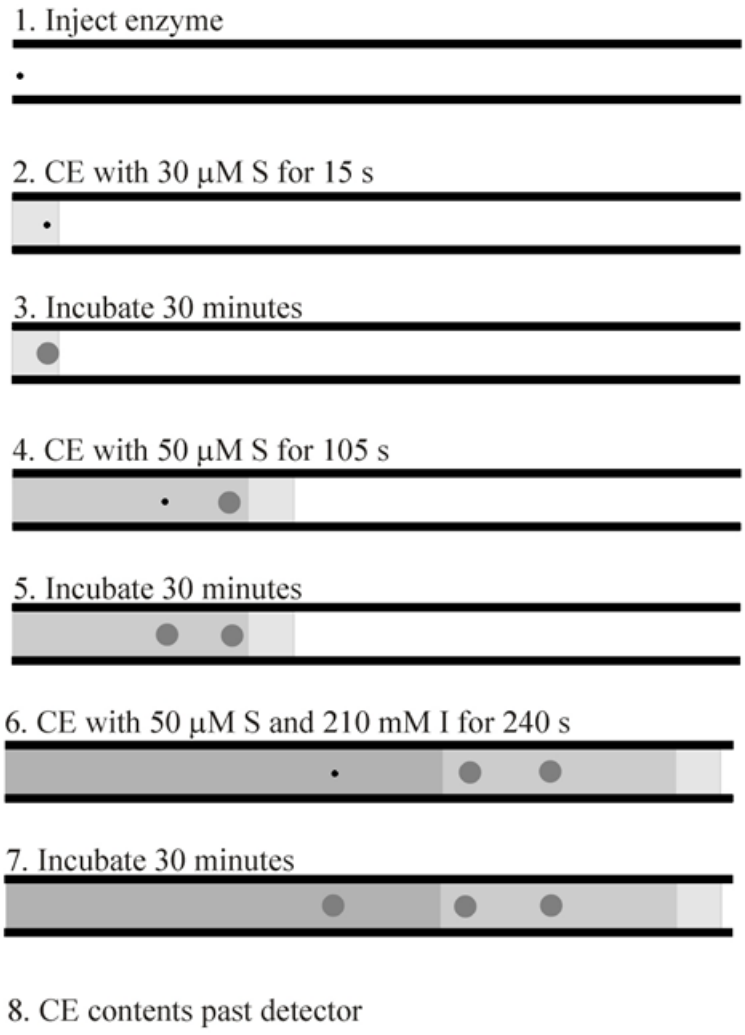

Figure 26: Protocol for a triple incubation of a single enzyme molecule with 3 different solutions.

7.2.4. Mathematical Modeling

Mathematical modeling was performed using Mathematica software (Wolfram) with the assistance of Dr. J. Hollett (University of Winnipeg).

7.3. Results and Discussion

7.3.1. Double Incubation Assays

The two double incubation assays performed include the same concentration of substrate repeated for both incubations and an assay where the second incubation

involved the substrate plus inhibitor solution. Both assays were measuring the conversion of DDAO-gal to the highly fluorescent DDAO product through the catalytic activity of β-galactosidase. Both DDAO-gal and L-ribose are uncharged and therefore have a mobility in the capillary equal to that of EOF. The DDAO product is anionic at pH 7.3 and under these assay conditions will have electrophoretic mobility that is directed towards the injection end of the capillary but not so much that it overtakes EOF. Therefore the net mobility of DDAO will still be in the direction of the detection end but less than that of EOF. The enzyme β-galactosidase has also been shown to have an overall negative charge at pH 7.3 and is even more negative in the presence of citrate. Its resulting net mobility is less than that of the DDAO under these conditions. This concept is crucial for the success of this study.

The concentration of enzyme used for injection was chosen based on its ability to provide an average of one enzyme molecule per 5 s injection volume. A trial and error approach was taken in determining this concentration. Although an average of one molecule was observed per electropherogram it is important to note that the actual number of molecules in a given injection volume is subject to a Poisson distribution. This means that 0, 1 or 2 enzyme molecules were injected most frequently with a small probability of 3 molecules and virtually no possibility of 4 or more. As it has been stated previously, individual molecules have been shown to possess different electrophoretic mobilities[124]. When more than 1 molecule was injected the resulting electropherogram was comprised of sets of overlapping peaks, complicating the mathematical resolution and integration of the peaks. In order to avoid this, only runs that consisted of a single molecule were considered in this study.

In the first double incubation assay a single molecule was introduced into the capillary and subjected to two incubations each being with the same concentration of substrate. The assay was represented previously by the Figure 21 illustration. Figure 24 is a representative data set of the 20 peak sets collected.

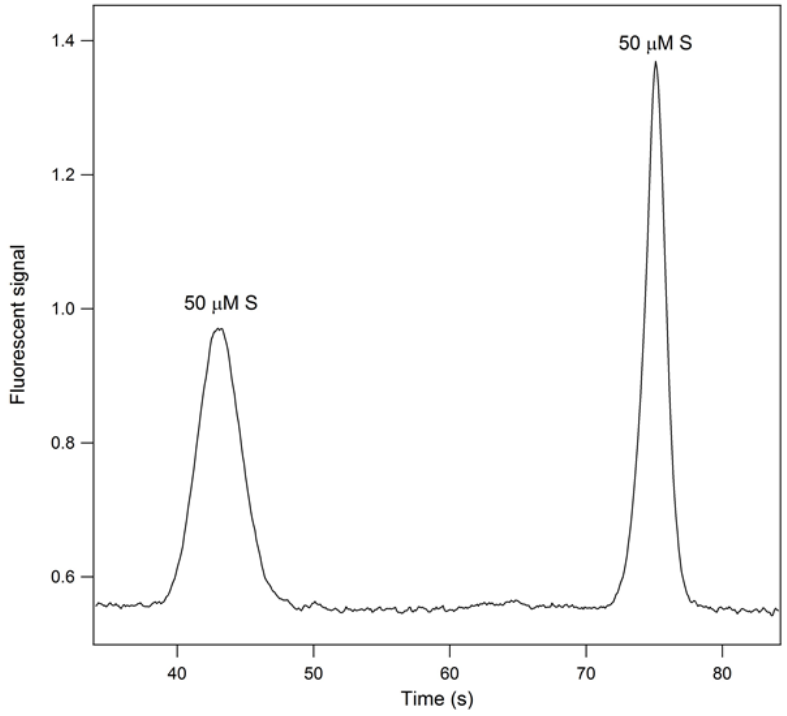

Figure 27: Resultant electropherogram from a double incubation assay with each incubation in 50 μM substrate.

The injected enzyme molecule was subjected to a period of electrophoresis with buffer containing substrate. Since the substrate has a higher net mobility, it quickly overtook the enzyme molecule. The enzyme was then statically incubated for 30 min, during which product was formed. A 30 min incubation was chosen in order to provide an accurate and reproducible average activity for each enzyme at each point of the assays. A shorter time may be taken for the incubation periods, however, a longer incubation time provides a more accurate average for the enzymes catalytic rate. The 30 min incubations for the assays did not provide enough time for significant background hydrolysis of the DDAO-

gal to take place. Also the total incubation time of 30 min did not provide enough time for the product zones to diffuse such that the resultant peak was distorted in the electropherogram. Therefore, the resulting product formed remained in the vicinity of the enzyme molecule until being mobilized. After the first incubation period the sample was again subjected to electrophoresis with buffer containing substrate. As the enzyme's net mobility is less than the product's and much less than the fresh substrate's the product was separated from the enzyme molecule and the molecule was subjected to a fresh substrate solution behind the product pool formed initially. The enzyme was then incubated for another 30 min in the fresh substrate solution and a new product pool was formed. Subsequently the capillary contents were mobilized past the detector, producing the two peaks observed above in Figure 24. The product that was formed during the first incubation was first to pass the detector, resulting in the left peak on the electropherogram. Since it was formed first, there was more time for the product pool to diffuse which is why the observed peak is shorter than the second incubation. As we will see the first peak is consistently shorter and wider than the subsequent peaks from later incubations which also means that peak height and width are not comparable traits of the electropherogram. Instead peak area was used to compare one incubation with the other. Areas of each peak were found through peak integration and compared by the quotient of the 2^{nd} peak area over the 1^{st} peak area. This resulted in a value of 0.96 ± 0.03 (N=20) with 5-fold observed difference between the most and least active enzymes observed in this set. This assay proved that the double incubation assay provided reproducible activities for the enzyme molecules. Using the findings from Chapter 5, it can be assumed that some variation would be expected even with the temperature and substrate

concentration remaining constant. The β-galactosidase enzyme was found to switch between active conformations to a small degree at ambient temperature so in between incubations for a given molecule this trait would be expected to be observed to a small degree.

The second double incubation assay, illustrated previously in Figure 22, was performed in an identical manner to the first, except that the second incubation was performed with a buffer solution containing an identical concentration of substrate plus the L-ribose inhibitor. As mentioned the DDAO-gal substrate and L-ribose inhibitor are both neutral molecules, therefore will have the same net mobility. This was an important property when considering inhibitors to use in this study. If the substrate and inhibitor had different net mobilities the solution would not travel uniformly through the capillary resulting in the separation of the components. The inhibitor was also chosen based on its low reported K_I value (210 μM).[148] An inhibitor that requires a higher concentration to produce the same inhibitory effects has the potential to introduce contaminants and to change the viscosity of the solution at increased concentration. For example, D-galactose was used in preliminary assays at a concentration of 300 mM. It was found to be a source of impurities in the solution even after filtration and autoclaving took place. Autoclaving introduced rapid degradation of the galactose solution, resulting in an observed colour change and an inconsistent rises in background signal. It was for these reasons that an inhibitor with a lower K_I was chosen for this study.

The two incubations of the double incubation assay provided data represented in Figure 25.

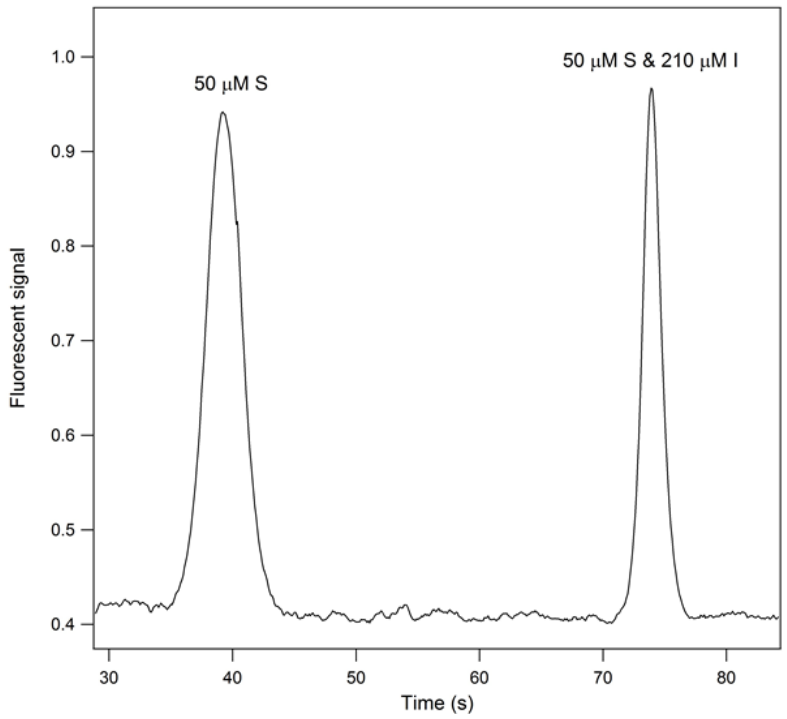

Figure 28: Resultant electropherogram from a double incubation of a single enzyme molecule in 50 μM substrate followed by 50 μM substrate plus 210 μM inhibitor.

The first peak (on the left) represents the first incubation at 50 μM substrate and the second peak (on the right) represents the second incubation with 50 μM substrate and 210 μM inhibitor. The quotient of the 2nd peak over the 1st was again compared and found to be 0.44 ± 0.23 (N=19). Initial observations suggest that the inhibitor does in fact causes a significant decrease. To confirm this the variances of the peak area quotients in the presence and absence of inhibitor were compared by 2-tailed F-test. It was found that these values differ significantly ($p < 0.01$) and that the presence of inhibitor affected the different enzymes differently. This would be consistent with K_I being a heterogeneous property of the enzyme. As [S] was not much less than K_m, and as K_m is a heterogeneous property[143], the double incubation assay did not permit quantification of K_I values for the individual enzyme molecules. In order to do so a value of K_m is required for each molecule in addition to the degree of inhibition.

7.3.2. Triple Incubation Assay

The triple incubation assay is illustrated in Figure 23. A single enzyme molecule was again injected into the capillary and quickly followed by a short injection and incubation in the presence of 30 µM substrate. After incubation, a second electrophoretic injection was performed such that a 50 µM substrate solution overtook the enzyme molecule followed by a second incubation in the new solution. The comparison of these two zones allows for the determination of K_m for the particular enzyme molecule according to equation 8.6. The sample was then subjected to electrophoresis where a solution 50 µM substrate and 210 µM inhibitor was able to overtake the enzyme once more, followed by a final incubation in the new solution. Three product zones were formed through the duration of the assay; the first two in the presence of 30 or 50 µM substrate in the absence of inhibitor and the third in the presence of 50 µM substrate and inhibitor. Comparison of the 50 µM substrate peak with the inhibition peak also in 50 µM substrate allowed for the quantification of K_I using equation 8.4 and 8.5.

During this study timing was absolutely crucial in that each injection provided sufficient separation of the enzyme and its product zone. This allowed for the enzyme to be overtaken by the new solution, and the entire injection time did not exceed the run time of the capillary. If the injections were not long enough, peak overlap was observed and it they were too long the product zones were lost out the end of the capillary before data was recorded. During the double incubation assays, this was not nearly as concerning as it was when attempting to achieve a triple incubation. A series of triple incubation assays were performed using a single substrate solution while varying the timing until sufficient separation was achieved. After the enzyme was injected, solution

injections of 15, 105 and 240 s were determined to be sufficient at satisfying the above criteria.

Initially a 10 µm internal diameter capillary was used in the triple incubation assay. A problem was encountered that can be observed on Figure 26.

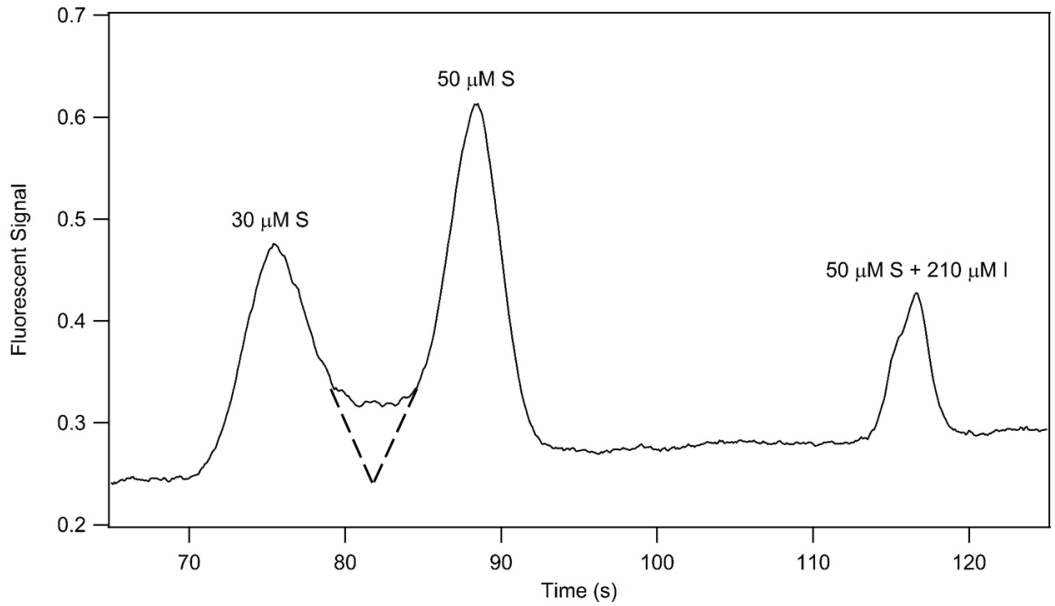

Figure 29: Electropherogram from a triple incubation using a 10 µm internal diameter capillary. Dashed lines represent peak extrapolation resulting in unaccounted area between the first and second peak.

The third peak was well separated from the first two and initial observation did not identify the problem. Upon peak area integration it was found that there was area unaccounted for between the first and second peak shown on Figure 26 by the dashed line. This was caused by a slight shift in the background signal that unfortunately coincided with one of the peaks, complicating the quantification of the area. The shift in background signal does not come unexpectedly, since the solution is changing throughout the capillary. A portion of the background signal is due to DDAO impurities in the substrate solution. It is expected that the concentration of impurities will be proportional to the concentration of substrate. Therefore, when the solution went from 30 µM to 50

µM substrate, there would be an expected rise in background signal to account for the increase in impurities. L-ribose was shown to not cause a significant shift in the background signal. The order of solution injection is not fixed to the order chosen in this study. The injection order was shown to be successful in the manner presented here and, for consistency, was kept the same. In order to deal with the issue of the background shift, a 5 µm internal diameter capillary was used in place of the 10 µm at the same 40 cm length. This smaller diameter capillary provides significantly lower background signal than the larger diameter capillary, thereby lowering the effects of the shift rather than attempting to remove it.

The 5 µM internal diameter capillary proved successful in reducing the effects of the background shift, allowing for baseline separation between the first and second peak. Figure 27 shows the resultant electropherogram from one of the three data sets collected.

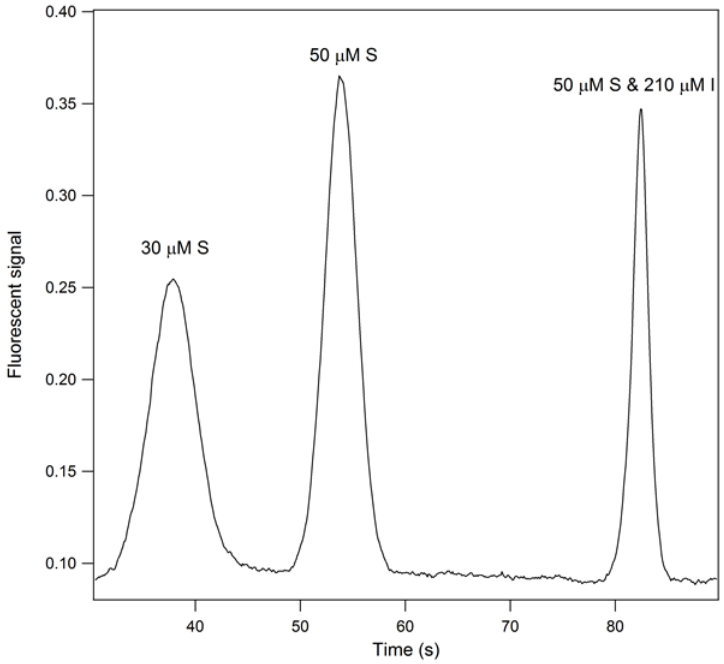

Figure 30: Electropherogram from a triple incubation using a 5 µm internal diameter capillary. Solutions were introduced into the capillary in the following order: 30 µM substrate, 50 µM substrate, and 50 µM substrate plus 210 µM inhibitor.

Each peak represents the product formed in the presence of each of the three solutions. Once again the earlier eluting peaks are wider due to more time for diffusion to occur. A total of 3 molecules were assayed with the relative peak areas along with the determined values for K_m and K_I are shown in Table 5.

Table 5: Data obtained from measuring the activities of three individual β-galactosidase molecules each during a triple incubation assay on a 5 μm internal diameter capillary. Calculated K_m and K_I values are presented for each molecule.

	Solution (Peak Area)			**K Constants**	
Molecule #	**30 μM S**	**50 μM S**	**50 μM S + 210 μM I**	***K_m* (μM)**	***K_I* (μM)**
1	0.85	0.96	0.45	13	38
2	0.25	0.33	0.21	43	170
3	0.26	0.30	0.12	17	35

This data proved consistent with the double incubation data with inhibitor which suggest that the enzyme is heterogeneous with respect to K_I. Although the data set is small, there appears to be a general pattern in which a low value for K_m coincides with a lower value for K_I and vice versa for a higher value of K_m. This property can be envisioned due to the nature of competitive inhibition. L-ribose and the substrate utilize the active site and if the enzyme has a high affinity for the binding of substrate it is proposed that the same affinity would be applied to any molecule using the active site. Therefore since competitive inhibitors share a common binding site with substrates and tend to have similar structural aspects there would be a relationship between the bindings of the two.

7.3.3. Mathematical Modeling

Heterogeneity amongst V_{max} values for given enzymes has been shown based on the relationship between V and [S] for single molecules. However, differences in values for K_m for individual enzyme molecules may be more interesting. The heterogeneity in V_{max} has the effect of altering a V vs. [S] curve by stretching or shrinking the Y-axis alone. This effect is also observed through the change in enzyme concentration and does

not result in a change to the hyperbolic shape of the curve for the Michaelis-Menten enzyme. Heterogeneity in K_m has the potential to cause the curve to deviate from its hyperbolic shape. In a previous study the effect of heterogeneity in K_m was modeled but was found to have little effect. Indeed, any effect found would not likely be discernable from experimental error. This was due to the effect of a molecule with a lower value for K_m largely averaging out the effect of a molecule with a higher K_m[143]. Here, the effect of heterogeneity with respect to K_I on the relationship between V and [S] for an enzyme which follows Michaelis-Menten kinetics in the presence of inhibitor was modeled.

The average rate, V_{av}, for an enzyme population following Michaelis-Menten kinetics in the presence of a competitive inhibitor in which the value of K_I falls within a Gaussian distribution, $f(K_I)$, is given be the equation:

$$V_{av} = \int f(K_I) V(K_I) dK_I \qquad [7.7]$$

Where

$$f(K_I) = e^{\frac{-1}{2\sigma^2}\left(K_I - \overline{K_I}\right)^2} \qquad [7.8]$$

The curves for a population of enzyme molecules with a value of K_m at 300 µM and a Gaussian distribution of K_I with a mean of 210 µM and a RSD of 50% when [I] is 100, 210 and 500 µM are shown in Figure 28, along with the curves when K_I is constant at 210 µM. At all three concentrations of I, there is a slight decrease in the enzyme rate when K_I is heterogeneous.

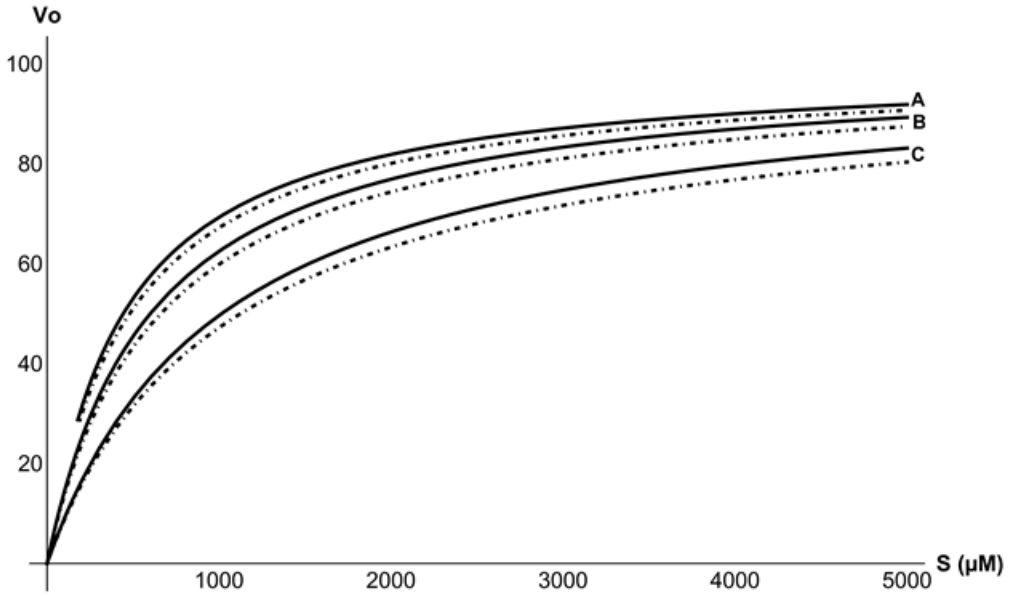

Figure 31: The theoretical Michaelis-Menten curves for a population of enzyme molecules that are homogeneous and heterogeneous with respect to K_I are shown. (A) solid line = 100 µM I with K_I = 210 µM and K_m = 300 µM, dashed line = 100 µM I with a Gaussian distribution of K_I where the mean = 210 µM and RSD = 50% and K_m = 300 µM. (B) solid line = 210 µM I with K_I = 210 µM and K_m = 300 µM, dashed line = 210 µM I with a Gaussian distribution of K_I where the mean = 210 µM and RSD = 50% and K_m = 300 µM. (C) solid line = 500 µM I with K_I = 210 µM and K_m = 300 µM, dashed line = 500 µM I with a Gaussian distribution of K_I where the mean = 210 µM and RSD = 50% and K_m = 300 µM.

Figure 29 represents the effects of increasing RSD for a Gaussian distribution of K_I when the mean value remains at 210 µM. When the RSD is 10% any effect would most likely not be discernable from experimental error. At 20% it may or may not be notable, however, at 30, 40 and 50% RSD the effect increases to a point where it is likely to be notable.

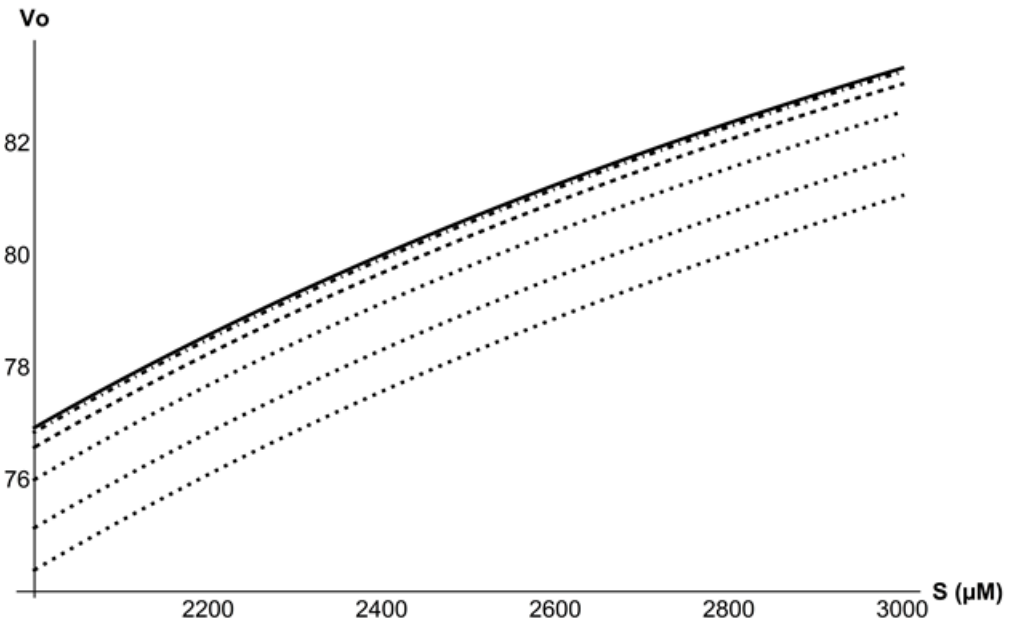

Figure 32: The theoretical Michaelis-Menten curves for a population of enzyme molecules that is heterogeneous with respect to K_I with and increasing RSD are shown. Solid line = 210 μM I with K_I = 210 μM. Dashed lines in order from the highest to lowest are 210 μM I with a Gaussian distribution of K_I where the mean = 210 μM and RSD = 10%, 20%, 30%, 40% and 50%. In all curves and K_m = 300 μM.

The modeling in Figures 28 and 29 does not incorporate any heterogeneity in K_m. In Figure 30 the relationship between V_{av} and [S] is shown when [I] is 210 μM and both K_m and K_I follow a Gaussian distribution according to:

$$V_{av} = \int\int g(K_I, K_m) V(K_I, K_m) dK_I dK_m \qquad [7.9]$$

Where

$$g(K_I, K_m) = f(K_I) e^{\frac{-1}{2\sigma^2}\left(K_m - \gamma \overline{K_I}\right)^2} \qquad [7.10]$$

And γ = 300 μM/ 210 μM.

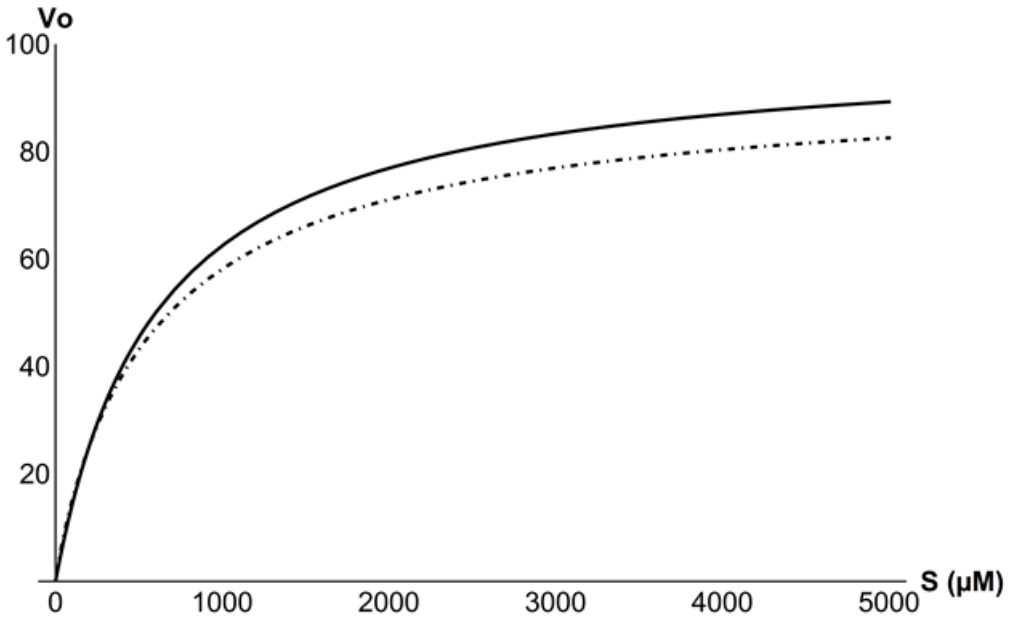

Figure 33: The theoretical Michaelis-Menten curves for a population of enzyme molecules that is heterogeneous with respect to both K_I and K_m. Solid line = 210 µM I with K_I = 210 µM and K_m = 300 µM for a homogeneous population. Dashed line = heterogeneous population where both K_I and K_m follow a Gaussian distribution where the mean is 210 µM and RSD is 50% and the mean is 300 µM and the RSD 50% respectively. K_m is linearly proportional to K_I.

K_m is given with a mean of 300 µM and an RSD of 50% and K_I with a mean of 210 µM and an RSD of 50%. In this study a relationship was determined between K_m and K_I. For the purpose of this modelling K_m was linearly proportional to K_I and follows a Gaussian distribution. This resulted in an increase in the deviation of the curve for the heterogeneous population from that of the homogeneous population.

From the data collected and the modelling performed it is suggested that there exists a relationship between K_m and K_I for single molecules. Proof of such a relationship would involve a sampling of much more than 3 molecules. Due to the probability factor of single molecule injections it was deemed sufficient to currently stop the study once 3 data sets were collected. However, it remains a future direction to gather the data in order to confirm or deny if such a relationship exists. Due to the constraints of "chasing" an enzyme molecule with new solution each time the current approach appears limited to a 3

solution maximum. The next chapter (8) outlines new methodology with the potential to subject a single molecule to an increased number of different solutions as it traverses the length of the capillary. As stated, a greater sample size is desired using the 3 solutions to measure K_m and K_I for single β-galactosidase molecules. Single molecule kinetics remains an active area of research and will be discussed in both Chapter 8 for alternative assays and Chapter 10 as future directions.

7.4. Summary and Conclusion

In this study, single molecules of the enzyme β-galactosidase were subjected to multiple solutions during the course of a single assay while the enzyme itself remained free in solution. Initial data collected showed that a double incubation of a single molecule in 50 μM substrate was reproducible, showing an averaged ratio of the second incubation over the first to be 0.96 ± 0.03 (N=20). The same double incubation principle was then applied while replacing the second solution to one containing 50 μM substrate and 210 μM inhibitor. The average ratio of the second peak area over the first was 0.44 ± 0.23 (N=19). This suggested that the inhibitor was in fact providing significant inhibition at this concentration and that individual molecules are each affected differently by the presence of inhibitor. This is consistent with heterogeneity for an enzyme population with respect to K_I. Since individual molecules have been previously found to be heterogeneous with respect to K_m, quantification of K_I for a single molecule would require its own specific value for K_m. In order to calculate both K_m and K_I from a single molecule, three data points were required; two points each at a different substrate concentration and then one point at one concentration of substrate with the presence of inhibitor. A novel assay for the introduction of three separate solutions to a single enzyme molecule in a capillary

was developed. Three separate enzyme molecules were assayed, being subjected to incubations in 30 µM substrate, 50 µM substrate and 50 µM substrate plus 210 µM inhibitor in that order. The assayed molecules were found to be heterogeneous with respect to both K_m and K_I. Furthermore there was indication that a higher or lower K_m was associated with a higher or lower K_I value respectively. A greater number of molecules in the ensemble would be able to prove or disprove this theory. Mathematical modeling was performed and it was found that heterogeneity in K_I alters the Michaelis-Menten curve for a population of enzyme molecules in the presence of a competitive inhibitor.

8. Single Molecule Michaelis-Menten Kinetics

The work presented in this chapter remains inconclusive at the present moment. Preliminary work has been performed and it has shown merit towards becoming a novel assay. The current stage of the study will be presented with further possibilities being discussed in the Future Directions chapter.

8.1. Objective

The purpose of this study was to create and apply a novel assay for which Michaelis-Menten kinetic properties may be obtained from a single enzyme molecule using a different approach than what was presented in the previous chapter. The study was focused on measuring both K_m and K_I for a single β-galactosidase molecule. In order to achieve this, a single β-galactosidase molecule must be subjected to a minimum of three different solutions. Chapter 7 outlines variables, equations and theory in detail as to why three different solutions are required in order to calculate both K values for a given enzyme. In brief, activity obtained from two different substrate concentrations for the enzyme are required in order to calculate K_m, which was previously determined a heterogeneous property. Then a third solution containing an inhibitor at a known concentration along with a substrate concentration equal to one of the previous solutions will provide numerical values for activity for an enzyme in the presence of an inhibitor. The measured activity value for the substrate and the inhibitor + substrate solutions provide the means to calculate K_I for the single molecule. As stated previously, K_I was also found to be a heterogeneous property for β-galactosidase.

8.2. Methodology

In order to achieve three different activities for a single enzyme as it traverses the capillary it must come into contact with each solution before the enzyme reaches the detection end and exits the capillary. The methodology described in Chapter 7 involved injecting a single enzyme molecule and then "chasing" the enzyme with a new solution each time until it was overtaken completely and left to incubate in the new solution for a period of time. This method proved successful in obtaining the three desired activities required for calculating K_m and K_I. However, it was limited in the amount of solutions a single molecule could be subjected to as every new solution introduced has to be electrokinetically injected for longer periods of time. This condition results in the enzyme being positioned close to the detection end of the capillary by the time the third solution was introduced, not allowing for a fourth to be injected. An assay was developed in order to reduce EOF to a very small value allowing for more selective control over the migration of the enzyme, DDAO-gal and DDAO through the capillary. As mentioned previously, EOF is a condition which arises from the negatively charged silica glass capillary interacting with the solvent creating a flow of solution through the capillary. By creating a barrier between the glass and solvent EOF can successfully be reduced or eliminated creating a situation where the molecules will move to or from the detector based on the applied potential to the capillary.

8.2.1. Capillary Coatings

Fused silica capillaries have a large negative charge density on the internal surface which is not always desired. This charge may be shielded with a variety of polymers resulting in a reduction or elimination of EOF. Genescan and PVP were two

polymers utilized in this study. Both polymers illustrate the same principles in binding to the capillary wall blocking the negative charge of the glass. The Genescan polymer is a trademarked compound of Applied Biosystems and its exact composition is not available to the public. Various capillary coatings are beneficial in that they can reduce band broadening or permanent retention of basic proteins which have a positive charge. Permanent coatings may also be used but as mentioned before they are quite costly and time consuming to prepare. The purpose of the capillary coatings in this study was to suppress EOF for the assay by dynamic capillary coating. Typically the coatings have not been used with narrow bore capillaries required for single molecule analysis due to the capillary becoming plugged. Dynamic coating has been shown to be successful with a 10 μm internal diameter capillary[149]. The benefits to dynamic coating with GS-6 and PVP is that they are relatively inexpensive and easy to prepare each day. Although, a major drawback is that the coating in the capillary degrades over time. This has the potential to create an uneven coating situation, resulting in uneven EOF through the capillary or the coating may be released from the capillary wall and form a complete or partial blockage, much like a blood clot in an artery.

The desired outcome of coating the capillary in this study was to reduce EOF as much as possible, evenly throughout the capillary. With EOF reduced to a very small value, charged molecules will move in the direction dictated by the potential applied to the capillary. With the coated capillary and applied potential such that the injection end was at a positive potential, EOF is of a small magnitude in the direction of the detector. This created conditions in which neutral or positive molecules will migrate into and through the capillary while negative species will remain in the injection vessel. If any

negatively charged molecules are already present in the capillary they will migrate away from the detector towards the injection end under these conditions. If the applied potential was switched such that the injection end was at a negative potential the resulting EOF remain low but would now be in the direction of the injection end of the capillary. Therefore negatively charged molecules would migrate in and throughout the capillary while neutral and positive species remain in the injection vessel. This is particularly useful since DDAO-gal is a neutral molecule while DDAO and β-galactosidase are negatively charged. This characteristic can be exploited to control the direction of the substrate and product, causing them to move in different directions. As negatively charged molecules will not migrate into the capillary with a positive injection potential the DDAO impurity present in a DDAO-gal solution will not enter the capillary through electrokinetic injection. Figure 31 illustrates four possible conditions that may be imposed on a solution containing β-galactosidase, DDAO-gal and DDAO. Relative mobilities are represented based on applied potential and whether a coating is present or not. The concepts illustrated provide the basis for the assay presented in this chapter. It will be shown how to utilize these various mobility conditions to execute a particular assay. The overall goal is; to subject a single β-galactosidase molecule to multiple, different solutions in order to measure its activity under each set of conditions and apply the results to equations, allowing for the calculation of K_m and K_I for a single molecule.

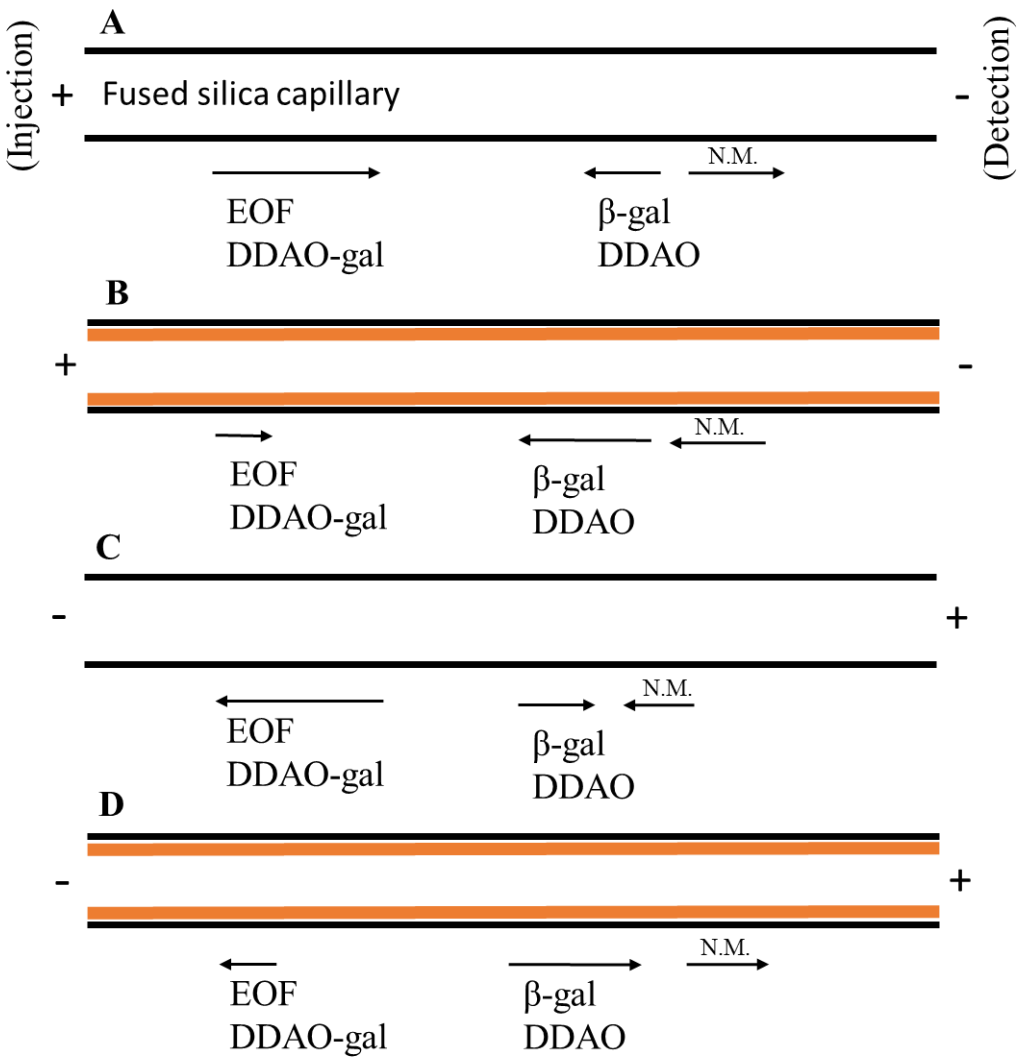

Figure 34: Electrophoretic mobility illustration for β-galactosidase, DDAO-gal and DDAO under coated and uncoated capillary conditions. Arrow indicate the direction and relative magnitude of the mobility for the given molecule. Exact mobilities not shown. A) Uncoated, positive injection potential. B) Coated, positive injection potential. C) Uncoated, negative injection potential. D) Coated, negative injection potential.

8.2.2. Materials and Methods

The materials and methods for GS-6 and PVP assays have been outlined in section 4.3.4. In this study DDAO-gal was not required to undergo the toluene washes. Due to the conditions of the assay and the principles represented in Figure 31 when DDAO-gal is electrokinetically injected into the coated capillary any DDAO impurity

will remain in the injection vessel. Figure 32 illustrates the protocol for performing the EOF suppression assay and is applicable for either coating. At the beginning of each day the capillary was electrophoretically injected with NaOH at 400 V/cm with a negative injection potential. All electrokinetic injections, positive or negative injection potential, were performed at 400 V/cm. The NaOH stripped any residual coating from the capillary allowing for a fresh start each day. The capillary was then dynamically coated with coating buffer for 30 minutes followed by running buffer. The purpose of this was to first coat the capillary evenly using a higher concentration of GS-6 or PVP and then rinse any excess coating from the capillary using a solution containing a lesser concentration of coating material. By using a rinsing solution that contained some amount of the coating polymer the established coating was preserved through the rinsing process. The capillary was then checked for alignment as previously stated. Once the coating and alignment were established, a negative injection potential was used to run substrate into the capillary. Specific injection times and substrate concentrations are not specified due to complications encountered that will be addressed in the discussion section of this chapter. The injection potential was then switched to a positive potential and a dilute enzyme solution in running buffer was injected until the run was completed.

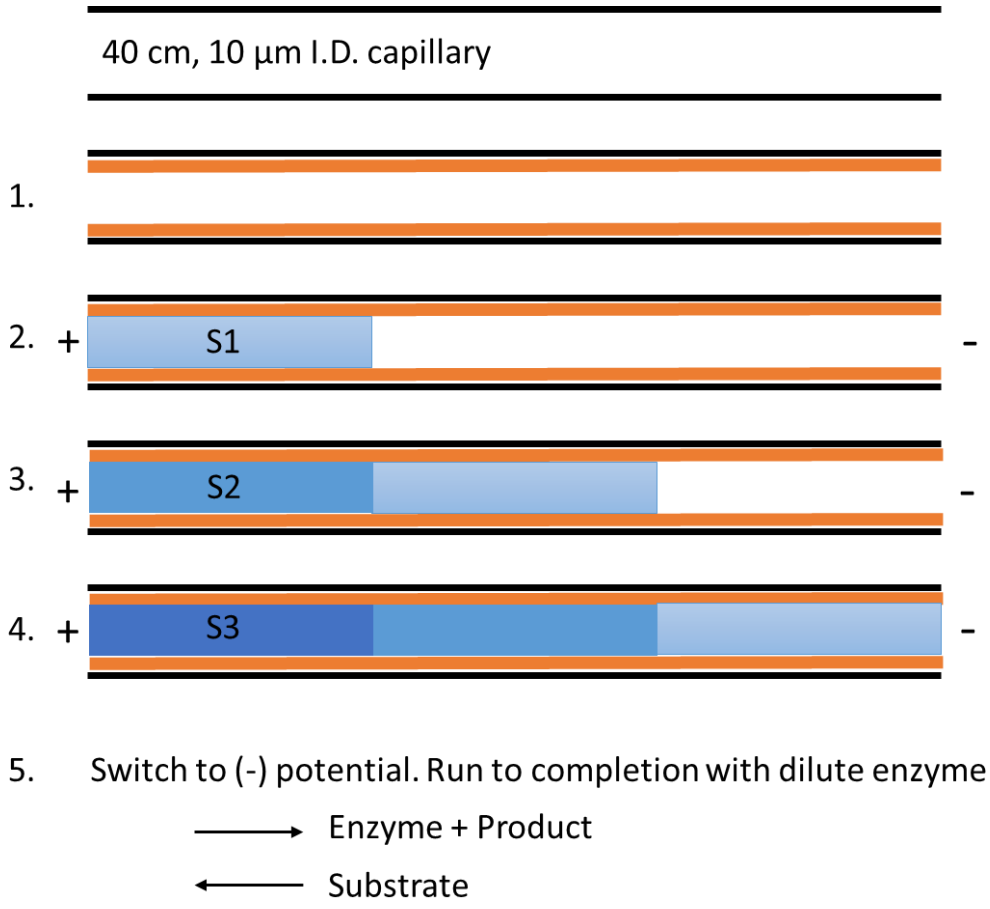

Figure 35: Capillary coating procedural outline. Step 1: Dynamic coating (GS-6 or PVP), Steps 2-4: Fill with various substrate concentrations electrokinetically. S1) Lowest concentration S2) Intermediate S3) Highest. Step 5: Switch potential, run with dilute enzyme in buffer.

8.3. Discussion

Once the capillary has been filled with the desired substrate gradient and the assay is taking place with a dilute enzyme solution, a single molecule will enter the capillary. As the enzyme enters the capillary, it will meet the substrate that was last to be injected during the set-up of the assay. It will then begin forming product as it moves through the first substrate concentration zone resulting in a box shaped peak with a height proportional to the activity of the enzyme at that concentration. The enzyme will then reach the second substrate concentration and its activity will change either increasing

with a higher substrate concentration or decreasing with a lower concentration. The final substrate concentration will have the same effect. Using Figure 32 as an example with S3 as the highest substrate concentration and S1 as the lowest the expected result would represent a staircase with decreasing steps. Figure 33 is an illustration of the staircase effect expected to be observed from this assay.

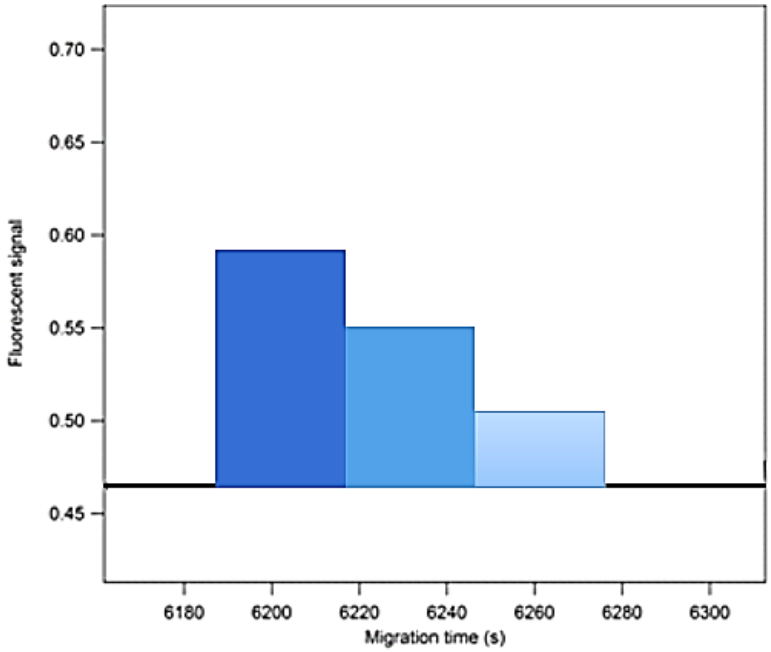

Figure 36: Theoretical data representation of the activity for a single enzyme being subjected to three different substrate concentrations. Dark blue represents the highest concentration and the lightest blue represents the lowest.

Each resulting box-shaped peak would come in contact with the next as there are no gaps in the substrate gradient where a baseline would be re-established. The results would provide an activity paired to each substrate concentration for each molecule analyzed. Using insight provided from previous studies here looking at static and dynamic heterogeneity, it is hypothesised that individual molecules will have different susceptibilities to changing substrate concentrations. For example it is possible that a particular enzyme retains most of its activity even as the concentration of substrate decreases. Or the opposite is possible where even a small drop in substrate concentration

cause the observed activity to decrease significantly. With catalytic rate data paired with each substrate concentration, it is possible to calculate K_m for individual molecules. If an inhibitor was to also be added to one of the substrate solutions it would be possible to calculate both K_m and K_I for individual molecules. This will be the focus of a later chapter and will be explained in detail there.

This assay would have provided a novel method for monitoring single molecule properties throughout a changing environment. Due to time constrictions and technical difficulties, data was not obtained at this time, however the assay remains as a future priority. Future directions include modification of the coating and running buffer concentrations in hopes to reduce the amount of loose material and plugs within the capillary. Once a stable and reproducible coating has been established, the time required for a neutral species to traverse the capillary can be recorded. This time will provide the intervals for filling the capillary with various solutions, provided that they are neutral or of opposite charge to the enzyme being studied. It is important to note that all of the solutions chosen to fill the capillary must have similar properties. The assay relies on the ability to inject the solutions at one injection potential and run the assay with the other potential. In theory it is possible to fill the capillary with more than three solutions as the only limit is capillary length and the ability to resolve the differences as the enzyme traverses from one solution to another. A variety of solution combinations may be chosen depending on what the experimenter desires as an end result. The assay was attempted (briefly), with a 2 μm internal diameter capillary which would make it the smallest dynamically coated capillary assay. There was evidence of viability with overnight dynamic coatings, although it was not investigated further at the present moment. Lastly

there is concern with the ability to coat and re-coat a capillary with consistency in that each day when the capillary is coated it will behave like a fresh coating. This means that the coating from the previous day must be entirely removed leaving the silica glass exposed to be recoated the following day. When NaOH was electrokinetically injected the following day there are uncertainties about the stage of deterioration of the coating in the capillary. This makes EOF unpredictable, therefore it becomes difficult to predict the mobility of NaOH and the extent to which it will be able to remove the residual coating. For this reason NaOH must be pressure injected into the capillary to remove the coating material prior to re-coating the capillary. These conditions applied to a 10 μm i.d. capillary are far easier to maintain, however, there is a signal to noise issue that arises. The continuous flow assay described in Chapter 5 involves an enzyme traversing the capillary with no static incubation period. The enzyme only forms product for the short time that it remains in the capillary. Due to the amount of product being small, the resulting signal is not as large as it would be if the enzyme was left static in the capillary for a period of time such as the assay described in Chapter 7. It is because of this that signal to noise is of greater concern. The smaller the internal diameter of the capillary, the lower the background signal will be, therefore the small amount of product formed by the enzyme will be better resolved in the electropherogram. The 10 μm i.d. capillary was unable to meet these conditions therefore a 5 μm i.d. was desired. This assay will be a future focus of the laboratory.

8.4. Summary and Conclusion

Although this study is not complete it has provided the groundwork for a novel assay in which a single enzyme molecule may be subjected to various solutions while

remaining free in solution. This is an alternative to traditional tethering techniques to fix the enzyme in place and have solutions wash over the enzyme. Assay optimization is a future goal and once that is complete it will be able to be utilized under many different experimental conditions.

8.5. Alternative Approach: Salt Reduction of EOF

8.5.1. Background

The ability to reduce EOF has led to the development of a novel assay for subjecting a single enzyme molecule to multiple solutions for the purposes of studying single molecule Michaelis-Menten kinetics. The following section outlines an attempted approach in achieving the desired data through the reduction of EOF by an increased salt concentration. EOF within a capillary is driven by the solutions interactions with the negatively charged glass wall. With a high concentration of positive ions in the buffer the negatively charged glass becomes entirely shielded with counter ions resulting in a drastically reduced EOF. If the salt is kept at the same high concentration throughout all of the solutions EOF will be permanently suppressed. In order to maintain a consistent current across the capillary the sheath flow buffer must also be made of an equal ionic strength solution. Once EOF is suppressed the capillary is expected to behave as was described with the capillary coatings. Both methods suppress EOF by blocking the charged capillary wall from the solution flowing through thereby reducing ζ, see equation 3.6. Typical CE buffers are prepared at low ionic strength, however a high ionic strength buffers can be used as long as the applied potential does not create a high enough current to damage the capillary. This increased salt concentration condition can be compared

normal cellular conditions, although we will see that this assay exceeds those amounts in order to achieve the desired EOF suppression.

8.5.2. Materials and Methods

The materials and methods for the salt suppression of EOF assay can be found in section 4.3.5. The assay was first attempted using 150 mM KCl and 10 mM $MgCl_2$ which did not exceed the current limitations of the capillary. From experience it is noted that the 2 µm internal diameter capillary should not exceed a current of 1 A as they become quite brittle at this point. The buffer was then made with the increased amounts of both salts as outlined previously for the assay, the current remained below 1 A.

8.5.3. Discussion

This assay provided sufficient suppression of EOF that may have use in future studies. The high ionic strength buffers were successful in reducing EOF. This was based on a negative injection potential and the detection of the alignment dye which would otherwise not have entered the capillary unless EOF was sufficiently reduced. The capillary was filled with two different concentrations of substrate, each representing half of the capillary volume. Data collected from this study was only able to identify a single peak which was much smaller than previous experience would dictate. It was determined that the decreased catalytic rate of the β-galactosidase enzyme was due to salt suppression. It has been stated that β-galactosidase requires Mg^{2+} for stability and activity so $MgCl_2$ concentrations are kept around 1 mM, however and increase [Mg^{2+}] may suppress catalytic rate. In order to determine whether KCl or increased $MgCl_2$ concentrations have an effect on activity, inhibition studies may be performed. Due to the overarching goal of the study to produce a solution gradient in the capillary, the effects of

increased salt concentrations were not studied further. The concept of subjecting a single molecule to multiple solutions while remaining free in solution remains a priority.

8.5.4. Summary and Conclusion

This study has provided insight into the ability to suppress EOF within a capillary by the salt concentration of the buffer. CE theory has explained this concept but it is yet to contribute to a successful assay. The potential of this novel assay is yet to be determined and remains a tool of CE. Future directions include testing various salt inhibitions with β-galactosidase and how the EOF reduction may contribute to further studies.

8.6. Cumulative Summary

Capillary coatings have been shown to be an excellent method in reducing EOF for specific assays, however some adjustments are required. The assay described in this study has the potential to investigate many characteristics simultaneously for a single enzyme molecule without the use of tethering methods. The development of a novel assay will include coating optimizations, capillary solution timing and resolution effects.

An increased salt concentration proved successful at reducing EOF. This method of EOF reduction provided the advantage that the EOF reduction agent could be included in all applicable solutions. Reproducibility of the coating and degradation are not factors with this method. However, the enzyme did not respond well to the increased salt concentration which was responsible for a significant decrease in activity.

9. General Discussion and Conclusions

The field of single molecule research has been a continuously growing body of work, as new techniques become available and current ones become more refined. There is an established principle that at the single molecule level, enzymes are in fact heterogeneous. Example areas include catalytic rates[2,3], requirements for cofactors[55], and activation energies[3]. Heterogeneity has gone from a skeptical enzymatic property to a moderately understood phenomenon. The understanding of both static and dynamic heterogeneity is currently limited based on the ability to analyze single molecule structures in detail. The history of single molecule research appears to follow a repetitive trend of high and low research periods based on the available techniques. Current advancements in high resolution structure determination and the ability to monitor these subtle changes is peaking the interest of researchers around the world to investigate systems at their most fundamental levels.[150] This includes areas of chemistry, biochemistry, biology, physics and many more areas of scientific research. All areas of research have components focusing on the smallest, most fundamental properties and as the world moves forward, these findings become more and more crucial. As it has been stated; in the area of single molecule enzymology, there is a well-established need for structure determination for single molecules in both the static and dynamic states. However, until such techniques become readily available, single molecule research will continue based on the indirect methods such as those presented in this body of work.

In Chapter 5, the role that static heterogeneity plays in determining a dynamic range was examined through temperature controlled incubations and measuring the before and after activity and mobility. A link was found in that an increase in temperature

causes a stable, long lived conformational alteration with an equal probability of the enzyme experiencing an increasing activity or mobility as it was to decrease in these two aspects. Static heterogeneity in both respects was observed by the range of activities and mobilities observed prior to any incubation period. When a sampling of enzyme molecules is assayed for either activity or mobility, a range of data is collected. This is a property of static heterogeneity determined at the time that the enzyme was synthesized and folded. From there, each molecule was determined to have a dynamic heterogeneity range stemming from its static formation. Conformational changes within an enzyme were determined to be small, as large changes would most likely result in a partial or complete unfolding of the enzyme. Therefore, the unique properties each enzyme obtains at the time of formation provide it with a limited range of dynamic heterogeneity that falls within a larger range determined by the population as a whole. The concept of catalytic heterogeneity does not come with much surprise, as proteins consist of well integrated short and long range networks throughout their structure. These networks govern protein stability[151], binding affinities[120], and conformational changes[152] related to catalysis. The network provides amplification to certain changes within the molecule such that a small structural change produces a measurable difference[71]. For example a small structural change far away from the active site has the potential to resonate through the protein, causing a significant change. Single amino acids variations cause alternations that range from unobservable to complete loss of activity through quaternary rearrangements. An example of a single amino acid substitution resulting in a large change is when a phenylalanine is converted to a leucine in human porphobilinogen synthase morpheeins[153]. A quaternary rearrangement from a hexamer to an octomer

occurs showing how vast of a change a single amino alteration can cause[154]. Although β-galactosidase does not undergo such drastic alterations such an example illustrates the potential that a molecule has for conformational alterations even at ambient temperature or below. This study has provided evidence supporting the link between static and dynamic heterogeneity in enzyme molecules through subtle conformational changes.

Heat shock proteins and their effects on β-galactosidase were examined through deletions in the DnaK-DnaJ-GrpE and GroEL-GroES heat shock chaperone systems (Chapter 6). *E. coli* was grown until normal (37°C) and heat shock (42°C) conditions and β-galactosidase was subsequently isolated from each category. No heterogeneity was observed between any of the 8 different β-galactosidase isolations. However, two hypotheses were presented from this finding. The first is that the enzymes observed in this study may only represent a small portion of properly folded, active enzymes. Much like enzymes are shown to be heterogeneous in aspects such as activity, mobility and conformational changes it is possible that some are simply more resilient to the temperature of the heat shock condition than others. Secondly, it remains a possibility that a single heat shock protein deletion is not sufficient to collapse the chaperone system. With one deletion, it is possible that the other proteins continue to ensure the proper folding of the enzyme.

The study presented in Chapter 7 provided a novel method in which a single enzyme molecule was subjected to a maximum of 3 different solutions in a single assay. Double and triple incubations were successful in providing the enzyme with a new solution, while separating it from a previously formed product zone. This allowed for the calculation of both K_m and K_I values from a single enzyme, both of which were found to

be heterogeneous properties. Mathematical modeling was used to show the relationship effects of a heterogeneous population of both K_m and K_I's.

Single molecule kinetics assays through capillary coatings and salt suppression of EOF (Chapter 8) were performed in hopes of creating a novel method for subjecting single molecules to multiple solutions one at time without the use of tethering methods. The current maximum number of solutions is at 3 before the enzyme exits the capillary. The use of capillary coatings described in the chapter outline the viability of such an assay providing that their reproducibility is stable. The assay has proven unsuccessful thus far but remains an active objective within the field of single molecule research and will be discussed further in the next chapter.

The main objective of this thesis and the research presented was to further the fundamental research and wealth of knowledge using the β-galactosidase molecule as model enzyme. β-galactosidase continues to remain one of the most highly studied enzymes in single molecule research to this date. This is in part due to relatively large amount of fluorogenic substrate options for the molecule, as fluorescence based detection techniques remain the most popular choices. Through the use of CE-LIF, static and dynamic heterogeneity have been studied along with the relationship between the two. Heat shock protein have been expressed in *E. coli*, containing a deletion and purified to provide the basis for the heterogenic effects of specific deletions. Although no significant results were found, the assay was a success and further questions were raised. Lastly, assays that are typically applied to bulk enzyme ensembles were interpreted and applied to single molecules through the development of a novel assay. Results provided further conformation on the heterogeneity of the values of K_m for a given enzyme and extended

that principle to values of K_I through competitive inhibition. An observational link between K_m and K_I was stated in that the values remain proportional to each other. If one value is larger the other is likely to be larger as well with the same effect if one is found to be smaller. Mathematical modeling was able to show that the relationship between heterogeneous K_m and K_I was in fact different from that of the homogeneous population.

Principles surrounding single molecule research rely on the assumption that heterogeneities observed for single molecules generally apply to all proteins. Although proteins are naturally made different the governing principle of encoded and assembled proteins remains consistent throughout. It has been proposed that this concept of heterogeneity in single molecules is the basis for polypeptide size constraints. It can be assumed that for each amino acid added to a protein, the probably of translational error increases, which has been identified as a source of static heterogeneity. A particular enzyme may be able to remain functional with "x" number of errors. However, if the protein doubled in size and the probability of error doubled as well, it could be assumed that twice as many errors would be present in the protein[155]. Due to a network of connections within the protein, the alterations[71] caused by those errors may have an exponential effect on the actual alterations in the protein, rendering it non-functional thus constraining the overall size of proteins[156,157].

Static and dynamic heterogenic observations made raise the question: What is the evolutionary purpose of heterogeneity? Would it not be increasingly beneficial for a cell to produce structurally "perfect" enzymes instead of a diverse population? It is possible for a cell to produce these flawless molecules, however the process becomes quite slow and tedious. Now it could be argued that the cell could simply just produce enzymes

within the high range of catalytic rates in order to reduce the need for a greater amount of them. This must be accompanied by evolutionary gain and some form of survival advantage. It can be shown through traditional evolutionary theories that diversity within a population creates strength and resilience. A former study suggested that the minor translational errors that exist in the heterogeneity of an enzyme population allow for the cell to explore possible evolutionary gain without the commitment of DNA alteration[61]. There may also be a method of adaptation to the stressful, ever changing environments in which mistranslations of DNA polymerase accelerate sub-population mutation rates[158]. It is possible that the catalytic heterogeneity observed in β-galactosidase does not actually have a major contribution to the overall fitness of the cell[159]. Diversity in enzyme molecules may play the same role as diversity in a plant species. If all of the components are identical in a system they become susceptible to a single interfering factor whereas diversity may allow a portion to go unaffected or minimally affected. For example, a genetically identical grouping of plants may be wiped out by a single virus, while a diverse population would certainly decrease but not necessarily by 100%. This appears to be observed with β-galactosidase in the presence of inhibitor where some enzymes show minimal decreases in activity.

It continues to remain unclear if single molecule heterogeneity has any significance within biological systems. From Chapter 5 it was observed that the statistical relevance of dynamic heterogeneity was lost in a 20 molecule ensemble average. Both static and dynamic heterogeneities are lost in a bulk ensemble average and with a sampling of 20 molecules illustrating this, would mean enzyme copy rates in a cell would have to be extremely low for it to have an effect. However, in terms of resiliency against

effectors outside the scope of the basic enzymatic functions heterogeneity continues to be expressed in the enzyme population. Regardless of the purpose static and dynamic heterogeneity plays in a cellular system, it continues to be a part of single molecule research. Enzymes were once thought of as a collection of identical microscopic machines and with the growing field of single molecule research there is more evidence that each molecule is in fact unique. A single cell hosts a collection of unique and diverse enzymes within a single population where each enzyme could be described as a unique snowflake.

10. Future Directions

In Chapter 5, β-galactosidase was determined to undergo conformational alterations between 10 and 50°C that were stable and long lived. The assay measured changing activities and mobilities of individual molecules which were inferred to be caused by these conformational changes. The modes of action remain unsolved for these alterations. In order to obtain this sort of information, structural analysis is required for each individual molecule. Techniques for doing such have been in constant development and have opened up a wealth of knowledge in the single molecule field although structural techniques are not employed in this laboratory. Two external techniques include; single molecule force spectroscopy[160] and smFRET[161]. Non-contact atomic force microscopy is also a high resolution technique able to distinguish subtle molecular motions without the use of probes.[162] These methods may provide further insight to current data and be sources of future collaborations.

The effects of heat shock protein deletions on β-galactosidase currently have shown no measurable effect on enzyme activity or mobility (Chapter 6). A couple of speculations were made as to if there were effects going unnoticed by the assay. The implications of this follow the same concepts that were listed above in that single molecule structural information would be of great use. The benefits to structural analysis is that the enzyme does not have to be active to be analyzed. It was proposed that many enzymes could have been misfolded into non-active conformations that are not able to be measured in the stated assay. It is also of interest to observe the protein folding mechanisms in the presence or absence of heat shock proteins. Another theory was that the remaining heat shock proteins in the chaperone set were able to compensate for the

deletion. Further investigation into the modes of action of the heat shock proteins may provide information about cell resilience. Within the measurements of catalytic rates and mobilities, there is further room to apply this heat shock study to more systems through transformed *E. coli* cells with the *lacZ* gene. The *rpoS* gene is known as a general stress response mechanism[163]. Along with heat as a stressor on the cellular system, other stress factors may be employed such as: cold shock, starvation and altered redox potentials while the enzyme production is induced. Two other genes of interest are the *hsp90*[164] and the *hsp70-lacZ* hybrid[165]. As the production of β-galactosidase is inducible and highly regulated, it is also of interest to test if heterogeneity will increase with a more rapid production of enzyme. Static heterogeneity is thought to be caused, in part, by errors in transcription and translation. A cell which is induced to produce enzyme at a rapid rate may introduce more error into each enzyme in order to meet its demands. It would be of interest to test whether static heterogeneity could be artificially amplified in the cell.

Both Chapters 7 and 8 were based on the fundamental goal of subjecting a single enzyme molecule to multiple solutions while the enzyme itself remains free in solution. Chapter 7 proved successful, however the assay has limitations. Through the use of capillary coatings to reduce EOF, the number of solutions that a single molecule could be subjected to would increase greatly. For example with enough solutions of different substrate concentrations, a Michaelis-Menton plot would be possible for a single molecule. It would also allow the experiment presented in Chapter 7 to be reproduced with a greater number of molecules with greater ease. In order to produce a working novel assay for such a method, a few properties need to be optimized; the first being the coating of the capillary. Coating the inside of a capillary by dynamic pressure injection

requires a certain concentration of polymer coating. This concentration must be enough that the capillary is evenly coated but not so much that aggregates of coating block the capillary. GS-6 and PVP solutions were used to coat the capillary at 0.2% and 0.5% w/v respectively. In order to reduce capillary plugs, either a decrease in concentration is required or possibly a longer coating and rinsing period to remove any loose polymer. A selection of concentrations and coating times are to be attempted in order to determine an optimum scenario. Reproducibility of the coating is the first necessary goal of the assay with either described coating polymer. Once a reproducible coating has been established, the resolution of the assay may be investigated. It is currently unknown what total number of solutions are able to be placed into the capillary while retaining peak resolution as an enzyme passes from one to the next. The time taken to fill the capillary must also be taken into account as diffusion will occur during long time periods. The diffusion in a capillary is quite low but if each plug of solution is small, diffusion becomes a greater factor. Solution plugs must be large enough that their volumes and spacings are reproducible. A benefit to this technique that has not been mentioned yet is the potential to analyze more than one molecule at a time. A continuous flow assay will be used, however the capillary solutions will flow towards the injection end which will dictate that length of the assay. Enzymes may enter at any time through the assay meaning that they may be subjected to less than the total number of solutions. If the data follows the predicted staircase pattern then the number of "steps" will be able to identify how many and which solutions that each particular enzyme experienced. A short length of capillary (10 μm I.D.) at 40 cm or less will be tested first but if successful, a longer capillary would allow more space for solutions while maintaining resolution.

Although the experiments conducted in this laboratory are fluorescence based, there is work worth mentioning in single molecule research that is independent of fluorescence detection. One study outlines the use of reverse-phase HPLC to create fractions that are then sent through a CE instrument coupled with a MS detector.[166] The technique proved sensitive enough to detect differences in acetylation, phosphorylation, deamidation and oxidized protein forms. Although unable to detect conformational differences, it is a technique that is able to provide a considerable amount of single molecule information.

Properties of individual molecules have shown potential in relation to how drugs may be modeled for certain treatments. β-galactosidase is an enzyme which follows Michaelis-Menten kinetics[5]. Originally, different activities observed in single molecules were thought to be due to varying K_{cat} values which implies that the activity was independent of substrate concentration[21]. Through previous work and work presented here, we see that this is not the case and K_m is different for each enzyme molecule. Along with that, K_I has also been shown to be a heterogeneous property. This would imply that drugs which act in competitive inhibition will also affect each enzyme in their own unique way. This has the potential of better identifying target molecules for specific enzymes. With the development of a novel assay to subject single molecules to multiple solutions, it would also be possible to test non-competitive inhibitions and their reversals. A molecule with an established activity may be non-competitively inhibited and then passed through various solutions to confirm whether or not the enzyme may be returned to its original state. This technique can be applied to on/off switches for enzymes allowing for fluctuations between the two states.

11.References

(1) Feynmann, R.P. There's Plenty of Room at the Bottom. *Miniaturization* **1961**.

(2) Q Xue; E. S. Yeung. Differences in the Chemical Reactivity of Individual Molecules of an Enzyme. *Nature* **1995**, *373*, 681–683.

(3) Craig, D. B.; Arriaga, E. A.; Wong, J. C.; Lu, H.; Dovichi, N. J. Studies on Single Alkaline Phosphatase Molecules: Reaction Rate and Activation Energy of a Reaction Catalyzed by a Single Molecule and the Effect of Thermal Denaturation The Death of an Enzyme. *J. Am. Chem. Soc.* **1996**, *118* (22), 5245–5253.

(4) Lu, H. P.; Xun, L.; Xie, X. S. Single-Molecule Enzymatic Dynamics. *Science* **1998**, *282* (5395), 1877–1882.

(5) English, B. P.; Min, W.; van Oijen, A. M.; Lee, K. T.; Luo, G.; Sun, H.; Cherayil, B. J.; Kou, S. C.; Xie, X. S. Ever-Fluctuating Single Enzyme Molecules: Michaelis-Menten Equation Revisited. *Nat. Chem. Biol.* **2006**, *2* (2), 87–94.

(6) Yildiz, A.; Forkey, J. N.; McKinney, S. A.; Ha, T.; Goldman, Y. E.; Selvin, P. R. Myosin V Walks Hand-Over-Hand: Single Fluorophore Imaging with 1.5-Nm Localization. *Science* **2003**, *300* (5628), 2061–2065.

(7) Kellermayer, M. S. Z.; Smith, S. B.; Granzier, H. L.; Bustamante, C. Folding-Unfolding Transitions in Single Titin Molecules Characterized with Laser Tweezers. *Science* **1997**, *276* (5315), 1112–1116.

(8) Min, W.; Luo, G.; Cherayil, B. J.; Kou, S. C.; Xie, X. S. Observation of a Power-Law Memory Kernel for Fluctuations within a Single Protein Molecule. *Phys. Rev. Lett.* **2005**, *94* (19).

(9) Cornish, P. V.; Ha, T. A Survey of Single-Molecule Techniques in Chemical Biology. *ACS Chem. Biol.* **2007**, *2* (1), 53–61.

(10) Chilvers, K. f.; Perry, J. d.; James, A. l.; Reed, R. h. Synthesis and Evaluation of Novel Fluorogenic Substrates for the Detection of Bacterial β-Galactosidase. *J. Appl. Microbiol.* **2001**, *91* (6), 1118–1130.

(11) Veigel, C.; Coluccio, L. M.; Jontes, J. D.; Sparrow, J. C.; Milligan, R. A.; Molloy, J. E. The Motor Protein Myosin-I Produces Its Working Stroke in Two Steps. *Nature* **1999**, *398* (6727), 530–533.

(12) Smith, S. B.; Cui, Y.; Bustamante, C. Overstretching B-DNA: The Elastic Response of Individual Double-Stranded and Single-Stranded DNA Molecules. *Science* **1996**, *271* (5250), 795–799.

(13) Marszalek, P. E.; Oberhauser, A. F.; Pang, Y.-P.; Fernandez, J. M. Polysaccharide Elasticity Governed by Chair–boat Transitions of the Glucopyranose Ring. *Nature* **1998**, *396* (6712), 661–664.

(14) Itoh, H.; Takahashi, A.; Adachi, K.; Noji, H.; Yasuda, R.; Yoshida, M.; Kinosita, K. Mechanically Driven ATP Synthesis by F1-ATPase. *Nature* **2004**, *427* (6973), 465–468.

(15) Wehry, E.L. Molecular Fluorescence and Phosphorescence Spectrometry. In *Handbook of Instrumental Techniques for Analytical Chemistry*; Prentice Hall Inc.: New Jersey, 1997; pp 507–539.

(16) Barnes, M. D.; Whitten, W. B.; Ramsay, J. M. Detecting Single Molecules in Liquids. *Anal. Chem.* **1995**, *67* (13), 418A – 423A.

(17) Nie, S.; Chiu, D. T.; Zare, R. N. Probing Individual Molecules with Confocal Fluorescence Microscopy. *Science* **1994**, *266* (5187), 1018–1021.

(18) *Comprehensive Sampling and Sample Preparation: Analytical Techniques for Scientists*; Pawliszyn, J., Ed.; Elsevier, Academic Press: Amsterdam, 2012.

(19) Polakowski, R.; Eggertson, M.; Craig, D. B.; Dovichi, N. J. The Chemistry of a Single Enzyme Molecule. In *Single Molecule Detection in Solution*; Zander, C., Enderlein, J., Keller, R. A., Eds.; Wiley-VCH Verlag GmbH & Co. KGaA, 2002; pp 293–301.

(20) Rotman, B. MEASUREMENT OF ACTIVITY OF SINGLE MOLECULES OF β-D-GALACTOSIDASE*. *Proc. Natl. Acad. Sci. U. S. A.* **1961**, *47* (12), 1981–1991.

(21) Rissin, D. M.; Gorris, H. H.; Walt, D. R. Distinct and Long-Lived Activity States of Single Enzyme Molecules. *J. Am. Chem. Soc.* **2008**, *130* (15), 5349–5353.

(22) Blom, H.; Kastrup, L.; Eggeling, C. Fluorescence Fluctuation Spectroscopy in Reduced Detection Volumes. *Curr. Pharm. Biotechnol.* **2006**, *7* (1), 51–66.

(23) Gratzl, M.; Lu, H.; Matsumoto, T.; Yi, C.; Bright, G. R. Fine Chemical Manipulations of Microscopic Liquid Samples. 1. Droplet Loading with Chemicals. *Anal. Chem.* **1999**, *71* (14), 2751–2756.

(24) Nakano, M.; Komatsu, J.; Matsuura, S.; Takashima, K.; Katsura, S.; Mizuno, A. Single-Molecule PCR Using Water-in-Oil Emulsion. *J. Biotechnol.* **2003**, *102* (2), 117–124.

(25) Hsin, T.-M.; Yeung, E. S. Single-Molecule Reactions in Liposomes. *Angew. Chem. Int. Ed Engl.* **2007**, *46* (42), 8032–8035.

(26) Rondelez, Y.; Tresset, G.; Tabata, K. V.; Arata, H.; Fujita, H.; Takeuchi, S.; Noji, H. Microfabricated Arrays of Femtoliter Chambers Allow Single Molecule Enzymology. *Nat. Biotechnol.* **2005**, *23* (3), 361–365.

(27) Rissin, D. M.; Walt, D. R. Digital Concentration Readout of Single Enzyme Molecules Using Femtoliter Arrays and Poisson Statistics. *Nano Lett.* **2006**, *6* (3), 520–523.

(28) Cheng, Y. F.; Dovichi, N. J. Subattomole Amino Acid Analysis by Capillary Zone Electrophoresis and Laser-Induced Fluorescence. *Science* **1988**, *242* (4878), 562–564.

(29) Noji, H.; Yasuda, R.; Yoshida, M.; Kinosita, K. Direct Observation of the Rotation of F1-ATPase. *Nature* **1997**, *386* (6622), 299–302.

(30) Walter, N. G.; Huang, C.-Y.; Manzo, A. J.; Sobhy, M. A. Do-It-Yourself Guide: How to Use the Modern Single-Molecule Toolkit. *Nat. Methods* **2008**, *5* (6), 475–489.

(31) Chen, D. Y.; Dovichi, N. J. Yoctomole Detection Limit by Laser-Induced Fluorescence in Capillary Electrophoresis. *J. Chromatogr. B Biomed. Appl.* **1994**, *657* (2), 265–269.

(32) Hirschfeld, T. Optical Microscopic Observation of Single Small Molecules. *Appl. Opt.* **1976**, *15* (12), 2965–2966.

(33) Dovichi, N. J.; Martin, J. C.; Jett, J. H.; Trkula, M.; Keller, R. A. Laser-Induced Fluorescence of Flowing Samples as an Approach to Single-Molecule Detection in Liquids. *Anal. Chem.* **1984**, *56* (3), 348–354.

(34) Betzig, E.; Chichester, R. J. Single Molecules Observed by Near-Field Scanning Optical Microscopy. *Science* **1993**, *262* (5138), 1422–1425.

(35) Xie, X. S.; Dunn, R. C. Probing Single Molecule Dynamics. *Science* **1994**, *265* (5170), 361–364.

(36) Ambrose, W. P.; Goodwin, P. M.; Keller, R. A.; Martin, J. C. Alterations of Single Molecule Fluorescence Lifetimes in Near-Field Optical Microscopy. *Science* **1994**, *265* (5170), 364–367.

(37) Vickery, S. A.; Dunn, R. C. Scanning near-Field Fluorescence Resonance Energy Transfer Microscopy. *Biophys. J.* **1999**, *76* (4), 1812–1818.

(38) Ha, T. Single-Molecule Fluorescence Resonance Energy Transfer. *Methods* **2001**, *25* (1), 78–86.

(39) Beckers, M.; Drechsler, F.; Eilert, T.; Nagy, J.; Michaelis, J. Quantitative Structural Information from Single-Molecule FRET. *Faraday Discuss.* **2015**, *184* (0), 117–129.

(40) Macklin, J. J.; Trautman, J. K.; Harris, T. D.; Brus, L. E. Imaging and Time-Resolved Spectroscopy of Single Molecules at an Interface. *Science* **1996**, *272* (5259), 255–258.

(41) Kapkiai, L. K.; Moore-Nichols, D.; Carnell, J.; Krogmeier, J. R.; Dunn, R. C. Hybrid near-Field Scanning Optical Microscopy Tips for Live Cell Measurements. *Appl. Phys. Lett.* **2004**, *84* (19), 3750–3752.

(42) Funatsu, T.; Harada, Y.; Tokunaga, M.; Saito, K.; Yanagida, T. Imaging of Single Fluorescent Molecules and Individual ATP Turnovers by Single Myosin Molecules in Aqueous Solution. *Nature* **1995**, *374* (6522), 555–559.

(43) Chen, Y.; Hu, D.; Vorpagel, E. R.; Lu, H. P. Probing Single-Molecule T4 Lysozyme Conformational Dynamics by Intramolecular Fluorescence Energy Transfer. *J. Phys. Chem. B* **2003**, *107* (31), 7947–7956.

(44) Schuler, B.; Eaton, W. A. Protein Folding Studied by Single-Molecule FRET. *Curr. Opin. Struct. Biol.* **2008**, *18* (1), 16–26.

(45) Yildiz, A.; Park, H.; Safer, D.; Yang, Z.; Chen, L.-Q.; Selvin, P. R.; Sweeney, H. L. Myosin VI Steps via a Hand-over-Hand Mechanism with Its Lever Arm Undergoing Fluctuations When Attached to Actin. *J. Biol. Chem.* **2004**, *279* (36), 37223–37226.

(46) Kural, C.; Kim, H.; Syed, S.; Goshima, G.; Gelfand, V. I.; Selvin, P. R. Kinesin and Dynein Move a Peroxisome in Vivo: A Tug-of-War or Coordinated Movement? *Science* **2005**, *308* (5727), 1469–1472.

(47) Yasuda, R.; Noji, H.; Yoshida, M.; Kinosita, K.; Itoh, H. Resolution of Distinct Rotational Substeps by Submillisecond Kinetic Analysis of F1-ATPase. *Nature* **2001**, *410* (6831), 898–904.

(48) Zhuang, X.; Kim, H.; Pereira, M. J. B.; Babcock, H. P.; Walter, N. G.; Chu, S. Correlating Structural Dynamics and Function in Single Ribozyme Molecules. *Science* **2002**, *296* (5572), 1473–1476.

(49) Hanson, J. A.; Duderstadt, K.; Watkins, L. P.; Bhattacharyya, S.; Brokaw, J.; Chu, J.-W.; Yang, H. Illuminating the Mechanistic Roles of Enzyme Conformational Dynamics. *Proc. Natl. Acad. Sci. U. S. A.* **2007**, *104* (46), 18055–18060.

(50) Tan, W.; Yeung, E. S. Monitoring the Reactions of Single Enzyme Molecules and Single Metal Ions. *Anal. Chem.* **1997**, *69* (20), 4242–4248.

(51) Herzenberg, L. A. Studies on the Induction of Beta-Galactosidase in a Cryptic Strain of Escherichia Coli. *Biochim. Biophys. Acta* **1959**, *31* (2), 525–538.

(52) Gorini, L. III. CONTROL BY REPRESSION OF A BIOCHEMICAL PATHWAY. *Bacteriol. Rev.* **1963**, *27* (2), 182–190.

(53) Craig, D. B.; Dovichi, N. J. Escherichia Coli β-Galactosidase Is Heterogeneous with Respect to the Activity of Individual Molecules. *Can. J. Chem.* **1998**, *76* (5), 623–626.

(54) Shoemaker, G. K.; Juers, D. H.; Coombs, J. M. L.; Matthews, B. W.; Craig, D. B. Crystallization of β-Galactosidase Does Not Reduce the Range of Activity of Individual Molecules †. *Biochemistry (Mosc.)* **2003**, *42* (6), 1707–1710.

(55) Craig, D. B.; Hall, T.; Goltz, D. M. Escherichia Coli \s S-Galactosidase Is Heterogeneous with Respect to a Requirement for Magnesium. *Biometals* **2000**, *13* (3), 223–229.

(56) Craig, D. B.; Nachtigall, J. T.; Ash, H. L.; Shoemaker, G. K.; Dyck, A. C.; Wawrykow, T. M.; Gudbjartson, H. L. Differences in the Average Single Molecule Activities of E. Coli β-Galactosidase: Effect of Source, Enzyme Molecule Age and Temperature of Induction. *J. Protein Chem.* **2003**, *22* (6), 555–561.

(57) Li, Q.; Seeger, S. Label-Free Detection of Single Protein Molecules Using Deep UV Fluorescence Lifetime Microscopy. *Anal. Chem.* **2006**, *78* (8), 2732–2737.

(58) Polakowski, R.; Craig, D. B.; Skelley, A.; Dovichi, N. J. Single Molecules of Highly Purified Bacterial Alkaline Phosphatase Have Identical Activity. *J. Am. Chem. Soc.* **2000**, *122* (20), 4853–4855.

(59) Dyck, A. C.; Craig, D. B. Individual Molecules of Thermostable Alkaline Phosphatase Support Different Catalytic Rates at Room Temperature. *Luminescence* **2002**, *17* (1), 15–18.

(60) Oijen, A. M. van; Blainey, P. C.; Crampton, D. J.; Richardson, C. C.; Ellenberger, T.; Xie, X. S. Single-Molecule Kinetics of λ Exonuclease Reveal Base Dependence and Dynamic Disorder. *Science* **2003**, *301* (5637), 1235–1238.

(61) Whitehead, D. J.; Wilke, C. O.; Vernazobres, D.; Bornberg-Bauer, E. The Look-Ahead Effect of Phenotypic Mutations. *Biol. Direct* **2008**, *3*, 18.

(62) Min, W.; English, B. P.; Luo, G.; Cherayil, B. J.; Kou, S. C.; Xie, X. S. Fluctuating Enzymes: Lessons from Single-Molecule Studies. *Acc. Chem. Res.* **2005**, *38* (12), 923–931.

(63) Craig, D. B.; Nichols, E. R. Continuous Flow Assay for the Simultaneous Measurement of the Electrophoretic Mobility, Catalytic Activity and Its Variation over Time of Individual Molecules of *Escherichia Coli* β-Galactosidase. *ELECTROPHORESIS* **2008**, *29* (21), 4298–4303.

(64) Edman, L.; Földes-Papp, Z.; Wennmalm, S.; Rigler, R. The Fluctuating Enzyme: A Single Molecule Approach. *Chem. Phys.* **1999**, *247* (1), 11–22.

(65) Hassler, K.; Rigler, P.; Blom, H.; Rigler, R.; Widengren, J.; Lasser, T. Dynamic Disorder in Horseradish Peroxidase Observed with Total Internal Reflection Fluorescence Correlation Spectroscopy. *Opt. Express* **2007**, *15* (9), 5366–5375.

(66) Yang, H.; Luo, G.; Karnchanaphanurach, P.; Louie, T.-M.; Rech, I.; Cova, S.; Xun, L.; Xie, X. S. Protein Conformational Dynamics Probed by Single-Molecule Electron Transfer. *Science* **2003**, *302* (5643), 262–266.

(67) Velonia, K.; Flomenbom, O.; Loos, D.; Masuo, S.; Cotlet, M.; Engelborghs, Y.; Hofkens, J.; Rowan, A. E.; Klafter, J.; Nolte, R. J. M.; et al. Single-Enzyme Kinetics of CALB-Catalyzed Hydrolysis. *Angew. Chem. Int. Ed.* **2005**, *44* (4), 560–564.

(68) Flomenbom, O.; Velonia, K.; Loos, D.; Masuo, S.; Cotlet, M.; Engelborghs, Y.; Hofkens, J.; Rowan, A. E.; Nolte, R. J. M.; Van der Auweraer, M.; et al. Stretched Exponential Decay and Correlations in the Catalytic Activity of Fluctuating Single Lipase Molecules. *Proc. Natl. Acad. Sci. U. S. A.* **2005**, *102* (7), 2368–2372.

(69) Cheatum, C. M.; Kohen, A. Relationship between Femtosecond-Picosecond Dynamics to Enzyme Catalyzed H-Transfer. *Top. Curr. Chem.* **2013**, *337*, 1–39.

(70) Dan, N. Understanding Dynamic Disorder Fluctuations in Single-Molecule Enzymatic Reactions. *Curr. Opin. Colloid Interface Sci.* **2007**, *12* (6), 314–321.

(71) Mesecar, A. D.; Stoddard, B. L.; Koshland, D. E. Orbital Steering in the Catalytic Power of Enzymes: Small Structural Changes with Large Catalytic Consequences. *Science* **1997**, *277* (5323), 202–206.

(72) Baldini, G.; Cannone, F.; Chirico, G.; Collini, M.; Campanini, B.; Bettati, S.; Mozzarelli, A. Evidence of Discrete Substates and Unfolding Pathways in Green Fluorescent Protein. *Biophys. J.* **2007**, *92* (5), 1724–1731.

(73) Gordon, M. J.; Huang, X.; Pentoney, S. L.; Zare, R. N. Capillary Electrophoresis. *Science* **1988**, *242* (4876), 224–228.

(74) Henk H. Lauer and Gerard P. Rozing. *High Performance Capillary Electrophoresis*, 2nd ed.; Agilent Technologies, Inc.: Germany, 2014.

(75) Deforce, D. L. D.; Millecamps, R. E. M.; Van Hoofstat, D.; Van den Eeckhout, E. G. Comparison of Slab Gel Electrophoresis and Capillary Electrophoresis for the Detection of the Fluorescently Labeled Polymerase Chain Reaction Products of Short Tandem Repeat Fragments. *J. Chromatogr. A* **1998**, *806* (1), 149–155.

(76) Mikkers, F. E. P.; Everaerts, F. M.; Verheggen, T. P. E. M. High-Performance Zone Electrophoresis. *J. Chromatogr. A* **1979**, *169*, 11–20.

(77) Jorgenson, J. W.; Lukacs, K. D. Zone Electrophoresis in Open-Tubular Glass Capillaries. *Anal. Chem.* **1981**, *53* (8), 1298–1302.

(78) Jorgenson, J. W.; Lukacs, K. D. Capillary Zone Electrophoresis. *Science* **1983**, *222* (4621), 266–272.

(79) Lauer, H. H.; McManigill, D. Capillary Zone Electrophoresis of Proteins in Untreated Fused Silica Tubing. *Anal. Chem.* **1986**, *58* (1), 166–170.

(80) Gassmann, E.; Kuo, J. E.; Zare, R. N. Electrokinetic Separation of Chiral Compounds. *Science* **1985**, *230* (4727), 813–814.

(81) Ewing, A.G et al. Electrochemical Detection IN MICROCOLUMN SEPARATIONS. *Anal. Chem.* **1994**, *66* (9), 527A – 537A.

(82) Sun, X.; Jin, W.; Li, D.; Bai, Z. Measurement of Alkaline Phosphatase Isoenzymes in Individual Mouse Bone Marrow Fibroblast Cells Based on Capillary Electrophoresis with on-Capillary Enzyme-Catalyzed Reaction and Electrochemical Detection. *ELECTROPHORESIS* **2004**, *25* (12), 1860–1866.

(83) Huck, C. W.; Bakry, R.; Huber, L. A.; Bonn, G. K. Progress in Capillary Electrophoresis Coupled to Matrix-Assisted Laser Desorption/ionization - Time of Flight Mass Spectrometry. *Electrophoresis* **2006**, *27* (11), 2063–2074.

(84) Chen, D. Y.; Adelhelm, K.; Cheng, X. L.; Dovichi, N. J. Communication. A Simple Laser-Induced Fluorescence Detector for Sulforhodamine 101 in a Capillary Electrophoresis System: Detection Limits of 10 Yoctomoles or Six Molecules. *Analyst* **1994**, *119* (2), 349–352.

(85) Dovichi, N. J. DNA Sequencing by Capillary Electrophoresis. *ELECTROPHORESIS* **1997**, *18* (12-13), 2393–2399.

(86) Whiting, C. E.; Arriaga, E. A. CE-LIF Analysis of Mitochondria Using Uncoated and Dynamically Coated Capillaries. *Electrophoresis* **2006**, *27* (22), 4523–4531.

(87) Shoemaker, G. K.; Lorieau, J.; Lau, L. H.; Gillmor, C. S.; Palcic, M. M. Multiple Sampling in Single-Cell Enzyme Assays Using CE-Laser-Induced Fluorescence to Monitor Reaction Progress. *Anal. Chem.* **2005**, *77* (10), 3132–3137.

(88) Hu, K.; Ahmadzadeh, H.; Krylov, S. N. Asymmetry between Sister Cells in a Cancer Cell Line Revealed by Chemical Cytometry. *Anal. Chem.* **2004**, *76* (13), 3864–3866.

(89) Adamson, N. J.; Reynolds, E. C. Rules Relating Electrophoretic Mobility, Charge and Molecular Size of Peptides and Proteins. *J. Chromatogr. B. Biomed. Sci. App.* **1997**, *699* (1-2), 133–147.

(90) Bolt, G. H. Determination of the Charge Density of Silica Sols. *J. Phys. Chem.* **1957**, *61* (9), 1166–1169.

(91) Stevens, T. S.; Cortes, H. J. Electroosmotic Propulsion of Eluent through Silica-Based Chromatographic Media. *Anal. Chem.* **1983**, *55* (8), 1365–1370.

(92) Gas, B.; Stedrý, M.; Kenndler, E. Peak Broadening in Capillary Zone Electrophoresis. *Electrophoresis* **1997**, *18* (12-13), 2123–2133.

(93) Cunliffe, J. M.; Baryla, N. E.; Lucy, C. A. Phospholipid Bilayer Coatings for the Separation of Proteins in Capillary Electrophoresis. *Anal. Chem.* **2002**, *74* (4), 776–783.

(94) MacDonald, A. M.; Lucy, C. A. Highly Efficient Protein Separations in Capillary Electrophoresis Using a Supported Bilayer/diblock Copolymer Coating. *J. Chromatogr. A* **2006**, *1130* (2), 265–271.

(95) Kaneta, T.; Ueda, T.; Hata, K.; Imasaka, T. Suppression of Electroosmotic Flow and Its Application to Determination of Electrophoretic Mobilities in a Poly(vinylpyrrolidone)-Coated Capillary. *J. Chromatogr. A* **2006**, *1106* (1-2), 52–55.

(96) Chang, W. W. P.; Hobson, C.; Bomberger, D. C.; Schneider, L. V. Rapid Separation of Protein Isoforms by Capillary Zone Electrophoresis with New Dynamic Coatings. *Electrophoresis* **2005**, *26* (11), 2179–2186.

(97) Zhao, J.-Y.; Chen, D.-Y.; Dovichi, N. J. Low-Cost Laser-Induced Fluorescence Detector for Micellar Capillary Zone Electrophoresis. *J. Chromatogr. A* **1992**, *608* (1), 117–120.

(98) Huang, X.; Gordon, M. J.; Zare, R. N. Bias in Quantitative Capillary Zone Electrophoresis Caused by Electrokinetic Sample Injection. *Anal. Chem.* **1988**, *60* (4), 375–377.

(99) Alpers, D. H.; Steers, E.; Shifrin, S.; Tomkins, G. Isozymes of the Lactose Operon of Escherichia Coli. *Ann. N. Y. Acad. Sci.* **1968**, *151* (1), 545–555.

(100) Matthews, B. W. The Structure of E. Coli Beta-Galactosidase. *C. R. Biol.* **2005**, *328* (6), 549–556.

(101) Jobe, A.; Bourgeois, S. Lac Repressor-Operator Interaction. VI. The Natural Inducer of the Lac Operon. *J. Mol. Biol.* **1972**, *69* (3), 397–408.

(102) Jacob, F.; Monod, J. Genetic Regulatory Mechanisms in the Synthesis of Proteins. *J. Mol. Biol.* **1961**, *3* (3), 318–356.

(103) Lewis, M. The Lac Repressor. *C. R. Biol.* **2005**, *328* (6), 521–548.

(104) Roderick, S. L. The Lac Operon Galactoside Acetyltransferase. *C. R. Biol.* **2005**, *328* (6), 568–575.

(105) Gilbert, W.; Müller-Hill, B. ISOLATION OF THE LAC REPRESSOR. *Proc. Natl. Acad. Sci. U. S. A.* **1966**, *56* (6), 1891–1898.

(106) Fowler, A. V.; Brake, A. J.; Zabin, I. Amino Acid Sequence of Beta-Galactosidase. VI. Limited Tryptic Digestion of the Citraconylated Protein and Sequences of Tryptic Peptides. *J. Biol. Chem.* **1978**, *253* (15), 5490–5498.

(107) Kalnins, A.; Otto, K.; Rüther, U.; Müller-Hill, B. Sequence of the lacZ Gene of Escherichia Coli. *EMBO J.* **1983**, *2* (4), 593–597.

(108) Jacobson, R. H.; Zhang, X. J.; DuBose, R. F.; Matthews, B. W. Three-Dimensional Structure of Beta-Galactosidase from E. Coli. *Nature* **1994**, *369* (6483), 761–766.

(109) Juers, D. H.; Jacobson, R. H.; Wigley, D.; Zhang, X.-J.; Huber, R. E.; Tronrud, D. E.; Matthews, B. W. High Resolution Refinement of β-Galactosidase in a New Crystal Form Reveals Multiple Metal-Binding Sites and Provides a Structural Basis for α-Complementation. *Protein Sci.* **2000**, *9* (9), 1685–1699.

(110) Marchesi, S. L.; Steers, E.; Shifrin, S. Purification and Characterization of the Multiple Forms of Beta-Galactosidase of Escherichia Coli. *Biochim. Biophys. Acta* **1969**, *181* (1), 20–34.

(111) Edwards, R. A.; Jacobson, A. L.; Huber, R. E. Thermal Denaturation of Beta-Galactosidase and of Two Site-Specific Mutants. *Biochemistry (Mosc.)* **1990**, *29* (49), 11001–11008.

(112) Craven, G. R.; Steers, E.; Anfinsen, C. B. Purification, Composition, and Molecular Weight of the β-Galactosidase of Escherichia Coli K12. *J. Biol. Chem.* **1965**, *240* (6), 2468–2477.

(113) Tenu, J. P.; Viratelle, O. M.; Yon, J. Kinetic Study of the Activation Process of -Galactosidase from Escherichia Coli by Mg 2+. *Eur. J. Biochem. FEBS* **1972**, *26* (1), 112–118.

(114) Huber, R. E.; Parfett, C.; Woulfe-Flanagan, H.; Thompson, D. J. Interaction of Divalent Cations with .beta.-Galactosidase (Escherichia Coli). *Biochemistry (Mosc.)* **1979**, *18* (19), 4090–4095.

(115) Ullmann, A.; Monod, J. On the Effect of Divalent Cations and Protein Concentration upon Renaturation of Beta-Galactosidase from E. Coli. *Biochem. Biophys. Res. Commun.* **1969**, *35* (1), 35–42.

(116) Bader, D. E.; Ring, M.; Huber, R. E. Site-Directed Mutagenic Replacement of Glu-461 with Gln in Beta-Galactosidase (E. Coli): Evidence That Glu-461 Is Important for Activity. *Biochem. Biophys. Res. Commun.* **1988**, *153* (1), 301–306.

(117) Ring, M.; Bader, D. E.; Huber, R. E. Site-Directed Mutagenesis of Beta-Galactosidase (E. Coli) Reveals That Tyr-503 Is Essential for Activity. *Biochem. Biophys. Res. Commun.* **1988**, *152* (3), 1050–1055.

(118) Yuan, J.; Martinez-Bilbao, M.; Huber, R. E. Substitutions for Glu-537 of Beta-Galactosidase from Escherichia Coli Cause Large Decreases in Catalytic Activity. *Biochem. J.* **1994**, *299* (Pt 2), 527–531.

(119) Roth, N. J.; Huber, R. E. The β-Galactosidase (Escherichia Coli) Reaction Is Partly Facilitated by Interactions of His-540 with the C6 Hydroxyl of Galactose. *J. Biol. Chem.* **1996**, *271* (24), 14296–14301.

(120) Huber, R. E.; Hakda, S.; Cheng, C.; Cupples, C. G.; Edwards, R. A. Trp-999 of β-Galactosidase (Escherichia Coli) Is a Key Residue for Binding, Catalysis, and Synthesis of Allolactose, the Natural Lac Operon Inducer. *Biochemistry (Mosc.)* **2003**, *42* (6), 1796–1803.

(121) Juers, D. H.; Heightman, T. D.; Vasella, A.; McCarter, J. D.; Mackenzie, L.; Withers, S. G.; Matthews, B. W. A Structural View of the Action of Escherichia Coli (lacZ) β-Galactosidase,. *Biochemistry (Mosc.)* **2001**, *40* (49), 14781–14794.

(122) Craig, D. B.; Schwab, T.; Sterner, R. Random Mutagenesis Suggests That Sequence Errors Are Not a Major Cause of Variation in the Activity of Individual Molecules of β-Galactosidase. *Biochem. Cell Biol.* **2012**, *90* (4), 540–547.

(123) Henn-Sax, M.; Thoma, R.; Schmidt, S.; Hennig, M.; Kirschner, K.; Sterner, R. Two $(\beta\alpha)_8$ -Barrel Enzymes of Histidine and Tryptophan Biosynthesis Have Similar Reaction Mechanisms and Common Strategies for Protecting Their Labile Substrates †, ‡. *Biochemistry (Mosc.)* **2002**, *41* (40), 12032–12042.

(124) Nichols, E. R.; Craig, D. B. Measurement of the Differences in Electrophoretic Mobilities of Individual Molecules of *E. Coli* β-Galactosidase Provides Insight into Structural Differences Which Underlie Enzyme Microheterogeneity. *ELECTROPHORESIS* **2008**, *29* (20), 4257–4269.

(125) Rojek, M. J.; Walt, D. R. Observing Single Enzyme Molecules Interconvert between Activity States upon Heating. *PloS One* **2014**, *9* (1), e86224.

(126) Johansson, E.; Majka, J.; Burgers, P. M. Structure of DNA Polymerase Delta from Saccharomyces Cerevisiae. *J. Biol. Chem.* **2001**, *276* (47), 43824–43828.

(127) Nichols, E. R.; Shadabi, E.; Craig, D. B. Effect of Alteration of Translation Error Rate on Enzyme Microheterogeneity as Assessed by Variation in Single Molecule Electrophoretic Mobility and Catalytic Activity. *Biochem. Cell Biol.* **2009**, *87* (3), 517–529.

(128) Craig, D. B.; Bayaraa, B.; Lee, D.; Charleton, J. Effect Of Induction Temperature And Partial Thermal Denaturation On The Catalytic And Electrophoretic Heterogeneity Of B-Galactosidase From Two *Escherichia Coli* Strains. *J. Liq. Chromatogr. Relat. Technol.* **2013**, *36* (20), 2944–2959.

(129) Compton, B. J.; O'Grady, E. A. Role of Charge Suppression and Ionic Strength in Free Zone Electrophoresis of Proteins. *Anal. Chem.* **1991**, *63* (22), 2597–2602.

(130) Kálmán, F.; Ma, S.; Fox, R. O.; Horváth, C. Capillary Electrophoresis of S. Nuclease Mutants. *J. Chromatogr. A* **1995**, *705* (1), 135–154.

(131) Neidhardt, F. C.; Curtiss, R. *Escherichia Coli and Salmonella: Cellular and Molecular Biology*; ASM Press: Washington, D.C., 1996.

(132) Yamamoto, N.; Nakahigashi, K.; Nakamichi, T.; Yoshino, M.; Takai, Y.; Touda, Y.; Furubayashi, A.; Kinjyo, S.; Dose, H.; Hasegawa, M.; et al. Update on the Keio Collection of Escherichia Coli Single-Gene Deletion Mutants. *Mol. Syst. Biol.* **2009**, *5*, 335.

(133) Feder, M. E.; Hofmann, G. E. HEAT-SHOCK PROTEINS, MOLECULAR CHAPERONES, AND THE STRESS RESPONSE: Evolutionary and Ecological Physiology. *Annu. Rev. Physiol.* **1999**, *61* (1), 243–282.

(134) Craig, D.B., Nichols, E.R. Sample Preparation for Single Molecules Using Capillary Electrophoresis with Fluorescence Detection. In *Comprehensive Sampling and Sample Preparation*; Elsevier, Academic Press, 2012; Vol. 3, pp 323–337.

(135) Eggertson, M. J.; Craig, D. B. β-Galactosidase Assay Using Capillary Electrophoresis Laser-Induced Fluorescence Detection and Resorufin-β-D-Galactopyranoside as Substrate. *Biomed. Chromatogr.* **1999**, *13* (8), 516–519.

(136) Craig, D. B.; Wong, J. C. Y.; Dovichi, N. J. Detection of Attomolar Concentrations of Alkaline Phosphatase by Capillary Electrophoresis Using Laser-Induced Fluorescence Detection. *Anal. Chem.* **1996**, *68* (4), 697–700.

(137) Thomas, J. G.; Baneyx, F. Protein Folding in the Cytoplasm of Escherichia Coli: Requirements for the DnaK-DnaJ-GrpE and GroEL-GroES Molecular Chaperone Machines. *Mol. Microbiol.* **1996**, *21* (6), 1185–1196.

(138) García-Fruitós, E.; Carrió, M. M.; Arís, A.; Villaverde, A. Folding of a Misfolding-Prone Beta-Galactosidase in Absence of DnaK. *Biotechnol. Bioeng.* **2005**, *90* (7), 869–875.

(139) Ferreira, N. L.; Alix, J.-H. The DnaK Chaperone Is Necessary for α-Complementation of β-Galactosidase in Escherichia Coli. *J. Bacteriol.* **2002**, *184* (24), 7047–7054.

(140) Young, J. C.; Agashe, V. R.; Siegers, K.; Hartl, F. U. Pathways of Chaperone-Mediated Protein Folding in the Cytosol. *Nat. Rev. Mol. Cell Biol.* **2004**, *5* (10), 781–791.

(141) McCallister, C.; Siracusa, M. C.; Shirazi, F.; Chalkia, D.; Nikolaidis, N. Functional Diversification and Specialization of Cytosolic 70-kDa Heat Shock Proteins. *Sci. Rep.* **2015**, *5*, 9363.

(142) Kuznetsova, S.; Zauner, G.; Aartsma, T. J.; Engelkamp, H.; Hatzakis, N.; Rowan, A. E.; Nolte, R. J. M.; Christianen, P. C. M.; Canters, G. W. The Enzyme Mechanism of Nitrite Reductase Studied at Single-Molecule Level. *Proc. Natl. Acad. Sci.* **2008**, *105* (9), 3250–3255.

(143) Craig, D. B.; Haslam, A. M.; Coombs, J. M. L.; Nichols, E. R. Kinetic Studies of Unmodified Individual Escherichia Coli β-Galactosidase Molecules in Free Solution. *Biochem. Cell Biol.* **2010**, *88* (3), 451–458.

(144) Dixon, M. The Determination of Enzyme Inhibitor Constants. *Biochem. J.* **1953**, *55* (1), 170–171.

(145) Gorris, H. H.; Rissin, D. M.; Walt, D. R. Stochastic Inhibitor Release and Binding from Single-Enzyme Molecules. *Proc. Natl. Acad. Sci.* **2007**, *104* (45), 17680–17685.

(146) Hadd, A. G.; Raymond, D. E.; Halliwell, J. W.; Jacobson, S. C.; Ramsey, J. M. Microchip Device for Performing Enzyme Assays. *Anal. Chem.* **1997**, *69* (17), 3407–3412.

(147) Seong, G. H.; Heo, J.; Crooks, R. M. Measurement of Enzyme Kinetics Using a Continuous-Flow Microfluidic System. *Anal. Chem.* **2003**, *75* (13), 3161–3167.

(148) Huber, R. E.; Brockbank, R. L. Strong Inhibitory Effect of Furanoses and Sugar Lactones On. Beta.-Galactosidase of Escherichia Coli. *Biochemistry (Mosc.)* **1987**, *26* (6), 1526–1531.

(149) Horvath, J.; Dolník, V. Polymer Wall Coatings for Capillary Electrophoresis. *ELECTROPHORESIS* **2001**, *22* (4), 644–655.

(150) Oteyza, D. G. de; Gorman, P.; Chen, Y.-C.; Wickenburg, S.; Riss, A.; Mowbray, D. J.; Etkin, G.; Pedramrazi, Z.; Tsai, H.-Z.; Rubio, A.; et al. Direct Imaging of Covalent Bond Structure in Single-Molecule Chemical Reactions. *Science* **2013**, *340* (6139), 1434–1437.

(151) Lockless, S. W.; Ranganathan, R. Evolutionarily Conserved Pathways of Energetic Connectivity in Protein Families. *Science* **1999**, *286* (5438), 295–299.

(152) Juers, D. H.; Hakda, S.; Matthews, B. W.; Huber, R. E. Structural Basis for the Altered Activity of Gly794 Variants of Escherichia Coli β-Galactosidase†. *Biochemistry (Mosc.)* **2003**, *42* (46), 13505–13511.

(153) Selwood, T.; Tang, L.; Lawrence, S. H.; Anokhina, Y.; Jaffe, E. K. Kinetics and Thermodynamics of the Interchange of the Morpheein Forms of Human Porphobilinogen Synthase. *Biochemistry (Mosc.)* **2008**, *47* (10), 3245–3257.

(154) Tang, L.; Breinig, S.; Stith, L.; Mischel, A.; Tannir, J.; Kokona, B.; Fairman, R.; Jaffe, E. K. Single Amino Acid Mutations Alter the Distribution of Human Porphobilinogen Synthase Quaternary Structure Isoforms (Morpheeins). *J. Biol. Chem.* **2006**, *281* (10), 6682–6690.

(155) Allan Drummond, D.; Wilke, C. O. The Evolutionary Consequences of Erroneous Protein Synthesis. *Nat. Rev. Genet.* **2009**, *10* (10), 715–724.

(156) Rosenberger, R. F.; Foskett, G. An Estimate of the Frequency of in Vivo Transcriptional Errors at a Nonsense Codon in Escherichia Coli. *Mol. Gen. Genet. MGG* **1981**, *183* (3), 561–563.

(157) Parker, J. Errors and Alternatives in Reading the Universal Genetic Code. *Microbiol. Rev.* **1989**, *53* (3), 273–298.

(158) Boe, L. Translational Errors as the Cause of Mutations in Escherichia Coli. *Mol. Gen. Genet. MGG* **1992**, *231* (3), 469–471.

(159) Dean, A. M.; Dykhuizen, D. E.; Hartl, D. L. Fitness Effects of Amino Acid Replacements in the Beta-Galactosidase of Escherichia Coli. *Mol. Biol. Evol.* **1988**, *5* (5), 469–485.

(160) Barrett, M. J.; Oliver, P. M.; Cheng, P.; Cetin, D.; Vezenov, D. High Density Single-Molecule-Bead Arrays for Parallel Single Molecule Force Spectroscopy. *Anal. Chem.* **2012**, *84* (11), 4907–4914.

(161) Li, Y.; Zhang, C. Analysis of MicroRNA-Induced Silencing Complex-Involved MicroRNA-Target Recognition by Single-Molecule Fluorescence Resonance Energy Transfer. *Anal. Chem.* **2012**, *84* (11), 5097–5102.

(162) Sasahara, A.; Uetsuka, H.; Onishi, H. Single-Molecule Analysis by Noncontact Atomic Force Microscopy. *J. Phys. Chem. B* **2001**, *105* (1), 1–4.

(163) Schaechter, M. Escherichia Coli and Salmonella 2000: The View From Here. *Microbiol. Mol. Biol. Rev.* **2001**, *65* (1), 119–130.

(164) Finkelstein, D. B.; Strausberg, S. Heat Shock-Regulated Production of Escherichia Coli Beta-Galactosidase in Saccharomyces Cerevisiae. *Mol. Cell. Biol.* **1983**, *3* (9), 1625–1633.

(165) Lis, J. T.; Simon, J. A.; Sutton, C. A. New Heat Shock Puffs and Beta-Galactosidase Activity Resulting from Transformation of Drosophila with an hsp70-lacZ Hybrid Gene. *Cell* **1983**, *35* (2 Pt 1), 403–410.

(166) Faserl, K.; Kremser, L.; Müller, M.; Teis, D.; Lindner, H. H. Quantitative Proteomics Using Ultralow Flow Capillary Electrophoresis–Mass Spectrometry. *Anal. Chem.* **2015**, *87* (9), 4633–4640.